

CBPF

Centro Brasileiro de
Pesquisas Físicas

**UNIVERSITÉ DE
GRENOBLE**

THÈSE

Pour obtenir le grade de

DOCTEUR DE L'UNIVERSITÉ DE GRENOBLE

**préparée dans le cadre d'une cotutelle entre
l'Université de Grenoble et CBPF – Centro Brasileiro
de Pesquisas Físicas**

Spécialité : **Physique**

Arrêté ministériel : le 6 janvier 2005 -7 août 2006

Présentée par

Fernanda DEUS DA SILVA

Thèse dirigée par **Mucio CONTINENTINO** et **Claudine LACROIX**
codirigée par **Mairbek CHSHIEV**

préparée au sein des **Institut Néel et CBPF**

dans le **École Doctorale de Physique de Grenoble et le CBPF**

Contributions aux Propriétés de Transport d'un Système à N Corps

Thèse soutenue publiquement le **11/03/2015**, devant le jury composé de :

Mme. Adeline CRÉPIEUX

Maitre de Conférences - Université Aix-Marseille, Rapporteur

Mme. Andrea LATGE

Chercheur/Professeur - UFF, Rapporteur

Mme. Claudine LACROIX

Chercheur - CNRS, Directeur de Thèse

Mr. Itzhak RODITI

Chercheur - CBPF, Membre

Mr. Mairbek CHSHIEV

Professeur - UJF, CoDirecteur de Thèse

Mr. Mucio CONTINENTINO

Chercheur - CBPF, Directeur de Thèse

Mr. Tobias MICKLITZ

Chercheur - CBPF, Membre

*Université Joseph Fourier / Université Pierre Mendès France /
Université Stendhal / Université de Savoie / Grenoble INP*





CBPF

**Centro Brasileiro de
Pesquisas Físicas**

Rua Dr. Xavier Sigaud, 150 Rio de Janeiro, Brasil
Tel:(0xx21) 2141-7100 Fax:(0xx21) 2141-7400 CEP:22290-180

Fernanda Deus da Silva

Contributions to the Transport Properties of Many-Body Systems

Rio de Janeiro, BR
Grenoble, FR
2015

Fernanda Deus da Silva

Contribuições para as Propriedades de
Transporte em Sistemas de Muitos
Corpos

Rio de Janeiro, BR
Grenoble, FR
2015

Agradecimento

Gostaria de agradecer as agências: CNPq, pelos 3 anos de financiamento em que estive realizando meu projeto de pesquisa de tese no CBPF; e a CAPES, pelo financiamento do ano em que estive na França aprimorando a minha formação. Também gostaria de agradecer ao apoio à mobilidade internacional de alunos de doutoramento em co-tutela dado pela Région Rhône Alpes.

Agradeço ao Prof. Dr. Mucio Amado Continentino, meu eterno orientador. Desde o tempo de iniciação científica aprendo com ele a me tornar uma verdadeira pesquisadora. Eu admiro seu encantamento com a Física e isso sempre me motiva a buscar o meu melhor. Obrigada pela oportunidade de trabalhar com você.

Durante minha estada na França eu tive a oportunidade de trabalhar com a Prof. Dra. Claudine Lacroix. Essa experiência foi enriquecedora para minha formação. Obrigada Prof. Dra. Claudine Lacroix pela atenção dispensada e pelo apoio. Também gostaria de agradecer ao Prof. Dr. Mairbek Chshiev, co-orientador desse trabalho

Obrigada aos meus amigos e familiares. Por sorte minha, precisaria de muitas páginas para escrever o nome de todos que me ajudaram, sendo assim não citarei nomes. A todos vocês que sabem que foram importantes, muito obrigada!

Ao Fillipe, que no período desta tese passou de namorado a noivo, e de noivo a esposo, eu agradeço pela paciência e pelo apoio. Nos momentos mais difíceis você foi indispensável. Obrigada por me acompanhar nessa tortuosa jornada, por entender a distância e pelas ótimas figuras feitas no Corel!

Por fim, eu agradeço aos meus pais, Ana Lucia e Gilson. Vocês são eternamente responsáveis por tudo de bom que eu faço. Vocês me dão força para superar meus medos e me apoiam incondicionalmente. Eu não somente agradeço, mas também dedico esse doutorado a vocês.

Acknowledgments

Thank CNPq and CAPES for the financing. I also thank the support of the international mobility of PhD students in *co-tutela* supervision given by the Région Rhône Alpes.

Thank the adviser of this thesis, Prof. Dr. Mucio Amado Continentino.

During the time I lived in France I had the opportunity to work with Prof. Dr. Claudine Lacroix. This experience was enriching for my training. Thank you Prof. Dr. Claudine Lacroix for your attention and support.

I also want to thank you Prof. Dr. Mairbek Chshiev, co-supervisor of this thesis.

I thank my family and friend.

Thank my husband, Fillipe.

Thank my parents, Ana Lucia e Gilson. This thesis is for you!

Abstract

In this thesis, we study some important problems related to the transport properties of many body systems. It is divided in three parts.

First we investigate the effect of dissipation and time - dependent external sources in the phase diagram of a superconducting film at zero and finite temperature. In the presence of time-dependent perturbations, dissipation is essential for the system to attain a steady, time independent state. In order to treat this time dependent problem, we use a Keldysh approach within an adiabatic approximation that allows us to study the phase diagram of this system as a function of the external parameters, including temperature. We also discuss the nature of the quantum phase transitions of the system.

Next, we study an important concept in the physics of metallic multi-band systems, that of hybridization, and how it affects the superconducting properties of a material. A constant or symmetric k -dependent hybridization in general acts in detriment of superconductivity. We show here that when hybridization between orbitals in different sites assumes an anti-symmetric character having odd-parity it *enhances* superconductivity. In chapter 3, we make use of the anti-symmetric property of hybridization to propose a new mechanism to generate Majorana fermions in a superconducting wire, even in the absence of spin-orbit interactions.

In the last part of this thesis we study the effect of spin-orbit coupling (SOC) on transport properties in magnetic nanostructures. In this system SOC plays an important role, because surfaces (or interfaces) introduce symmetry breaking which is a source of spin-orbit interaction. We study the role of Dzyaloshinskii-Moriya (DM) interaction on spin-transport in a 3 layer system. We show that there is a DM interaction between magnetic ions in the layers and spin of conduction electrons. We study the influence of this DM interaction on transport within a simple model where each layer is represented by a point.

Resumo

Nós estudamos alguns problemas relacionados as propriedades de transporte de sistemas de muitos corpos. Essa tese pode ser dividida em três partes, cada uma focada em um tópico específico. Os resultados obtidos ajudam a entender melhor os problemas aqui abordados.

Nós investigamos o efeito da dissipação e de fontes externas dependentes do tempo no diagrama de fase de um sistema a temperatura zero e finita. Na presença das perturbações dependentes do tempo, a dissipação é essencial para a obtenção de um estado estático independente do tempo. Para tratar esse problema, nós usamos o formalismo de Keldysh com uma aproximação adiabática. Isso nos permite estudar o diagrama de fase como função dos parâmetros do sistema e da temperatura. Nós também investigamos a natureza das transições de fases quânticas do sistema.

Depois, realizamos estudos sobre hibridização, um conceito importante na física de sistemas multi bandas. Uma hibridização constante ou simétrica em k atua destruindo as propriedades supercondutoras de um material. Nós mostramos aqui que se a hibridização possuir paridade ímpar, ela atua reforçando a supercondutividade. Nós estudamos um problema em que a hibridização anti-simétrica nos permite propor um novo sistema para estudar férmions de Majorana, mesmo da ausência de interações de spin-órbita.

Na última parte nós estudamos o efeito do acoplamento spin-órbita (SOC) nas propriedades de transporte em nano estruturas magnéticas. Nesses sistemas o SOC tem uma grande importância pois superfícies introduzem quebra de simetria, que é uma fonte do SOC. Mais especificamente, nós estudamos a interação de Dzyaloshinskii-Moriya (DM) no transporte de spin em um sistema de 3 camadas. Nós consideramos a interação de DM entre os íons magnéticos e os spins dos elétrons de condução. Nós propusemos um modelo simples para estudar como a interação de DM influencia o transporte de spin nesse sistema de 3 camadas.

Résumé

Nous étudions plusieurs problèmes reliés aux propriétés de transport dans les systèmes corrélés. La thèse contient 3 parties distinctes, chacune d'entre elles décrivant un aspect particulier. Nous avons obtenu dans chacun des cas des résultats qui permettent une meilleure compréhension du transport.

Nous étudions l'effet de la dissipation et d'une perturbation extérieure dépendant du temps sur le diagramme de phases d'un système à N corps à température nulle et à température finie. En présence de perturbation dépendant du temps, la dissipation joue un rôle important dans l'évolution vers un état stable indépendant du temps. Nous utilisons le formalisme de Keldysh dans l'approximation adiabatique qui permet d'étudier le diagramme de phases du système en fonction de paramètre et de la température.

Dans la 2^{ième} partie, nous étudions un concept important pour la physique des systèmes métalliques à plusieurs bandes, le concept d'hybridation, et la façon dont l'hybridation affecte la supraconductivité du métal. De façon générale, une hybridation dépendante ou non du vecteur d'onde k a tendance à détruire la supraconductivité. Nous montrons dans ce chapitre qu'une hybridation antisymétrique a l'effet inverse et renforce la supraconductivité. Nous montrons que si l'hybridation est antisymétrique, la supraconductivité a des propriétés non-triviales. Nous proposons que dans un tel système, il puisse exister des fermions de Majorana, même en l'absence de couplage spin-orbite.

Le dernier chapitre de la thèse porte sur les effets du couplage spin-orbite sur le transport dans les nanostructures magnétiques. Dans les nanostructures, le couplage spin-orbite joue un rôle important en raison de la brisure de symétrie à la surface ou aux interfaces. En particulier, nous étudions l'effet de l'interaction Dzyaloshinskii-Moriya (DM) sur le transport de spin dans un système tri-couche. Nous montrons qu'il existe une interaction DM entre les moments des couches et les électrons de conduction, et l'influence de cette interaction sur le transport est étudiée dans un modèle simplifié où chaque couche est représentée par un point.

Contents

Agradecimiento	i
Acknowledgments	ii
Abstract	iii
Resumo	iv
Résumé	v
1 Introduction	1
2 Dissipative and Non-equilibrium Effects Near a Superconductor-Metal Quantum Critical Point	5
2.1 Model	6
2.2 The Non-equilibrium Keldysh Formalism	8
2.3 Adiabatic Approximation	12
2.4 Zero-order Solution	17
2.4.1 Nature of the dissipation induced transition when $\vec{A} = \vec{0}$	22
2.5 First Order Approach	23
2.5.1 Zero Temperature Phase Diagram	27
2.5.2 Phase Diagram for $T \neq 0K$	32
2.6 Conclusions	32
3 Influence of an Odd-Parity Hybridization in the Superconducting State	35
3.1 Origin of an Odd-Parity Hybridization	36
3.2 Model	40
3.3 Calculations	42
3.3.1 Excitation Energies	46
3.3.2 Inter-band Order Parameter - Δ_{ab}	47
3.3.3 Intra-band Order Parameter - Δ_{bb}	49

3.3.4	Occupation Number	50
3.3.5	Induced Order Parameter - Δ_{aa}	52
3.4	Self Consistent Equations	54
3.5	Particular Case	55
3.5.1	Special Case I - $g_{bb} = 0$	55
3.5.2	Special Case II - $g_{ab} = 0$	58
3.6	Conclusion	60
4	Spin Current in the Presence of Dzyaloshinskii-Moriya Interaction	61
4.1	Introduction: Spin-Orbit Coupling (SOC)	62
4.2	Dzyaloshinskii-Moriya Interaction	63
4.3	DM Interaction between Magnetic Ions and Conduction Electrons	66
4.4	Model	70
4.4.1	Model I: Three Sites Problem for the study of interlayer DM	74
4.4.2	Model II: Two Sites Problem	76
4.5	Results and Discussion	79
4.5.1	Model I	79
4.5.2	Model II	84
4.5.3	Spin Accumulation	87
4.6	Perspective: A More Realistic Description	91
5	Conclusions and Perspectives	92
A	Adiabatic Expansion of Green's Function	94
B	Retarded Green's Function	96
C	Spin Orbit Coupling Induces p-wave Superconductors	98
D	List of Publications	103

List of Figures

2.1	Schematic picture of the system. Superconducting layer coupled to a metallic bath. The external electric field is applied only in the layer.	7
2.2	Mean-field critical line $\hat{T}_c(\Gamma)$ (full line) separating the normal and the superconducting phases, for $\lambda\nu = 0.25$. For convenience we used the variable $\hat{T} = eEv_F/\Gamma_c$ or $\hat{T} = (\Gamma/\Gamma_c)\hat{T}$. The dotted line, $\hat{T}_f \propto g ^\psi$, with $\psi = 1$ for $\Gamma/\Gamma_c < 1$, represents the expected shape of the critical line when fluctuations are included. The dashed line, $\hat{T}_x \propto g ^{\nu z}$, with $\nu z = 1$ is the crossover line separating the quantum critical from the quantum disordered, low field, regimes. The transition at $\Gamma = 0$, $\hat{T}_c = \Delta_0$ corresponding to the critical current in a dissipationless film (see text) appears in the variable \hat{T} at $\hat{T} = 0$	31
2.3	Finite temperature phase diagram T/Ω_{BCS} versus $\hat{T}_c/\Omega_{BCS} = eEv_F\tau/\Omega_{BCS}$ for fixed $\Gamma/\Gamma_c = 0.7$ and $\lambda\nu = 0.25$	33
3.1	Schematic picture of an inversion of coordinates in spherical coordinates.	37
3.2	We present here the solution of the two self-consistent equations for $\alpha = 0.5$ and $1/k_F a_s = -0.25$	57
3.3	We present here the solution of the two self-consistent equations for $\alpha = 0.5$ and two values of $1/k_F a_{sb}$: $1/k_F a_{sb} = -0.5$ and $1/k_F a_{sb} = -0.25$	59
4.1	DM interaction between two Fe (dark and light grey) ions mediated by a nearby oxygen ion (red). Red arrows represent two adjacent spins \vec{S}_i and \vec{S}_j lying in a plane (yellow). The DM coupling vector \vec{D} lies a different plane (blue), the orientation of which depends on local symmetry.	65
4.2	Site 1 is the magnetic site, site 2 corresponds to the conduction electron. In (a) is shown the superexchange process and in (b) the direct exchange one.	68

4.3	A physical system with three layers: two ferromagnetic layers (FL and FR) and a non-magnetic one (NM). Dzyaloshinskii-Moriya interaction is considered at both interfaces FL/NM and FR/NM	71
4.4	A schematic picture of the three sites approximation. \vec{S}_L represents the left (FL) and \vec{S}_R the right (FR) ferromagnetic layer. A non-magnetic layer is represented by the central site NM . Conduction electrons can travel on all sites.	72
4.5	This graphic shows the 4 energy levels in model II, the lowest one is represented by the blue curve. θ is the angle between the 2 spins \vec{S}_L and \vec{S}_R . Here, $J_0/t_{LR} = 0.5$, $ \vec{D}' /t_{LR} = 0.05$ and $\theta_D = \pi/4$	77
4.6	Model I: The x , y and z components of the spin current flowing from the left (L) to the right (R) site for occupation number of one electron. Parameters are: $J_0/\tau = 0.5$, $t_{LR}/\tau = 0.1$, $\theta_D = \pi/4$ and $V/\tau = 1$. Here, each line represents one value of $ \vec{D} /\tau$: Red thick line is $ \vec{D} /\tau = 0$, Blue dotted line is $ \vec{D} /\tau = 0.1$, Green dot dashed line is $ \vec{D} /\tau = 0.4$ and Black dotted line is $ \vec{D} /\tau = 1.0$	80
4.7	Model I: The x , y and z components of the spin current flowing from the left (L) to the central non-magnetic (NM) site for occupation number of one electron. Parameters are: $J_0/\tau = 0.5$, $t_{LR}/\tau = 0.1$, $\theta_D = \pi/4$ and $V/\tau = 1$. Here, each line represents one value of $ \vec{D} /\tau$: Red thick line is $ \vec{D} /\tau = 0$, Blue dotted line is $ \vec{D} /\tau = 0.1$, Green dot dashed line is $ \vec{D} /\tau = 0.4$ and Black dotted line is $ \vec{D} /\tau = 1.0$	81
4.8	Model I: The x , y and z components of the spin current flowing from the central non-magnetic (NM) to right (R) site for occupation number of one electron. Parameters are: $J_0/\tau = 0.5$, $t_{LR}/\tau = 0.1$, $\theta_D = \pi/4$ and $V/\tau = 1$. Here, each line represents one value of $ \vec{D} /\tau$: Red thick line is $ \vec{D} /\tau = 0$, Blue dotted line is $ \vec{D} /\tau = 0.1$, Green dot dashed line is $ \vec{D} /\tau = 0.4$ and Black dotted line is $ \vec{D} /\tau = 1.0$	82
4.9	Model I: The three components of spin current flowing from the left (L) to the right (R) site when the occupation is one electron. Parameters are: $J_0/\tau = 0.5$, $t_{LR}/\tau = 0.1$, $\theta_D = \pi/4$ and $ \vec{D} /J_0 = 1$. Here, each line represents one value of V/τ : Red line is $V/\tau = 5.0$, Blue dashed lines $V/\tau = 0$ and Green dot dashed line is $V/\tau = -5.0$	83

4.10	Model II - One Electron Occupation: The three components of the spin current. Parameters are: $J_0/t_{LR} = 0.5$ and $\theta_D = \pi/4$. Here, each line represents one value of $ \vec{D} /\tau$: Red thick line is $ \vec{D} /\tau = 0$, Blue dotted line is $ \vec{D} /\tau = 0.1$, Green dot dashed line is $ \vec{D} /\tau = 0.4$ and Black dotted line is $ \vec{D} /\tau = 1.0$	85
4.11	Model II - Two Electrons Occupation: The x , y and z components of spin current. Where $J_0/t_{LR} = 0.5$ and $\theta_D = \pi/4$. Here, each line represents one value of $ \vec{D} /\tau$: Red thick line is $ \vec{D} /\tau = 0$, Blue dotted line is $ \vec{D} /\tau = 0.1$, Green dot dashed line is $ \vec{D} /\tau = 0.4$ and Black dotted line is $ \vec{D} /\tau = 1.0$	86
4.12	Model I - This figure shows the spin accumulation in site L. Parameters are: $J_0/\tau = 0.5$, $t_{LR}/\tau = 0.1$, $\theta_D = \pi/4$ and $V/\tau = 1$. Here, each line represents one value of $ \vec{D} /\tau$: Red thick line is $ \vec{D} /\tau = 0$, Blue dotted line is $ \vec{D} /\tau = 0.1$, Green dot dashed line is $ \vec{D} /\tau = 0.4$ and Black dotted line is $ \vec{D} /\tau = 1.0$	88
4.13	Model I - The spin accumulation in site R. Parameters are: $J_0/\tau = 0.5$, $t_{LR}/\tau = 0.1$, $\theta_D = \pi/4$ and $V/\tau = 1$. Here, each line represents one value of $ \vec{D} /\tau$: Red thick line is $ \vec{D} /\tau = 0$, Blue dotted line is $ \vec{D} /\tau = 0.1$, Green dot dashed line is $ \vec{D} /\tau = 0.4$ and Black dotted line is $ \vec{D} /\tau = 1.0$	89
4.14	Model I - This figure shows the spin accumulation in site R. Parameters are: $J_0/\tau = 0.5$, $t_{LR}/\tau = 0.1$, $\theta_D = \pi/4$ and $V/\tau = 1$. Here, each line represents one value of $ \vec{D} /\tau$: Red thick line is $ \vec{D} /\tau = 0$, Blue dotted line is $ \vec{D} /\tau = 0.1$, Green dot dashed line is $ \vec{D} /\tau = 0.4$ and Black dotted line is $ \vec{D} /\tau = 1.0$	90
C.1	Schematic picture of how k -inversion affects ϕ	101

Chapter 1

Introduction

The quantum theory of many-particle systems is a powerful tool to understand the properties of real systems that deal with interacting particles. This theory enable us to solve the many-particle Schrödinger equation with interparticle potential through some special techniques, such as linear response [1], non-equilibrium Green's function method (Keldysh formalism) [2, 3], density functional theory (DFT) [4], etc. Among many-particle systems, we can mention some important problems as for example Bose-Einstein condensation (BEC), superconductivity, superfluity, etc [5]. The development of this field is crucial for the advance of electronics devices and also of sophisticated engineering instruments. Almost all new technological equipments, like cell phones, TVs, microscopes, lasers, etc., makes use of some properties of many-particle systems (magnetism, superconductivity). However there are still some open problems and behaviors not entirely understood in this field. Motived by this, we have studied some important problems related with transport properties of many body systems.

The superconductivity was discovered by H. Kamerlingh Onnes in 1911 [6]. A fundamental understanding of this phenomenon was only possible during the 1950's when Ginzburg and Landau proposed the phenomenological theory known as Ginzburg-Landau theory (1950) [7] and Bardeen, Cooper and Schrieffer proposed a microscopic BCS theory (1957) [8]. However, in 1986, Bednorz and Müller [9] discovered a new class of superconductors which, because of the basic microscopic mechanism, cannot be described by BCS theory. Until today there are many open problems with respect to the understanding of superconductivity and after more than 100 years after the discovery of superconductivity, this topic remains fascinating. In this thesis we devote two chapters to superconducting systems.

The first problem that we have investigated is presented in chapter 2. Motivated by the interest to understand decoherence that arises from the

coupling between nano-systems and the surrounding, we investigate the problem of a superconducting film submitted to a electric field, that gives rise to a time dependent vector potential in the Hamiltonian, that acts exclusively in the layer that is coupled to a metallic substrate. We study this problem near a superconductor-metal quantum critical point (QCP). The coupling between the superconducting layer and the bath is the source of dissipation that is related with decoherence. The behavior of nanomaterials under the action of external time-dependent perturbations is also an interesting problem. Here, the combination between the time-dependent perturbation and the dissipation is essential to attain a steady-state, time-independent situation. We explore the effects of dissipation and of an electric field on the phase diagram of the system.

The system proposed in this work was studied by others authors using phenomenological effective theories, like Landau theory using the non-equilibrium Schwinger round-trip Green's function formalism [10] and scaling arguments when there is no extrinsic dissipation [11]. Another work develop a fully microscopic derivation of the Keldysh effective theory using a mean-field treatment out of equilibrium [12]. Here we also use a non-equilibrium Keldysh approach [2, 3] and develop a formalism that allows to obtain the time dependence of the Green's functions necessary to calculate the superconducting order parameter, for an arbitrary time dependence of the vector potential under an adiabatic condition. The knowledge of these functions is fundamental in the time-dependent problem because, if the perturbation is strong enough, the ground state properties can be modified. Besides introducing the method, we will be mainly concerned with the phase diagram of the superconducting layer, and its modifications by dissipation and perturbation (the external applied electrical field introduced in the Hamiltonian by the time-dependent vector potential) in a steady state regime.

The nature of the phase transition in the presence of the time-dependent external perturbation it also examined here. However our method does not resort to the time dependent Landau-Ginzburg equation neither to Boltzmann's equation. To deal with this problem we introduce an alternative approach that allow us to include fluctuations to the zero order solution [13] (in our approach fluctuations only appear in first order solution). The big advantage to use this alternative approach is that we have now a full dynamic description of the quantum phase transition, so that we can write an effective action, at the Gaussian level, which describes this QCP. Thus we fully characterize the quantum critical point associated with the dissipation induced superconductor-normal metal transition.

In chapter 3 we focus on another important many body problem related with superconductivity. We investigate a two-band metal with an attractive

interaction between quasi-particles in different bands and an attractive intra-band interaction in one of these bands. The hybridization is assumed to be anti-symmetric. We show that the metal has non-trivial superconducting properties if the hybridization is anti-symmetric. The study of the effects of hybridization is quite common in literature since it can be easily controlled externally, by doping or applying pressure in the system [14, 15, 16]. In superconductors, for example, hybridization strongly affects the properties of a material and it can change the phase diagram on the superconductor. When hybridization is constant or has even-parity in k -space, it acts in detriment of superconductivity and can even destroy it at a superconducting quantum critical point (SQCP) [15, 17, 18]. However, the effect of an anti-symmetric hybridization is not a widely studied topic. We will dedicate chapter 3 to understand the effects of hybridization with odd-parity symmetry in the superconducting properties of multi-band systems.

Based on the work of Drzazga and Zipper [19], we discuss under which conditions the hybridization assumes an anti-symmetric character. We conclude that the odd-parity hybridization occurs when it mixes orbitals with different parities in neighboring lattice site, i.e., when the crystalline potential mixes orbitals with angular momentum l and $l + n$, where n is any odd number. There are some results in literature considering this anti-symmetric character in the hybridization [20, 21]. Here we studied the direct effect of the odd-parity hybridization in superconductivity properties. We calculate the order parameters and total occupation number in both strong and weak coupling regime and we find a remarkable result: the superconductivity is enhanced when the hybridization is anti-symmetric. This result opens new possibilities in the study of superconductors.

This anti-symmetric hybridization implies another important result. The combination of odd-parity hybridization and the proximity effect gives rise to attractive interactions in the originally non-interacting band. It is possible to calculate a parameter that we called “induced order parameter” and observe that, under certain conditions, it is proportional to the anti-symmetric hybridization, i.e., the spacial space part of the induced order parameter is anti-symmetric. This property is related with p -wave superconductivity [22]. Kitaev proposed a model for a p -wave superconducting chain that presents a non-trivial topological phase with Majorana fermions at its ends [23]. The combination between our results and the outcome of Kitaev allows us to propose a new mechanism to produce a Kitaev’s chain without the necessity of spin orbit coupling or an external magnetic field.

The *spintronics* is a relative new field in physics and also can be considered as a many-body problem. It emerges from some important discoveries in 1980’s, such as the observation of spin polarized electron injection from

a ferromagnetic metal to a normal metal [24] or the discovery of the giant magnetoresistance [25, 26]. Spintronics incorporates the electronic spin moment in the description of the system. It has a universal goal to develop a broad range of applications in electronics and nanoscale devices [27]. However to use all the potential of spintronics it is important to understand all possible effects that occurs in this process of miniaturization. The Spin Orbit Coupling (SOC), for example, is a small effect that plays an important role in magnetic nanostructures since space inversion symmetry is broken near surface and interfaces. For example, it was shown that spin-orbit coupling induces some changes of magneto-crystalline anisotropy [28] at surfaces and that Dzyaloshinskii-Moriya (DM) interactions exist near the surface [29]. We focus on the study of DM interaction and some consequences of this interaction in magnetic nanostructures.

The Dzyaloshinskii-Moriya [30, 31] interaction is driven by SOC and only appears in structures that lack inversion symmetry. In this thesis we considered a system composed by a non-magnetic layer between two ferromagnetic layers. At each interface breaking of symmetry occurs. We propose a very simple model where each layer is replaced by a site, taking account conduction electrons. On the magnetic sites, a classical spin represents the magnetization of the ferromagnetic layer while the non-magnetic site has only conduction electrons. Our purpose is to study the role of DM interaction on spin transport in this three-layer system. Usually, studies of SOC on transport is made by including Rashba interaction [32]. The effect of DM interaction has not been yet studied in this type of system.

Zarea *et al.* [33] have shown that DM interaction between magnetic ions and conduction electrons may exist. Based in this work, we can write the correct expression for the DM Hamiltonian and solve a three sites problem that represents the three layers system. Thus we can find the wave functions and solve the time-independent Schrödinger equation. Once the wave functions are well determined, we can calculate the spin current. We conclude that the DM interaction affects the spin current and should be taken account in nanostructures.

This work was done in four years, three years in CBPF - Brazil and the other one in Institute Néel - France. We studied this three problems and found some interesting new results, but there are still many issues to be studied in the three problems presented here. Thus in the last chapter we present our general conclusions and perspectives.

Chapter 2

Dissipative and Non-equilibrium Effects Near a Superconductor-Metal Quantum Critical Point

Recently with the advent of nanotechnology, great interest and effort have been devoted to the study of decoherence in nanosystems that arise from its coupling to the environment [34]. This coupling is also a crucial feature since it gives rise to dissipation. Due to the small sizes of the studied materials and consequently reduced degrees of freedom decoherence and dissipation, there are fundamental aspects that are going to determine their properties and eventual applications. Equally important is to understand the behavior of these nanomaterials under the action of external perturbations.

It turns out that, even in macroscopic many-body systems, if the strength of the perturbation is sufficiently strong, its ground state properties and phase diagram can be severely modified. If a physical system is subjected to a time-dependent perturbation, dissipation is essential to attain a steady-state, time-independent situation [35]. In this case, the non-equilibrium properties depend on the intensity of the perturbation and on how strong is the coupling of the system to the outside world.

Another important and substantial question concerns the nature of the phase transitions in non-equilibrium systems, both classical and quantum. In the quantum case, due to the entanglement of time and space dimensions, including dissipation, it is sometimes essential to give a correct description of the quantum critical phenomena.

It is important to emphasize that when we consider the effect of time dependent perturbations, beyond the regime of linear response, it is necessary

to appeal for more unconventional mathematical approaches in order to deal with the non-equilibrium situation, even in the steady state. In this case, there is a breakdown of the fluctuation-dissipation theorem [50] due to the explicit time dependence of the parameters in the Hamiltonian describing the system. The mathematical approach that we used in this work is the non-equilibrium Keldysh formalism [2, 3].

In the next sections we present in detail all progress we have made concerning this topic.

2.1 Model

We focus on a system consisting of a superconducting layer under the action of an external electric field, that arises from a time dependent vector potential that acts exclusively in the superconducting layer. The layer is coupled to a metallic substrate, representing a source of dissipation and allowing the perturbed system to attain a non-equilibrium steady state, time-independent situation. The microscopic mechanism for dissipation is the transfer of electrons between the two systems [36], the same type of coupling which gives rise to the proximity effect. We show in Fig. (2.1) a schematic picture of the system that we will study.

This system is described by the following Hamiltonian [12]

$$H = H_{layer} + H_{bath} + H_{bath-layer}, \quad (2.1)$$

where H_{layer} describes the two-dimensional (2D) superconductor whose physical properties we are interested in. H_{bath} takes into account the reservoir and $H_{bath-layer}$ in an obvious notation describes the coupling between the 2D superconductor and the bulk metal. This coupling represents a source for dissipation. Explicitly, these Hamiltonians are given by,

$$H_{layer} = \sum_{k,\sigma} \frac{1}{2m} \left(\frac{\vec{\nabla}}{i} - \frac{e}{\hbar c} \vec{A}(t) \right)^2 d_{k,\sigma}^\dagger d_{k,\sigma} - \lambda \sum_k d_{k,\uparrow}^\dagger d_{k,\downarrow}^\dagger d_{-k,\downarrow} d_{-k,\uparrow} \quad (2.2)$$

$$H_{bath} = \sum_{k_z k \sigma} \epsilon_{k_z, k, \sigma}^b c_{k_z, k, \sigma}^\dagger c_{k_z, k, \sigma}; \quad (2.3)$$

$$H_{bath-layer} = \sum_{k_z k \sigma} \left(t_z c_{k_z, k, \sigma}^\dagger d_{k, \sigma} + H.c. \right). \quad (2.4)$$

Notice that $c^{(\dagger)}$ and $d^{(\dagger)}$ are electron destruction (creation) operators in metallic bath and in superconductivity layer, respectively. The vector potential $\vec{A}(t) = -c\vec{E}t$ ($\hbar = 1$) gives rise to an electric field $\vec{E} = -1/c(\partial\vec{A}/\partial t)$ that acts

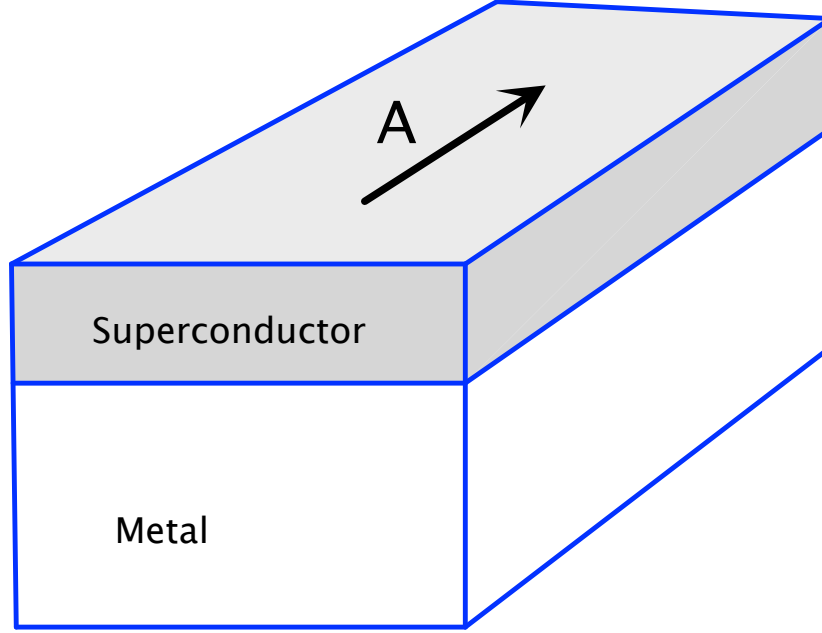


Figure 2.1: Schematic picture of the system. Superconducting layer coupled to a metallic bath. The external electric field is applied only in the layer.

only in the superconducting layer. The quantity $\epsilon_{k_z, k, \sigma}^b$ is the kinetic energy of the electrons in the metallic bath (substrate). Notice that $\vec{k} = (k_\perp, k_z)$ and for simplicity we write $k_\perp = k$. The coupling between the layer and substrate [Eq. (2.4)] has an intensity t_z and transfers electrons from the layer to the substrate and vice-versa. It does not conserve momentum since the superconductor is strictly 2D [37].

Applying a BCS decoupling to H_{layer} [8], we get

$$H_{layer} = \sum_{k, \sigma} \epsilon \left(k - \frac{e\vec{A}(t)}{\hbar c} \right) d_{k\sigma}^\dagger d_{k\sigma} - \frac{1}{2} \sum_k \left(\Delta_k d_{k\uparrow}^\dagger d_{-k\downarrow}^\dagger + H.c. \right), \quad (2.5)$$

where $k = k_\perp$ and

$$\Delta_k = \lambda \left\langle d_{k\uparrow}^\dagger d_{-k\downarrow}^\dagger \right\rangle \quad (2.6)$$

is the superconducting order parameter of the layer. This Hamiltonian has also been recently studied by Mitra [12].

The system considered above is a classical one in the study of superconductivity from both experimental and theoretical aspects. It has been treated

in the literature by many authors and at different times [36, 37, 38, 39, 40, 41, 42], always with renewed interest [10, 11, 12, 43, 44, 45, 46, 47]. As fabrication and experimental techniques improve, new aspects of this problem are revealed, requiring more sophisticated theoretical approaches. The present work introduces a novel theoretical treatment and focuses on the new aspects of quantum criticality in this paradigmatic system.

2.2 The Non-equilibrium Keldysh Formalism

Based on experience from previous works [48, 49], in this section we introduce the Keldysh formalism [2, 3] in order to obtain the normal and anomalous Green's functions, relevant to solve the problem. We use this type of formalism to deal with the explicit time dependence of the kinetic term in the Hamiltonian H_{layer} when the potential vector is present – remember that the potential vector is directly related to the electric field. A direct consequence of this time dependence is that the Green's function is now function of (t, t') and not of $(t - t')$, as in the case $\vec{A} = 0 \rightarrow \vec{E} = 0$.

We can define the time-dependent Green's functions according with the temporal evolution of operators as follows

$$\begin{aligned} G_{AB}^r(t, t') &= \langle\langle A(t)|B(t') \rangle\rangle^r = \theta(t - t')\langle[A(t), B(t')]_\eta\rangle, \\ G_{AB}^a(t, t') &= \langle\langle A(t)|B(t') \rangle\rangle^a = \theta(t' - t)\langle[A(t), B(t')]_\eta\rangle, \\ G_{AB}^<(t, t') &= \langle\langle A(t)|B(t') \rangle\rangle^< = \langle T_\eta A(t)B(t') \rangle, \end{aligned} \quad (2.7)$$

where r is the retarded component, a is the advanced component and $<$ is the lesser Green's function. We use the following definition:

$$\begin{aligned} [A(t), B(t')]_\eta &= A(t)B(t') - \eta B(t')A(t) \\ T_\eta A(t)B(t') &= \theta(t - t')A(t)B(t') + \eta\theta(t' - t)B(t')A(t), \end{aligned} \quad (2.8)$$

where $\eta = 1$ is used for bosons and $\eta = -1$ is for fermions. Here we deal with electrons, so we always assume $\eta = -1$.

The normal and anomalous Green's functions are given respectively by

$$G_L(t, t') \equiv \langle\langle d_{k\sigma}(t)|d_{k\sigma}^\dagger(t') \rangle\rangle, \quad (2.9)$$

$$\mathcal{F}(t, t') \equiv \langle\langle d_{-k-\sigma}^\dagger(t)|d_{k\sigma}^\dagger(t') \rangle\rangle, \quad (2.10)$$

where we follow the notation of Tyablikov [50]. In this definition $G_L(t, t')$ and $\mathcal{F}(t, t')$ can be r , a or $<$ components. We will specify in the future which of

these components are dealing according with the calculations. Notice that G_L is the Green's function related to the layer and \mathcal{F} is the anomalous Green's function related to the Cooper pairs involved with the superconducting state.

We use the equation of motion method [50] to write

$$i\hbar \frac{\partial}{\partial t} \langle \langle d_{k'\sigma'}(t) | d_{k'\sigma'}^\dagger(t') \rangle \rangle = \delta(t-t') \langle \{ d_{k'\sigma'}(t), d_{k'\sigma'}^\dagger(t') \} \rangle + \langle \langle [d_{k'\sigma'}(t), H] | d_{k'\sigma'}^\dagger(t') \rangle \rangle, \quad (2.11)$$

$$i\hbar \frac{\partial}{\partial t} \langle \langle d_{-k'-\sigma'}^\dagger(t) | d_{k'\sigma'}^\dagger(t') \rangle \rangle = \delta(t-t') \langle \{ d_{-k'-\sigma'}^\dagger(t), d_{k'\sigma'}^\dagger(t') \} \rangle + \langle \langle [d_{-k'-\sigma'}^\dagger(t), H], d_{k'\sigma'}^\dagger(t') \rangle \rangle. \quad (2.12)$$

By calculating the commutators (in Ref. [48] see the calculation of similar commutators in detail), we have

$$\begin{aligned} \left(i\hbar \frac{\partial}{\partial t} + \epsilon_k(t) \right) \mathcal{F}(t, t') &= -\Delta_k(t) G_L(t, t') - \sum_{k_z} t_z \langle \langle c_{k_z - k - \sigma'}^\dagger(t) | d_{k\sigma}^\dagger(t') \rangle \rangle, \\ \left(i\hbar \frac{\partial}{\partial t} - \epsilon_k(t) \right) G_L(t, t') &= \delta(t-t') - \Delta_k(t) \mathcal{F}(t, t') + \\ &\quad + \sum_{k_z} t_z^* \langle \langle c_{k_z k \sigma}(t) | d_{k\sigma}^\dagger(t') \rangle \rangle, \end{aligned}$$

where we defined

$$\epsilon \left(k - \frac{e\vec{A}(t)}{\hbar c} \right) \equiv \epsilon_k(t), \quad (2.13)$$

remember that $k = k_\perp$.

Notice that we generate two new Green's functions. We repeat the process and write the equation of motion for these two new Green's functions:

$$i\hbar \frac{\partial}{\partial t} \langle \langle c_{k'_z - k' - \sigma'}^\dagger(t) | d_{k'\sigma'}^\dagger(t') \rangle \rangle = \delta(t-t') \langle \{ c_{k'_z - k' - \sigma'}^\dagger(t), d_{k'\sigma'}^\dagger(t') \} \rangle + \langle \langle [c_{k'_z - k' - \sigma'}^\dagger(t), H] | d_{k'\sigma'}^\dagger(t') \rangle \rangle, \quad (2.14)$$

$$i\hbar \frac{\partial}{\partial t} \langle \langle c_{k'_z k' \sigma'}(t) | d_{k\sigma}^\dagger(t') \rangle \rangle = \delta(t-t') \langle \{ c_{k'_z k' \sigma'}(t), d_{k'\sigma'}^\dagger(t') \} \rangle + \langle \langle [c_{k'_z k' \sigma'}(t), H], d_{k'\sigma'}^\dagger(t') \rangle \rangle. \quad (2.15)$$

Or

$$\begin{aligned} \left(i\hbar \frac{\partial}{\partial t} + \epsilon_{k_z, k, \sigma}^b \right) \langle \langle c_{k_z - k - \sigma}^\dagger(t) | d_{k\sigma}^\dagger(t') \rangle \rangle &= -t_z^* \mathcal{F}(t, t'), \\ \left(i\hbar \frac{\partial}{\partial t} - \epsilon_{k_z, k, \sigma}^b \right) \langle \langle c_{k_z k\sigma}(t) | d_{k\sigma}^\dagger(t') \rangle \rangle &= t_z G_L(t, t'). \end{aligned}$$

where $\epsilon_{k_z, k, \sigma}^b$ is the kinetic energy of the electrons in the metallic bath.

In order to solve the system above, we need to introduce four auxiliary Green's functions through their equations of motion:

$$\left(i\hbar \frac{\partial}{\partial t} + \epsilon_{k_z, k, \sigma}^b \right) g_{k_z k\sigma}(t - t') \equiv \delta(t - t'), \quad (2.16)$$

$$\left(i\hbar \frac{\partial}{\partial t} - \epsilon_{k_z, k, \sigma}^b \right) g'_{k_z k\sigma}(t - t') \equiv \delta(t - t'), \quad (2.17)$$

$$\left(i\hbar \frac{\partial}{\partial t} + \epsilon_k(t) \right) F(t, t') \equiv \delta(t - t'), \quad (2.18)$$

$$\left(i\hbar \frac{\partial}{\partial t} - \epsilon_k(t) \right) g_L(t, t') \equiv \delta(t - t'). \quad (2.19)$$

Notice that this four Green's functions are the Green's functions of the decoupled bath [Eqs. (2.16) and (2.17)] and decoupled layer [Eqs. (2.18) and (2.19)]. Again we can use the definitions (2.7) and we will specify which function we are dealing in the calculations.

Using the following property of Green's function:

If we have two equation such that:

$$[\partial_t + A(t)] g(t, t') = \delta(t - t')$$

and

$$[\partial_t + A(t)] G(t, t') = h(t, t')$$

We have:

$$G(t, t') = \int dt_1 g(t, t_1) h(t_1, t').$$

We can write

$$\langle\langle c_{k_z-k-\sigma}^\dagger(t)|d_{k\sigma}^\dagger(t')\rangle\rangle = - \int dt_1 t_z^* g_{k_z k\sigma}(t, t_1) \mathcal{F}(t_1, t'), \quad (2.20)$$

$$\langle\langle c_{k_z k\sigma}(t)|d_{k\sigma}^\dagger(t')\rangle\rangle = \int dt_1 t_z g'_{k_z k\sigma}(t, t_1) G_L(t_1, t'), \quad (2.21)$$

$$\begin{aligned} \mathcal{F}(t, t') &= - \int dt_1 F(t, t_1) \Delta_k(t_1) G_L(t_1, t') - \\ &\quad - \sum_{k_z} t_z \int dt_1 F(t, t_1) \langle\langle c_{k_z-k-\sigma}^\dagger(t_1)|d_{k\sigma}^\dagger(t')\rangle\rangle, \end{aligned} \quad (2.22)$$

$$\begin{aligned} G_L(t, t') &= g_L(t, t') - \int dt_1 t_z^* g_L(t, t_1) \Delta_k(t_1) \mathcal{F}(t_1, t') + \\ &\quad + \sum_{k_z} t_z^* \int dt_1 g_L(t, t_1) \langle\langle c_{k_z k\sigma}(t_1)|d_{k\sigma}^\dagger(t')\rangle\rangle. \end{aligned} \quad (2.23)$$

Using the results above, we define two self-energies

$$\Sigma(t_1, t_2) = \sum_{k_z} |t_z|^2 g_{k_z k\sigma}(t_1, t_2), \quad (2.24)$$

$$\bar{\Sigma}(t_1, t_2) = \sum_{k_z} |t_z|^2 g'_{k_z k\sigma}(t_1, t_2). \quad (2.25)$$

Further on, we will assume that $\Sigma(t, t') = \bar{\Sigma}(t, t')$ Ref. [12]. This is equivalent, in reciprocal space, to $\rho(\omega) = \rho(-\omega)$, where $\rho(\omega)$ is the density of states of the metallic bath. This approach facilitates posterior calculations and does not significantly alter our results.

Once the self-energy is defined, we reduce our system to two equations that link anomalous and normal Green's functions,

$$\begin{aligned} \mathcal{F}(t, t') &= - \int dt_1 F(t, t_1) \Delta_k(t_1) G_L(t_1, t') + \\ &\quad + \int dt_1 \int dt_2 F(t, t_1) \Sigma(t_1, t_2) \mathcal{F}(t_2, t'), \end{aligned} \quad (2.26)$$

$$\begin{aligned} G_L(t, t') &= g_L(t, t') - \int dt_1 g_L(t, t_1) \Delta_k(t_1) \mathcal{F}(t_1, t') + \\ &\quad + \int dt_1 \int dt_2 g_L(t, t_1) \Sigma(t_1, t_2) G_L(t_2, t'). \end{aligned} \quad (2.27)$$

In the next section, we introduce an adiabatic approximation. This approximation will restrict our result to the limit of validity of the approach, and without this, it is impossible to continue our calculations.

2.3 Adiabatic Approximation

Before doing the approximation, it is convenient to write the functions according to other characteristic time of the problem. A convenient choice is to introduce a *slow time*: $(t + t')/2$ and a *fast time*: $t - t'$ [51], such that,

$$(t, t') \rightarrow \left(t - t', \frac{t + t'}{2} \right) = (t - t', \bar{t}).$$

In terms of this time scale, equations (2.26) and (2.27) become,

$$\begin{aligned} \mathcal{F}(t - t', \bar{t}) = & - \int dt_1 F \left(t - t_1, \frac{t + t_1}{2} \right) \Delta_k(t_1) G_L \left(t_1 - t', \frac{t_1 + t'}{2} \right) + \\ & + \int dt_1 \int dt_2 F \left(t - t_1, \frac{t + t_1}{2} \right) \Sigma \left(t_1 - t_2, \frac{t_1 + t_2}{2} \right) \mathcal{F} \left(t_2 - t', \frac{t_2 + t'}{2} \right), \end{aligned} \quad (2.28)$$

$$\begin{aligned} G_L(t - t', \bar{t}) = & g_L(t - t', \bar{t}) - \int dt_1 g_L \left(t - t_1, \frac{t + t_1}{2} \right) \Delta_k(t_1) \mathcal{F} \left(t_1 - t', \frac{t_1 + t'}{2} \right) \\ & + \int dt_1 \int dt_2 g_L \left(t - t_1, \frac{t + t_1}{2} \right) \Sigma \left(t_1 - t_2, \frac{t_1 + t_2}{2} \right) G_L \left(t_2 - t', \frac{t_2 + t'}{2} \right). \end{aligned} \quad (2.29)$$

Once we have distinguished between the fast and the slow time scales, we can implement an adiabatic approximation [51, 49] which, in our case, consists in taking into account terms up to the linear order in the variables associated with the slow time scale. The validity of this approximation requires the characteristic time associated with the change of the external parameter (the vector potential) to be large compared to the lifetime of an electron in the superconducting layer before it is scattered to the metallic substrate. Since the time derivative of the vector potential is related to the electric field, the adiabatic condition turns out to involve the electric field. This condition will be given and discussed in more details below.

Mathematically, the adiabatic approximation tells us how to expand the relevant Green's functions to linear order in deviation from the slow time scale up to first order,

$$G \left(t - t', \frac{t + t'}{2} \right) \approx G(t - t', t) + \left(\frac{t' - t}{2} \right) \frac{\partial}{\partial \bar{t}} G(t - t', \bar{t}) \Big|_{\bar{t}=t} + O[(\bar{t} - t)^2], \quad (2.30)$$

which is rewritten as,

$$G(t-t', t) = G^{(0)}(t-t', \bar{t}) + G^{(1)}(t-t', \bar{t}), \quad (2.31)$$

where the zeroth order term refers to equilibrium quantities and the first order terms refer to first corrections in slow time scale.

Using the expansion (2.30) in equations (2.28) and (2.29), up to linear order in the slow variable [In Appendix A we show how to process this expansion], we get,

$$\begin{aligned} \mathcal{F}(t-t', \bar{t}) = & - \int dt_1 \left[F(t-t_1, \bar{t}) \Delta_k(\bar{t}) G_L(t_1-t', \bar{t}) + \right. \\ & + \left(\frac{t_1-t}{2} \right) F(t-t_1, \bar{t}) \Delta_k(\bar{t}) \frac{\partial G_L}{\partial \bar{t}}(t_1-t', \bar{t}) + \\ & + (t'-t_1) F(t_1-\bar{t}, \bar{t}) \frac{\partial \Delta_k}{\partial \bar{t}}(\bar{t}) G_L(t_1-t', \bar{t}) + \\ & \left. + \left(\frac{t_1-t'}{2} \right) \frac{\partial F}{\partial \bar{t}}(t-t_1, \bar{t}) \Delta_k(\bar{t}) G_L(t_1-t', \bar{t}) \right] + \\ & + \int dt_1 \int dt_2 \left[F(t-t_1, \bar{t}) \Sigma(t_1-t_2, \bar{t}) \mathcal{F}(t_2-t', \bar{t}) + \right. \\ & + \left(\frac{t_1-t}{2} + \frac{t_2-t'}{2} \right) F(t-t_1, \bar{t}) \frac{\partial \Sigma}{\partial \bar{t}}(t_1-t_2, \bar{t}) \mathcal{F}(t_2-t', \bar{t}) + \\ & + \left(\frac{t_1-t'}{2} \right) \frac{\partial F}{\partial \bar{t}}(t-t_1, \bar{t}) \Sigma(t_1-t_2, \bar{t}) \mathcal{F}(t_2-t', \bar{t}) + \\ & \left. + \left(\frac{t_2-t}{2} \right) F(t-t_1, \bar{t}) \Sigma(t_1-t_2, \bar{t}) \frac{\partial \mathcal{F}}{\partial \bar{t}}(t_2-t', \bar{t}) \right] \end{aligned} \quad (2.32)$$

and

$$\begin{aligned}
G_L(t-t', \bar{t}) = & g_L(t-t', \bar{t}) - \int dt_1 \left[g_L(t-t_1, \bar{t}) \Delta_k(\bar{t}) \mathcal{F}(t_1-t', \bar{t}) + \right. \\
& + \left(\frac{t_1-t}{2} \right) g_L(t-t_1, \bar{t}) \Delta_k(\bar{t}) \frac{\partial \mathcal{F}}{\partial \bar{t}}(t_1-t', \bar{t}) + \\
& + (t'-t_1) g_L(t_1-\bar{t}, \bar{t}) \frac{\partial \Delta_k}{\partial \bar{t}}(\bar{t}) \mathcal{F}(t_1-t', \bar{t}) + \\
& \left. + \left(\frac{t_1-t'}{2} \right) \frac{\partial g_L}{\partial \bar{t}}(t-t_1, \bar{t}) \Delta_k(\bar{t}) \mathcal{F}(t_1-t', \bar{t}) \right] + \\
& + \int dt_1 \int dt_2 \left[g_L(t-t_1, \bar{t}) \Sigma(t_1-t_2, \bar{t}) G_L(t_2-t', \bar{t}) + \right. \\
& + \left(\frac{t_1-t}{2} + \frac{t_2-t'}{2} \right) g_L(t-t_1, \bar{t}) \frac{\partial \Sigma}{\partial \bar{t}}(t_1-t_2, \bar{t}) G_L(t_2-t', \bar{t}) + \\
& + \left(\frac{t_1-t'}{2} \right) \frac{\partial g_L}{\partial \bar{t}}(t-t_1, \bar{t}) \Sigma(t_1-t_2, \bar{t}) G_L(t_2-t', \bar{t}) + \\
& \left. + \left(\frac{t_2-t}{2} \right) g_L(t-t_1, \bar{t}) \Sigma(t_1-t_2, \bar{t}) \frac{\partial G_L}{\partial \bar{t}}(t_2-t', \bar{t}) \right].
\end{aligned} \tag{2.33}$$

Our next step is to do a Fourier transform in the *fast time*. We use the following definition for the Fourier transform [52]

$$h(\omega, \bar{t}) = \mathfrak{F} \left[h(t-t', \bar{t}) \right] = \int_{-\infty}^{\infty} d(t-t') e^{i\omega(t-t')} h(t-t', \bar{t}). \tag{2.34}$$

It is also important to remember the concept of convolution [52]:

$$(f * g)(x) = h(x) = \int_{-\infty}^{\infty} f(u)g(x-u)du. \tag{2.35}$$

Now, we can invoke the convolution theorem to write the Fourier transform of this new function $h(x)$

$$\mathfrak{F} [h(x)] = \mathfrak{F} [(f * g)(x)] = \mathfrak{F} [f(x)] \cdot \mathfrak{F} [g(x)]. \tag{2.36}$$

Equations (2.32) and (2.33) can be rewritten doing the Fourier transform

in fast time:

$$\begin{aligned}
\mathcal{F}(\omega, \bar{t}) = & - \left[F(\omega, \bar{t}) \Delta_k(\bar{t}) G_L(\omega, \bar{t}) - \frac{i}{2} \frac{\partial F}{\partial \omega}(\omega, \bar{t}) \Delta_k(\bar{t}) \frac{\partial G_L}{\partial \bar{t}}(\omega, \bar{t}) - \right. \\
& - \frac{i}{2} \frac{\partial F}{\partial \omega}(\omega, \bar{t}) \frac{\partial \Delta_k}{\partial \bar{t}}(\bar{t}) G_L(\omega, \bar{t}) + \frac{i}{2} F(\omega, \bar{t}) \frac{\partial \Delta_k}{\partial \bar{t}}(\bar{t}) \frac{\partial G_L}{\partial \omega}(\omega, \bar{t}) + \\
& \left. + \frac{i}{2} \frac{\partial F}{\partial \bar{t}}(\omega, \bar{t}) \Delta_k(\bar{t}) \frac{\partial G_L}{\partial \omega}(\omega, \bar{t}) \right] + F(\omega, \bar{t}) \Sigma(\omega, \bar{t}) \mathcal{F}(\omega, \bar{t}) - \\
& - \frac{i}{2} \frac{\partial F}{\partial \omega}(\omega, \bar{t}) \frac{\partial \Sigma}{\partial \bar{t}}(\omega, \bar{t}) \mathcal{F}(\omega, \bar{t}) + \frac{i}{2} F(\omega, \bar{t}) \frac{\partial \Sigma}{\partial \bar{t}}(\omega, \bar{t}) \frac{\partial \mathcal{F}}{\partial \omega}(\omega, \bar{t}) + \\
& + \frac{i}{2} \frac{\partial F}{\partial \bar{t}}(\omega, \bar{t}) \frac{\partial \Sigma}{\partial \omega}(\omega, \bar{t}) \mathcal{F}(\omega, \bar{t}) + \frac{i}{2} \frac{\partial F}{\partial \bar{t}}(\omega, \bar{t}) \Sigma(\omega, \bar{t}) \frac{\partial \mathcal{F}}{\partial \omega}(\omega, \bar{t}) - \\
& - \frac{i}{2} F(\omega, \bar{t}) \frac{\partial \Sigma}{\partial \omega}(\omega, \bar{t}) \frac{\partial \mathcal{F}}{\partial \bar{t}}(\omega, \bar{t}) - \frac{i}{2} \frac{\partial F}{\partial \omega}(\omega, \bar{t}) \Sigma(\omega, \bar{t}) \frac{\partial \mathcal{F}}{\partial \bar{t}}(\omega, \bar{t})
\end{aligned}$$

and

$$\begin{aligned}
G_L(\omega, \bar{t}) = & g_L(\omega, \bar{t}) - \left[g_L(\omega, \bar{t}) \Delta_k(\bar{t}) \mathcal{F}(\omega, \bar{t}) - \frac{i}{2} \frac{\partial g_L}{\partial \omega}(\omega, \bar{t}) \Delta_k(\bar{t}) \frac{\partial \mathcal{F}}{\partial \bar{t}}(\omega, \bar{t}) - \right. \\
& - \frac{i}{2} \frac{\partial g_L}{\partial \omega}(\omega, \bar{t}) \frac{\partial \Delta_k}{\partial \bar{t}}(\bar{t}) \mathcal{F}(\omega, \bar{t}) + \frac{i}{2} g_L(\omega, \bar{t}) \frac{\partial \Delta_k}{\partial \bar{t}}(\bar{t}) \frac{\partial \mathcal{F}}{\partial \omega}(\omega, \bar{t}) + \\
& \left. + \frac{i}{2} \frac{\partial g_L}{\partial \bar{t}}(\omega, \bar{t}) \Delta_k(\bar{t}) \frac{\partial \mathcal{F}}{\partial \omega}(\omega, \bar{t}) \right] + g_L(\omega, \bar{t}) \Sigma(\omega, \bar{t}) \mathcal{F}(\omega, \bar{t}) - \\
& - \frac{i}{2} \frac{\partial g_L}{\partial \omega}(\omega, \bar{t}) \frac{\partial \Sigma}{\partial \bar{t}}(\omega, \bar{t}) G_L(\omega, \bar{t}) + \frac{i}{2} g_L(\omega, \bar{t}) \frac{\partial \Sigma}{\partial \bar{t}}(\omega, \bar{t}) \frac{\partial G_L}{\partial \omega}(\omega, \bar{t}) + \\
& + \frac{i}{2} \frac{\partial g_L}{\partial \bar{t}}(\omega, \bar{t}) \frac{\partial \Sigma}{\partial \omega}(\omega, \bar{t}) G_L(\omega, \bar{t}) + \frac{i}{2} \frac{\partial g_L}{\partial \bar{t}}(\omega, \bar{t}) \Sigma(\omega, \bar{t}) \frac{\partial G_L}{\partial \omega}(\omega, \bar{t}) - \\
& - \frac{i}{2} g_L(\omega, \bar{t}) \frac{\partial \Sigma}{\partial \omega}(\omega, \bar{t}) \frac{\partial G_L}{\partial \bar{t}}(\omega, \bar{t}) - \frac{i}{2} \frac{\partial g_L}{\partial \omega}(\omega, \bar{t}) \Sigma(\omega, \bar{t}) \frac{\partial G_L}{\partial \bar{t}}(\omega, \bar{t}).
\end{aligned}$$

In Ref. [48], it is possible to see the transformation as done previously in detail. The two equations above can be further simplified:

$$\begin{aligned}
\mathcal{F} = & F \Sigma \mathcal{F} - F \Delta_k(\bar{t}) G_L + \frac{i}{2} \frac{\partial F}{\partial \omega} \frac{\partial}{\partial \bar{t}} [\Delta_k(\bar{t}) G_L] - \frac{i}{2} \frac{\partial}{\partial \bar{t}} [F \Delta_k(\bar{t})] \frac{\partial G_L}{\partial \omega} + \\
& + \frac{i}{2} \frac{\partial F}{\partial \bar{t}} \frac{\partial}{\partial \omega} [\Sigma \mathcal{F}] - \frac{i}{2} \frac{\partial}{\partial \omega} [F \Sigma] \frac{\partial \mathcal{F}}{\partial \bar{t}} - \frac{i}{2} \frac{\partial F}{\partial \omega} \frac{\partial \Sigma}{\partial \bar{t}} \mathcal{F} + \frac{i}{2} F \frac{\partial \Sigma}{\partial \bar{t}} \frac{\partial \mathcal{F}}{\partial \omega}
\end{aligned} \tag{2.37}$$

and

$$\begin{aligned}
G_L = & g_L - g_L \Delta_k(\bar{t}) \mathcal{F} + g_L \Sigma G_L + \frac{i}{2} \frac{\partial g_L}{\partial \omega} \frac{\partial}{\partial \bar{t}} [\Delta_k(\bar{t}) \mathcal{F}] - \frac{i}{2} \frac{\partial}{\partial \bar{t}} [g_L \Delta_k(\bar{t})] \frac{\partial \mathcal{F}}{\partial \omega} + \\
& + \frac{i}{2} \frac{\partial g_L}{\partial \bar{t}} \frac{\partial}{\partial \omega} [\Sigma G_L] - \frac{i}{2} \frac{\partial}{\partial \omega} [g_L \Sigma] \frac{\partial G_L}{\partial \bar{t}} - \frac{i}{2} \frac{\partial g_L}{\partial \omega} \frac{\partial \Sigma}{\partial \bar{t}} G_L + \frac{i}{2} g_L \frac{\partial \Sigma}{\partial \bar{t}} \frac{\partial G_L}{\partial \omega},
\end{aligned} \tag{2.38}$$

where we do not explicitly write the dependence on (ω, \bar{t}) , for simplicity.

Now, we use equation (2.31). This allows us to separate the Green's functions and the order parameter in two contributions, respectively, in zero order and first order in the slow variable \bar{t} :

$$\begin{aligned}
g_L(\omega, \bar{t}) &\approx g_L^{(0)}(\omega, \bar{t}=0) + g_L^{(1)}(\omega, \bar{t}), \\
F(\omega, \bar{t}) &\approx F^{(0)}(\omega, \bar{t}=0) + F^{(1)}(\omega, \bar{t}), \\
G_L(\omega, \bar{t}) &\approx G_L^{(0)}(\omega, \bar{t}=0) + G_L^{(1)}(\omega, \bar{t}), \\
\mathcal{F}(\omega, \bar{t}) &\approx \mathcal{F}^{(0)}(\omega, \bar{t}=0) + \mathcal{F}^{(1)}(\omega, \bar{t}), \\
\Delta_k(\bar{t}) &\approx \Delta_k^{(0)} + \Delta_k^{(1)}(\bar{t}).
\end{aligned} \tag{2.39}$$

Multiplying the terms and considering only terms up to the first order in $(t - t')$, we can write the contributions of zero and first order separately

$$\mathcal{F}^{(0)} = F^{(0)}\Sigma\mathcal{F}^{(0)} - F^{(0)}\Delta_k^{(0)}G_L^{(0)}, \tag{2.40}$$

where the functions \mathcal{F}^0, F^0 and Σ are only ω -dependent.

$$\begin{aligned}
\mathcal{F}^{(1)} &= F^{(0)}\Sigma\mathcal{F}^{(1)} + F^{(1)}\Sigma\mathcal{F}^{(0)} - F^{(0)}\Delta_k^{(1)}(\bar{t})G_L^{(0)} - \\
&\quad - F^{(1)}\Delta_k^{(0)}G_L^{(0)} - F^{(0)}\Delta_k^{(0)}G_L^{(1)} + \frac{i}{2}\frac{\partial F^{(0)}}{\partial\omega}\frac{\partial}{\partial\bar{t}}\left[\Delta_k^{(0)}G_L^{(0)}\right] - \\
&\quad - \frac{i}{2}\frac{\partial}{\partial\omega}\left[F^{(0)}\Sigma\right]\frac{\partial\mathcal{F}^{(0)}}{\partial\bar{t}} - \frac{i}{2}\frac{\partial F^{(0)}}{\partial\omega}\frac{\partial\Sigma}{\partial\bar{t}}\mathcal{F}^{(0)} + \frac{i}{2}F^{(0)}\frac{\partial\Sigma}{\partial\bar{t}}\frac{\partial\mathcal{F}^{(0)}}{\partial\omega} - \\
&\quad - \frac{i}{2}\frac{\partial}{\partial\bar{t}}\left[F^{(0)}\Delta_k^{(0)}\right]\frac{\partial G_L^{(0)}}{\partial\omega} + \frac{i}{2}\frac{\partial F^{(0)}}{\partial\bar{t}}\frac{\partial}{\partial\omega}\left[\Sigma\mathcal{F}^{(0)}\right].
\end{aligned} \tag{2.41}$$

where zero order contributions of Green's functions and self-energy are ω -dependent and first order contributions has dependence on (ω, \bar{t}) . And

$$G_L^{(0)} = g_L^{(0)} + g_L^{(0)}\Sigma G_L^{(0)} - g_L^{(0)}\Delta_k^{(0)}\mathcal{F}^{(0)}, \tag{2.42}$$

$$\begin{aligned}
G_L^{(1)} &= g_L^{(1)} + g_L^{(0)}\Sigma G_L^{(1)} + g_L^{(1)}\Sigma G_L^{(0)} - g_L^{(0)}\Delta_k^{(1)}(\bar{t})\mathcal{F}^{(0)} - \\
&\quad - g_L^{(1)}\Delta_k^{(0)}\mathcal{F}^{(0)} - g_L^{(0)}\Delta_k^{(0)}\mathcal{F}^{(1)} + \frac{i}{2}\frac{\partial g_L^{(0)}}{\partial\omega}\frac{\partial}{\partial\bar{t}}\left[\Delta_k^{(0)}\mathcal{F}^{(0)}\right] - \\
&\quad - \frac{i}{2}\frac{\partial}{\partial\omega}\left[g_L^{(0)}\Sigma\right]\frac{\partial G_L^{(0)}}{\partial\bar{t}} - \frac{i}{2}\frac{\partial g_L^{(0)}}{\partial\omega}\frac{\partial\Sigma}{\partial\bar{t}}G_L^{(0)} + \frac{i}{2}g_L^{(0)}\frac{\partial\Sigma}{\partial\bar{t}}\frac{\partial G_L^{(0)}}{\partial\omega} - \\
&\quad - \frac{i}{2}\frac{\partial}{\partial\bar{t}}\left[g_L^{(0)}\Delta_k^{(0)}\right]\frac{\partial\mathcal{F}^{(0)}}{\partial\omega} + \frac{i}{2}\frac{\partial g_L^{(0)}}{\partial\bar{t}}\frac{\partial}{\partial\omega}\left[\Sigma G_L^{(0)}\right],
\end{aligned} \tag{2.43}$$

remembering that the zero order Green's functions and the self-energy are ω -dependent and the first order functions depend on (ω, \bar{t}) .

In the next section, we will present the calculations considering terms of the same order separately.

2.4 Zero-order Solution

We shall consider first the zero order problem. At this level of approximation, the slow time is taken as fixed at an arbitrary time $\bar{t} = t_0$, which for simplicity we take as zero ($t_0 = 0$). This corresponds to taking the electric field as zero, such that, there is no explicit time dependence in the problem. We want to obtain the retarded, advanced and Keldysh (lesser) components of the Green's functions [5]. For the retarded and advanced Green's functions in zero order, we get:

$$\begin{cases} \mathcal{F}^{(0)r(a)} = F^{(0)r(a)} \Sigma^{r(a)} \mathcal{F}^{(0)r(a)} - \Delta_k^{(0)} F^{(0)r(a)} G_L^{(0)r(a)} \\ G_L^{(0)r(a)} = g_L^{(0)r(a)} - \Delta_k^{(0)} g_L^{(0)r(a)} \mathcal{F}^{(0)r(a)} + g_L^{(0)r(a)} \Sigma^{r(a)} G_L^{(0)r(a)}, \end{cases} \quad (2.44)$$

which are ω -dependent. Notice that we have a system of two equations and two unknown variables that can be easily solved:

$$\begin{aligned} \mathcal{F}^{(0)r(a)} &= -\frac{g_L^{(0)r(a)} F^{(0)r(a)} \Delta_k^{(0)}}{\left(1 - g_L^{(0)r(a)} \Sigma^{r(a)}\right) \left(1 - F^{(0)r(a)} \Sigma^{r(a)}\right) - \Delta_k^{(0)2} g_L^{(0)r(a)} F^{(0)r(a)}}, \\ G_L^{(0)r(a)} &= \frac{\left(1 - F^{(0)r(a)} \Sigma^{r(a)}\right) g_L^{(0)r(a)}}{\left(1 - g_L^{(0)r(a)} \Sigma^{r(a)}\right) \left(1 - F^{(0)r(a)} \Sigma^{r(a)}\right) - \Delta_k^{(0)2} g_L^{(0)r(a)} F^{(0)r(a)}}. \end{aligned} \quad (2.45)$$

Notice that F and g_L are defined in equations (2.18) and (2.19). By solving these two equations, we find the explicit expression for these two functions:

$$F^{(0)r(a)} = \frac{1}{\omega + \epsilon_k(\bar{t} = 0) \pm i\delta} \quad \text{and} \quad g_L^{(0)r(a)} = \frac{1}{\omega - \epsilon_k(\bar{t} = 0) \pm i\delta}, \quad (2.46)$$

where δ is an infinitesimal parameter, such that $\delta \rightarrow 0$. Substituting this result at (2.44), we write

$$\begin{aligned} \mathcal{F}^{(0)r(a)} &= -\frac{\Delta_k^{(0)}}{(\omega \pm i\delta - \Sigma^{r(a)})^2 - \epsilon_k^2(\bar{t} = 0) - \Delta_k^{(0)2}}, \\ G_L^{(0)r(a)} &= \frac{\omega \pm i\delta - \Sigma^{r(a)}}{(\omega \pm i\delta - \Sigma^{r(a)})^2 - \epsilon_k^2(\bar{t} = 0) - \Delta_k^{(0)2}}. \end{aligned} \quad (2.47)$$

Actually, we want to find the lesser component of the Green's function. This is related to the retarded and advanced components through the fluctuation-dissipation theorem [50]:

$$\begin{aligned}\mathcal{F}^{(<)}(\omega, \bar{t}) &= f(\omega) [\mathcal{F}^{(a)}(\omega, \bar{t}) - \mathcal{F}^{(r)}(\omega, \bar{t})], \\ G_L^{(<)}(\omega, \bar{t}) &= f(\omega) [G_L^{(a)}(\omega, \bar{t}) - G_L^{(r)}(\omega, \bar{t})],\end{aligned}\quad (2.48)$$

where $f(\omega)$ is the Fermi-Dirac distribution. This theorem is valid to any correlation function. Using this, we can conclude that

$$F^{(0)<} = 2\pi i f(\omega) \delta(\omega - \epsilon_k(\bar{t} = 0)) \quad \text{and} \quad g_L^{(0)<} = 2\pi i f(\omega) \delta(\omega + \epsilon_k(\bar{t} = 0)). \quad (2.49)$$

This result will be useful later.

The self-energy was defined by equation (2.39). We want to find an expression for this self-energy. First, we need the analytical expression for the function $g_{k_z k \sigma}$ defined by equation (2.16):

$$g_{k_z k \sigma}^{r(a)} = \mathcal{P} \left(\frac{1}{\omega + \epsilon_{k_z k \sigma}^b} \right) \mp i\pi \delta(\omega - \epsilon_{k_z k \sigma}^b).$$

The main part can be neglected and $\sum_k \delta(\omega - \epsilon_{k_z k \sigma}^b) = \rho(\omega)$, where $\rho(\omega)$ is the density of state of metallic bath. So, $\sum_{k_z k \sigma} g_{k_z k \sigma} \approx \mp i\pi \rho(\omega)$. Replacing this result in (2.24), we get

$$\Sigma^{r(a)}(\omega) = \mp i\pi |t_z|^2 \rho(\omega),$$

where $-$ is the retarded component and $+$ is the advanced one. We can replace the density of states by the density of states in the Fermi level: $\rho(E_F) = \nu$. So,

$$\Sigma^{r(a)} = \mp i\pi |t_z|^2 \rho(E_F).$$

Now, we will define

$$\Gamma \equiv \pi |t_z|^2 \rho(E_F), \quad (2.50)$$

and we can write the self-energy in a very common way

$$\Sigma^{r(a)}(\omega, \bar{t}) = \mp i \frac{\Gamma}{2}, \quad (2.51)$$

$$\Sigma^{<}(\omega, \bar{t}) = i f(\omega) \Gamma, \quad (2.52)$$

where we use the fluctuation-dissipation theorem to find the lesser component of the self-energy.

Now we have all the ingredients to calculate the lesser component of normal and anomalous Green's functions:

$$\mathcal{F}^{(0)<}(\omega, \bar{t} = 0) = -\frac{2if(\omega)\omega\Gamma\Delta_k^{(0)}}{\left(\omega^2 - \epsilon_k^2 - \Delta_k^{(0)2} - \Gamma^2/4\right)^2 + \omega^2\Gamma^2} \quad (2.53)$$

and

$$G_L^{(0)<}(\omega, \bar{t} = 0) = \frac{if(\omega)\Gamma\left(\omega^2 + \omega - \epsilon_k^2 - \Delta_k^{(0)2} + \Gamma^2/4\right)}{\left(\omega^2 - \epsilon_k^2 - \Delta_k^{(0)2} - \Gamma^2/4\right)^2 + \omega^2\Gamma^2}. \quad (2.54)$$

We are interested in obtaining the phase diagram of the system. We need to calculate $\Delta_k^{(0)}$ in order to find this diagram. We relate the gap equation for $\Delta_k^{(0)}$ to the anomalous correlation function throughout the relation:

$$\Delta_k^{(0)} = \sum_k \int \frac{\lambda}{2\pi i} \mathcal{F}^{(0)<}(\omega, \bar{t} = 0) d\omega. \quad (2.55)$$

So,

$$\Delta_k^{(0)} = \frac{1}{\pi} \sum_k \int d\omega \frac{f(\omega)\lambda\Delta_k^{(0)}}{4E_k} \left[\frac{\Gamma}{(\omega + E_k)^2 + \Gamma^2/4} - \frac{\Gamma}{(\omega - E_k)^2 + \Gamma^2/4} \right], \quad (2.56)$$

where $E_k \equiv \sqrt{\epsilon_k^2 + \Delta_k^{(0)2}}$.

Here, we will make a parenthesis to test the limit of $\Gamma \rightarrow 0$ from the above equation. We rewrite the equation (2.56) considering $\Delta_k^{(0)}$ independent of k , as follows

$$\frac{1}{\lambda} = \frac{1}{\pi} \sum_k \int d\omega \frac{f(\omega)}{4E_k} \left[\frac{\Gamma}{(\omega + E_k)^2 + \Gamma^2/4} - \frac{\Gamma}{(\omega - E_k)^2 + \Gamma^2/4} \right] \Bigg|_{\Gamma \rightarrow 0}.$$

$$\frac{1}{\lambda} = \frac{1}{\pi} \sum_k \int d\omega \frac{f(\omega)}{2E_k} [\delta(\omega - E_k) - \delta(\omega + E_k)]$$

$$\frac{1}{\lambda} = \frac{1}{\pi} \sum_k \frac{1}{2E_k} [f(-E_k) - f(E_k)].$$

The Fermi-Dirac distribution obeys the relation:

$$f(-E_k) - f(E_k) = \pi \tanh(\beta E_k/2).$$

So, we can write

$$\frac{1}{\lambda} = \sum_k \frac{1}{E_k} \tanh\left(\frac{\beta E_k}{2}\right), \quad (2.57)$$

where $\beta = 1/k_B T$ and k_B is the Boltzmann constant. This result is the usual equation for the transition temperature in mean field BCS theory [53].

Now, we go back to equation (2.56) and focus on the case of $T = 0K$. In this case, the Fermi-Dirac distribution is equal to 1 when $\omega \rightarrow [-\infty, \mu]$ and we can write

$$\Delta_k^{(0)} = \frac{1}{\pi} \sum_k \int_{-\infty}^{\mu} d\omega \frac{\lambda \Delta_k^{(0)}}{4E_k} \left[\frac{\Gamma}{(\omega + E_k)^2 + \Gamma^2/4} - \frac{\Gamma}{(\omega - E_k)^2 + \Gamma^2/4} \right]. \quad (2.58)$$

The significant events which occur near μ we need not integrate across the limit $[-\infty, \mu]$. It is enough to integrate a region $[\mu - \Omega_{BCS}, \mu + \Omega_{BCS}]$. We can consider, without loss of generality $\mu = 0$. This equation can be solved to yield the superconducting order parameter as a function of temperature and of the coupling to the metallic substrate through the damping parameter Γ .

$$\Delta_k^{(0)} = \frac{1}{\pi} \sum_k \frac{\lambda \Delta_k^{(0)}}{2E_k} \left[\arctan\left(\frac{\omega + E_k}{\Gamma/2}\right) - \arctan\left(\frac{\omega - E_k}{\Gamma/2}\right) \right] \Bigg|_{-\Omega_{BCS}}^{\Omega_{BCS}}. \quad (2.59)$$

We take $\Delta_k^{(0)}$ independent of k , i.e., $\Delta_k^{(0)} = \Delta^{(0)}$. So,

$$\frac{1}{\lambda} = \frac{1}{\pi} \sum_k \frac{1}{2E_k} \left[2 \arctan\left(\frac{E_k}{\Gamma/2}\right) - \arctan\left(\frac{\Omega_{BCS} + E_k}{\Gamma/2}\right) + \arctan\left(\frac{\Omega_{BCS} - E_k}{\Gamma/2}\right) \right]. \quad (2.60)$$

Now, we take the limit $\Omega_{BCS} \rightarrow \infty$

$$\frac{1}{\lambda} = \frac{1}{\pi} \sum_k \frac{1}{E_k} \arctan\left(\frac{E_k}{\Gamma/2}\right). \quad (2.61)$$

We can consider k continuous. This allows us to use the following transformation

$$\sum_k \rightarrow \frac{A}{2\pi} k_F \int_{k_F-\delta}^{k_F+\delta} dk, \quad (2.62)$$

where k_F is the 2D Fermi vector and $k_F = 2\pi\nu v_F/A$, being v_F the Fermi velocity and ν is the density of state in the Fermi level. So

$$\frac{1}{\lambda\nu} = \frac{v_F}{\pi} \int_{k_F-\delta}^{k_F+\delta} dk \frac{1}{E_k} \arctan\left(\frac{E_k}{\Gamma/2}\right), \quad (2.63)$$

from this equation we can find the phase diagram at $T = 0K$.

Finally, to find the critical coupling, Γ_c , we assume $\Delta^{(0)} = 0$. We also use that: $\epsilon_k = v_F(k - k_F)$:

$$\frac{1}{\lambda\nu} = \frac{1}{\pi} \int_{k_F-\delta}^{k_F+\delta} dk \frac{1}{k - k_F} \arctan\left(\frac{v_F(k - k_F)}{\Gamma_c/2}\right). \quad (2.64)$$

The solution of the integral (2.64) converges to a series of functions with the argument Ω_{BCS}/Γ_c . This series does not bring us much information about Γ_c . So, we will expand that series considering $\Omega_{BCS}/\Gamma \rightarrow \infty$:

$$\frac{1}{\lambda\nu} = \frac{1}{\pi} \left[-\pi \ln\left(\frac{\Gamma_c}{\Omega_{BCS}}\right) + 2\left(\frac{\Gamma_c}{\Omega_{BCS}}\right) + O\left(\frac{\Gamma_c}{\Omega_{BCS}}\right)^2 \right],$$

and we consider only the dominant term of expansion

$$\frac{1}{\lambda\nu} = \ln\left(\frac{\Omega_{BCS}}{\Gamma_c}\right), \quad (2.65)$$

where remember that ν is the density of state in the Fermi level. Considering that the gap in the 2D layer in equilibrium is $\Delta_0 = 2\Omega_{BCS}e^{-1/\lambda\nu}$ we can write

$$\Gamma_c = \frac{\Delta_0}{2}. \quad (2.66)$$

The result (2.66) coincide with the result obtained by Mitra [12]. This is expected because until here both description, in this thesis and Mitra's paper, is the same.

2.4.1 Nature of the dissipation induced transition when $\vec{A} = \vec{0}$

We have shown above that, for a sufficiently strong coupling between the layer and the normal substrate, superconductivity can be suppressed at a quantum critical point (QCP) at Γ_c . An important question, for which the mean-field approach above cannot give an appropriate answer, concerns the nature of this transition. Which is the universality class of the dissipation induced QCP and in particular, the value of its associated dynamic exponent z ?

To investigate this problem we need to include fluctuations to the zero order solution. For this purpose, we use an alternative approach which consists of calculating the response of the layer, in the absence of the vector potential, to a fictitious, frequency and wave-vector dependent field of intensity h that couples to the superconducting order parameter [13]. This response is given in terms of a generalized susceptibility $\chi(q, \omega)$, such that,

$$\delta\Delta_k^{(0)}(\omega) = \frac{\chi(q, \omega)}{1 - \lambda\chi(q, \omega)}h. \quad (2.67)$$

The condition

$$1 - \lambda\chi(q = 0, \omega = 0) = 0, \quad (2.68)$$

signals an instability to a homogeneous superconducting state, since $\Delta^{(0)}$ can be finite even in the absence of the fictitious field. On the other hand, considering the frequency and wave vector dependence of the generalized susceptibility amounts to take into account the fluctuations close to this instability.

The quantity $\chi(q, \omega)$ is the q-dependent dynamic pair susceptibility [54] of the layer, that we generalize here to include a finite lifetime of the quasi-particles in the normal phase. It is given by:

$$\chi(q, \omega) = \frac{1}{2} \sum_k \left[\frac{\tanh(\beta\epsilon_k/2)}{\epsilon_{k+q} + \epsilon_k - (\omega + i\tau_{SC}^{-1}/2)} + \frac{\tanh(\beta\epsilon_k/2)}{\epsilon_{k-q} + \epsilon_k - (\omega + i\tau_{SC}^{-1}/2)} \right], \quad (2.69)$$

where $\beta = (k_B T)^{-1}$. Dissipation is included in the term $i\tau_{SC}^{-1}$. We take $\tau_{SC} = \tau = \Gamma^{-1}$ which is the lifetime of the quasi-particles in the layer due to the coupling with the metallic substrate.

When $T = 0$ and close to $q = 0$ and $\omega = 0$, we can calculate this susceptibility and obtain:

$$\chi(q \approx 0, \omega \approx 0) = \frac{\nu}{4} \ln \left(\frac{\Omega_{BCS}^4}{\Gamma^4} \right) - \frac{\nu(qv_F)^2}{2\Gamma^2} + i \frac{\nu\omega}{\Gamma}. \quad (2.70)$$

Notice that the relevant wave-vector to expand is near $q = 0$ since we are interested in an instability to a uniform superconducting state. The Thouless condition $1 - \lambda \Re \chi(q = 0, \omega = 0) = 0$ yields,

$$\frac{1}{\lambda \nu} = \ln \left(\frac{\Omega_{BCS}}{\Gamma_c} \right), \quad (2.71)$$

which coincides with Eq. (2.65) obtained previously. Consequently, the present approach that incorporates the finite lifetime of the quasi-particles in the layer through the dynamic pair susceptibility yields the same dissipation induced quantum critical point obtained previously. The advantage, of course, is that we have now a full dynamic description of the quantum phase transition. Following the approach of Hertz [35], we can write an effective action, at the Gaussian level, which describes this QCP,

$$S = \int dq \int d\omega \left[\left(\frac{\Gamma - \Gamma_c}{\Gamma_c} \right) + \frac{(qv_F)^2}{2\Gamma^2} + \frac{|\omega|}{\Gamma} \right] |\Delta^{(0)}(q, \omega)|^2, \quad (2.72)$$

where $\Gamma_c = \Delta_0/2$ as before. The dynamic exponent turns out to be $z = 2$ and the effective dimension of the QCP, $d_{eff} = d + z = 4$ [55]. Then, the quantum normal-to-superconductor phase transition in the layer when its coupling to the metallic substrate is reduced occurs at the upper critical dimension $d_c = 4$, in which case logarithmic corrections to the Gaussian or mean-field critical behavior are expected.

2.5 First Order Approach

Let us now consider the first order terms of the Green's functions and of the order parameter. First, we notice that due to the time re-parametrization, we can show that

$$g^r(t, t') = -\frac{i}{\hbar} \theta(t - t') \exp \left[-\frac{i}{\hbar} \int_{t'}^t dt_1 \epsilon_k(t_1) \right].$$

Solving the integration expanding $\epsilon_k(t_1)$ near $\bar{t} \rightarrow \epsilon_k(t_1) \approx \epsilon_k(\bar{t}) + (t_1 - \bar{t}) \dot{\epsilon}_k(\bar{t})$

$$\begin{aligned}
\int_{t'}^t dt_1 \epsilon_k(t_1) &= \int_{t'}^t [\epsilon_k(\bar{t}) + (t_1 - \bar{t}) \dot{\epsilon}_k(\bar{t})] \\
&= t_1 \epsilon_k(\bar{t}) + \frac{t_1^2}{2} \dot{\epsilon}_k(\bar{t}) - \bar{t} t_1 \dot{\epsilon}_k(\bar{t}) + O(\ddot{\epsilon}_k) \Big|_{t'}^t \\
&= (t - t') \epsilon_k(\bar{t}) + \left(\frac{t^2 - t'^2}{2} \right) \dot{\epsilon}_k(\bar{t}) - \bar{t} (t - t') \dot{\epsilon}_k(\bar{t}) + O(\ddot{\epsilon}_k) \\
&= (t - t') \epsilon_k(\bar{t}) + \left(\frac{t^2 - t'^2}{2} \right) \dot{\epsilon}_k(\bar{t}) - \left(\frac{t^2 - t'^2}{2} \right) \dot{\epsilon}_k(\bar{t}) + O(\ddot{\epsilon}_k) \\
&= (t - t') \epsilon_k(\bar{t}) + O(\ddot{\epsilon}_k), \tag{2.73}
\end{aligned}$$

this procedure can be repeated for all components: retarded, advanced and lesser. So we can affirm that $F^{(1)} = g_L^{(1)} = 0$. Using this simplification and the Langreth rule ¹ [56] to write the advanced and retarded component of anomalous and normal Green's function, we find

$$\begin{aligned}
\boxed{\mathcal{F}^{(1)r(a)}} &= F^{(0)r(a)} \Sigma^{r(a)} \mathcal{F}^{(1)r(a)} - F^{(0)r(a)} \Delta_k^{(1)}(\bar{t}) G_L^{(0)r(a)} + \\
&+ \frac{i}{2} \frac{\partial F^{(0)r(a)}}{\partial \omega} \frac{\partial}{\partial \bar{t}} \left[\Delta_k^{(0)} G_L^{(0)r(a)} \right] - \frac{i}{2} \frac{\partial}{\partial \omega} \left[F^{(0)r(a)} \Sigma^{r(a)} \right] \frac{\partial \mathcal{F}^{(0)r(a)}}{\partial \bar{t}} - \\
&- \frac{i}{2} \frac{\partial}{\partial \bar{t}} \left[F^{(0)r(a)} \Delta_k^{(0)} \right] \frac{\partial G_L^{(0)r(a)}}{\partial \omega} + \frac{i}{2} \frac{\partial F^{(0)r(a)}}{\partial \bar{t}} \frac{\partial}{\partial \omega} \left[\Sigma^{r(a)} \mathcal{F}^{(0)r(a)} \right] - \\
&- \frac{i}{2} \frac{\partial F^{(0)r(a)}}{\partial \omega} \frac{\partial \Sigma^{r(a)}}{\partial \bar{t}} \mathcal{F}^{(0)r(a)} + \frac{i}{2} F^{(0)r(a)} \frac{\partial \Sigma^{r(a)}}{\partial \bar{t}} \frac{\partial \mathcal{F}^{(0)r(a)}}{\partial \omega} - \\
&- F^{(0)r(a)} \Delta_k^{(0)} \boxed{G_L^{(1)r(a)}} \tag{2.74}
\end{aligned}$$

and

$$\begin{aligned}
\boxed{G_L^{(1)r(a)}} &= g_L^{(0)r(a)} \Sigma^{r(a)} G_L^{(1)r(a)} - g_L^{(0)r(a)} \Delta_k^{(1)}(\bar{t}) \mathcal{F}^{(0)r(a)} + \\
&+ \frac{i}{2} \frac{\partial g_L^{(0)r(a)}}{\partial \omega} \frac{\partial}{\partial \bar{t}} \left[\Delta_k^{(0)} \mathcal{F}^{(0)r(a)} \right] - \frac{i}{2} \frac{\partial}{\partial \omega} \left[g_L^{(0)r(a)} \Sigma^{r(a)} \right] \frac{\partial G_L^{(0)r(a)}}{\partial \bar{t}} - \\
&- \frac{i}{2} \frac{\partial}{\partial \bar{t}} \left[g_L^{(0)r(a)} \Delta_k^{(0)} \right] \frac{\partial \mathcal{F}^{(0)r(a)}}{\partial \omega} + \frac{i}{2} \frac{\partial g_L^{(0)r(a)}}{\partial \bar{t}} \frac{\partial}{\partial \omega} \left[\Sigma^{r(a)} G_L^{(0)r(a)} \right] - \\
&- \frac{i}{2} \frac{\partial g_L^{(0)r(a)}}{\partial \omega} \frac{\partial \Sigma^{r(a)}}{\partial \bar{t}} G_L^{(0)r(a)} + \frac{i}{2} g_L^{(0)r(a)} \frac{\partial \Sigma^{r(a)}}{\partial \bar{t}} \frac{\partial G_L^{(0)r(a)}}{\partial \omega} - \\
&- g_L^{(0)r(a)} \Delta_k^{(0)} \boxed{\mathcal{F}^{(1)r(a)}}. \tag{2.75}
\end{aligned}$$

¹Langreth rule to find advanced and retarded correlation function is very simple: $A = \int_c BCD \rightarrow A^{r(a)} = \int_t B^{r(a)} C^{r(a)} D^{r(a)}$. As we will show below, this is not the case for the lesser Green's function.

Again, we have a system of equations. The terms highlighted are the unknown variables of the system of equations. This system is much more complicated to solve, but it is feasible. We show the solutions in Appendix B. We will not write the result of the system because later we will study some specific limits of these equations.

We will use the Langreth rules [56] to find the lesser component of normal and anomalous Green's function. We can summarize these rules for two functions

$$C = \int_c AB \rightarrow C^< = \int_t A^r B^< + A^< B^a \quad (2.76)$$

and in the case of three functions

$$D = \int_c ABC \rightarrow D^< = \int_t A^r B^r C^< + A^r B^< C^a + A^< B^a C^a. \quad (2.77)$$

It is important to remember that now we are dealing with the time dependent part of the problem. So, we can not use the fluctuation-dissipation theorem.

Applying the rule described below, we have

$$\begin{aligned} \boxed{\mathcal{F}^{(1)<}} &= F^{(0)r\Sigma^<} \mathcal{F}^{(1)a} + F^{(0)<\Sigma^a} \mathcal{F}^{(1)a} - F^{(0)r} \Delta_k^{(1)}(\bar{t}) G_L^{(0)<} - \\ &- F^{(0)<\Delta_k^{(1)}(\bar{t})} G_L^{(0)a} - F^{(0)r} \Delta_k^{(0)} \boxed{G_L^{(1)<}} + F^{(0)r} \Sigma^r \boxed{\mathcal{F}^{(1)<}} - \\ &- F^{(0)<\Delta_k^{(0)}} G_L^{(1)a} + \frac{i}{2} \frac{\partial F^{(0)r}}{\partial \omega} \frac{\partial}{\partial \bar{t}} \left(\Delta_k^{(0)} G_L^{(0)<} \right) + \\ &+ \frac{i}{2} \frac{\partial F^{(0)<}}{\partial \omega} \frac{\partial}{\partial \bar{t}} \left(\Delta_k^{(0)} G_L^{(0)a} \right) - \frac{i}{2} \frac{\partial}{\partial \omega} (F^{(0)r} \Sigma^r) \frac{\partial \mathcal{F}^{(0)<}}{\partial \bar{t}} - \\ &- \frac{i}{2} \frac{\partial}{\partial \omega} (F^{(0)r} \Sigma^<) \frac{\partial \mathcal{F}^{(0)a}}{\partial \bar{t}} - \frac{i}{2} \frac{\partial}{\partial \omega} (F^{(0)<\Sigma^a}) \frac{\partial \mathcal{F}^{(0)a}}{\partial \bar{t}} - \\ &- \frac{i}{2} \frac{\partial}{\partial \bar{t}} \left(F^{(0)r} \Delta_k^{(0)} \right) \frac{\partial G_L^{(0)<}}{\partial \omega} - \frac{i}{2} \frac{\partial}{\partial \bar{t}} \left(F^{(0)<\Delta_k^{(0)}} \right) \frac{\partial G_L^{(0)a}}{\partial \omega} + \\ &+ \frac{i}{2} \frac{\partial F^{(0)r}}{\partial \bar{t}} \frac{\partial}{\partial \omega} (\Sigma^r \mathcal{F}^{(0)<}) + \frac{i}{2} \frac{\partial F^{(0)r}}{\partial \bar{t}} \frac{\partial}{\partial \omega} (\Sigma^< \mathcal{F}^{(0)a}) + \\ &+ \frac{i}{2} \frac{\partial F^{(0)<}}{\partial \bar{t}} \frac{\partial}{\partial \omega} (\Sigma^a \mathcal{F}^{(0)a}) - \frac{i}{2} \frac{\partial F^{(0)r}}{\partial \omega} \frac{\partial \Sigma^r}{\partial \bar{t}} \mathcal{F}^{(0)<} - \\ &- \frac{i}{2} \frac{\partial F^{(0)r}}{\partial \omega} \frac{\partial \Sigma^<}{\partial \bar{t}} \mathcal{F}^{(0)a} - \frac{i}{2} \frac{\partial F^{(0)<}}{\partial \omega} \frac{\partial \Sigma^a}{\partial \bar{t}} \mathcal{F}^{(0)a} + \\ &+ \frac{i}{2} F^{(0)r} \frac{\partial \Sigma^r}{\partial \bar{t}} \frac{\partial \mathcal{F}^{(0)<}}{\partial \omega} + \frac{i}{2} F^{(0)r} \frac{\partial \Sigma^<}{\partial \bar{t}} \frac{\partial \mathcal{F}^{(0)a}}{\partial \omega} + \frac{i}{2} F^{(0)<} \frac{\partial \Sigma^a}{\partial \bar{t}} \frac{\partial \mathcal{F}^{(0)a}}{\partial \omega} \end{aligned} \quad (2.78)$$

and

$$\begin{aligned}
\boxed{G_L^{(1)<}} &= g_L^{(0)r} \Sigma^< G_L^{(1)a} + g_L^{(0)<} \Sigma^a G_L^{(1)a} - g_L^{(0)r} \Delta_k^{(1)}(\bar{t}) \mathcal{F}^{(0)<} - \\
&- g_L^{(0)<} \Delta_k^{(1)}(\bar{t}) \mathcal{F}^{(0)a} - g_L^{(0)r} \Delta_k^{(0)} \boxed{\mathcal{F}^{(1)<}} + g_L^{(0)r} \Sigma^r \boxed{G_L^{(1)<}} - \\
&- g_L^{(0)<} \Delta_k^{(0)} \mathcal{F}^{(1)a} + \frac{i}{2} \frac{\partial g_L^{(0)r}}{\partial \omega} \frac{\partial}{\partial \bar{t}} \left(\Delta_k^{(0)} \mathcal{F}^{(0)<} \right) + \\
&+ \frac{i}{2} \frac{\partial g_L^{(0)<}}{\partial \omega} \frac{\partial}{\partial \bar{t}} \left(\Delta_k^{(0)} \mathcal{F}^{(0)a} \right) - \frac{i}{2} \frac{\partial}{\partial \omega} \left(g_L^{(0)r} \Sigma^r \right) \frac{\partial G_L^{(0)<}}{\partial \bar{t}} - \\
&- \frac{i}{2} \frac{\partial}{\partial \omega} \left(g_L^{(0)r} \Sigma^< \right) \frac{\partial G_L^{(0)a}}{\partial \bar{t}} - \frac{i}{2} \frac{\partial}{\partial \omega} \left(g_L^{(0)<} \Sigma^a \right) \frac{\partial G_L^{(0)a}}{\partial \bar{t}} - \\
&- \frac{i}{2} \frac{\partial}{\partial \bar{t}} \left(g_L^{(0)r} \Delta_k^{(0)} \right) \frac{\partial \mathcal{F}^{(0)<}}{\partial \omega} - \frac{i}{2} \frac{\partial}{\partial \bar{t}} \left(g_L^{(0)<} \Delta_k^{(0)} \right) \frac{\partial \mathcal{F}^{(0)a}}{\partial \omega} + \\
&+ \frac{i}{2} \frac{\partial g_L^{(0)r}}{\partial \bar{t}} \frac{\partial}{\partial \omega} \left(\Sigma^r G_L^{(0)<} \right) + \frac{i}{2} \frac{\partial g_L^{(0)r}}{\partial \bar{t}} \frac{\partial}{\partial \omega} \left(\Sigma^< G_L^{(0)a} \right) + \\
&+ \frac{i}{2} \frac{\partial g_L^{(0)<}}{\partial \bar{t}} \frac{\partial}{\partial \omega} \left(\Sigma^a G_L^{(0)a} \right) - \frac{i}{2} \frac{\partial g_L^{(0)r}}{\partial \omega} \frac{\partial \Sigma^r}{\partial \bar{t}} G_L^{(0)<} - \\
&- \frac{i}{2} \frac{\partial g_L^{(0)r}}{\partial \omega} \frac{\partial \Sigma^<}{\partial \bar{t}} G_L^{(0)a} - \frac{i}{2} \frac{\partial g_L^{(0)<}}{\partial \omega} \frac{\partial \Sigma^a}{\partial \bar{t}} G_L^{(0)a} + \\
&+ \frac{i}{2} g_L^{(0)r} \frac{\partial \Sigma^r}{\partial \bar{t}} \frac{\partial G_L^{(0)<}}{\partial \omega} + \frac{i}{2} g_L^{(0)r} \frac{\partial \Sigma^<}{\partial \bar{t}} \frac{\partial G_L^{(0)a}}{\partial \omega} + \frac{i}{2} g_L^{(0)<} \frac{\partial \Sigma^a}{\partial \bar{t}} \frac{\partial G_L^{(0)a}}{\partial \omega}.
\end{aligned} \tag{2.79}$$

Equations (2.78) and (2.79) form a closed set of equations where the high-lighted terms need to be determined.

The first order contribution to the order parameter $\Delta_k^{(1)}$ is obtained from the equation:

$$\Delta_k^{(1)}(\bar{t}) = \lambda \sum_k \int \frac{1}{2\pi i} \mathcal{F}^{(1)<}(\omega, \bar{t}) d\omega. \tag{2.80}$$

The equations above provide a fully self-consistent solution for the time dependent order parameter in the adiabatic approximation for an arbitrary time dependence of the vector potential. It can be obtained numerically, as a function of temperature and of the electric field.

Now that we will introduce the lifetime τ of the electrons in the layer, we can discuss and obtain the adiabatic condition under which the results above are valid. The relevant time scales to be compared are the electronic lifetime τ and the characteristic time associated with the time variation of the vector potential ($\propto (\partial \vec{A} / \partial t)^{-1}$) in the layer. This adiabatic condition

requires that the time variation of the vector potential is much slower than the relaxation time of the electrons. Mathematically, this implies that the first order adiabatic corrections that involve the time and frequency derivatives of all quantities appearing in the expression for the lesser Green's function $\mathcal{F}^{(1)<}$ are small compared to the zero order terms. Ultimately, due to the equality $\vec{E} = (-1/c)\partial\vec{A}/\partial t$, the adiabatic condition involves a constraint on the electric field in the film. This implies that the time variation of the potential is slow compared to the characteristic relaxation time of the electrons in the layer and guarantees that the first order correction is small with respect to the zeroth order term.

In the next section, using the first order correction for the order parameter, we calculate the phase diagram of the dissipative superconducting film under the action of the electric field when the system has reached a steady state regime. In this stationary regime, the properties of the system remain unchanged in time and the time \bar{t} can be replaced by the lifetime τ of the electrons in the layer ($\bar{t} = \tau = 1/\Gamma$). This is the actual time the current carriers remain under the action of the electric field before being scattered to different quasi-particle states.

2.5.1 Zero Temperature Phase Diagram

In order to obtain the quantum critical points and critical lines separating the normal and superconducting phases, we take $\Delta_k = \Delta_k^{(0)} + \Delta_k^{(1)} = 0$ and $T = 0$. Here Δ_k is the actual (measurable) value of the order parameter in the presence of the electric field, under the conditions of validity of the first order adiabatic approximation. We take initially $\Delta_k^{(0)} = 0$ and $T = 0K$:

$$\begin{aligned}
\mathcal{F}^{(1)<} = & F^{(0)r}\Sigma^<\mathcal{F}^{(1)a} - F^{(0)<}\Sigma^r\mathcal{F}^{(1)a} - F^{(0)r}\Delta_k^{(1)}(\bar{t})G_L^{(0)<} - \\
& - F^{(0)<}\Delta_k^{(1)}G_L^{(0)a} + F^{(0)r}\Sigma^r\mathcal{F}^{(1)<} - \frac{i}{2}\frac{\partial F^{(0)r}}{\partial\omega}\Sigma^r\frac{\partial\mathcal{F}^{(0)<}}{\partial\bar{t}} - \\
& - \frac{i}{2}\frac{\partial}{\partial\omega}(F^{(0)r}\Sigma^<)\frac{\partial\mathcal{F}^{(0)a}}{\partial\bar{t}} + \frac{i}{2}\frac{\partial F^{(0)<}}{\partial\omega}\Sigma^r\frac{\partial\mathcal{F}^{(0)a}}{\partial\bar{t}} - \\
& + \frac{i}{2}\frac{\partial F^{(0)r}}{\partial\bar{t}}\Sigma^r\frac{\partial\mathcal{F}^{(0)<}}{\partial\omega} + \frac{i}{2}\frac{\partial F^{(0)r}}{\partial\bar{t}}\frac{\partial}{\partial\omega}(\Sigma^<\mathcal{F}^{(0)a}) - \\
& - \frac{i}{2}\frac{\partial F^{(0)<}}{\partial\bar{t}}\Sigma^r\frac{\partial\mathcal{F}^{(0)a}}{\partial\omega}.
\end{aligned} \tag{2.81}$$

By simplifying this equation, we get

$$\mathcal{F}^{(1)<} = \frac{\Delta_k^{(1)}}{[\Gamma^2 + (\omega - \epsilon_k(\bar{t}))^2][\Gamma^2 + (\omega + \epsilon_k(\bar{t}))^2]} \left(-2\Gamma\pi[\omega + \epsilon_k(\bar{t})]^2\delta(\omega + \epsilon_k(\bar{t})) + 2i[2\Gamma\omega + \pi(\omega - \epsilon_k(\bar{t}))(\omega + \epsilon_k(\bar{t}))^2\delta(\omega + \epsilon_k(\bar{t}))] \right). \quad (2.82)$$

Making use of the delta functions, the integral (2.80) is simplified and we get,

$$\Delta_k^{(1)}(\bar{t}) = \sum_k \frac{\lambda\Gamma\Delta_k^{(1)}(\bar{t})}{\pi} \int_{-\Omega_{BCS}}^{\Omega_{BCS}} d\omega \frac{\omega}{[\Gamma^2/4 + (\omega - \epsilon_k(\bar{t}))^2][\Gamma^2/4 + (\omega + \epsilon_k(\bar{t}))^2]}. \quad (2.83)$$

We use the transformation (2.62) and replace the *average* or *slow* time by the electronic lifetime in the layer ($\bar{t} \rightarrow \tau$) to describe the steady state

$$\Delta_k^{(1)}(\tau) = \frac{A}{2\pi} k_F \int_{k_F - \delta}^{k_F + \delta} dk \frac{\lambda\Gamma\Delta_k^{(1)}(\tau)}{\pi} \times \int_{-\Omega_{BCS}}^{\Omega_{BCS}} d\omega \frac{\omega}{[\Gamma^2/4 + (\omega - \epsilon_k(\tau))^2][\Gamma^2/4 + (\omega + \epsilon_k(\tau))^2]}.$$

Using that $k_F = 2\pi\nu v_F/A$,

$$\Delta_k^{(1)}(\tau) = \frac{\lambda\nu v_F \Gamma}{\pi} \int_{k_F - \delta}^{k_F + \delta} dk \Delta_k^{(1)}(\tau) \times \int_{\Omega_{BCS}}^0 d\omega \frac{\omega}{[\Gamma^2/4 + (\omega - \epsilon_k(\tau))^2][\Gamma^2/4 + (\omega + \epsilon_k(\tau))^2]}.$$

Considering $\Delta_k^{(1)}$ independent of k , this quantity, which also vanishes at the phase transition, cancels out. Solving the ω integration, we can simplify

$$\frac{1}{\lambda\nu} = \int_{k_F - \delta}^{k_F + \delta} dk \frac{v_F}{2\pi\epsilon_k} \left(-2 \arctan\left(\frac{\epsilon_k(\tau)}{\Gamma/2}\right) + \arctan\left(\frac{\epsilon_k(\tau) - \Omega_{BCS}}{\Gamma/2}\right) + \arctan\left(\frac{\epsilon_k(\tau) + \Omega_{BCS}}{\Gamma/2}\right) \right).$$

Now, we assume that $\Omega_{BCS} \rightarrow \infty$. So,

$$\frac{1}{\lambda\nu} = \int_{-\pi}^{\pi} d\theta \int_{k_F - \delta}^{k_F + \delta} dk \frac{v_F}{(2\pi)^2} \frac{v_F}{\pi(k - k_F) - \pi e E \tau \cos \theta} \times \left(-\arctan\left(\frac{v_F(k - k_F) - v_F e E \tau \cos \theta}{\Gamma/2}\right) \right). \quad (2.84)$$

where we use that $\epsilon_k(\vec{t}) = \frac{1}{2m}(\vec{k} - e\vec{E}\vec{t})^2 - \frac{1}{2m}k_F^2 \approx v_F(k - k_F) - eEv_F\tau \cos\theta$. Notice that in transformation (2.57), there is no integration in θ . This happens because such integration has been done resulting in $(2\pi)^2$. Now, our function depends on θ . So, the result of this integration is not simply $(2\pi)^2$. Therefore, we include in the equation above.

It is interesting to consider first the limit $\Gamma \rightarrow 0$ of this expression, but with the product $E\tau = E/\Gamma$ finite, when the layer decouples from the substrate. In this limit, performing the integrations, first in θ and then in k , we get:

$$\frac{1}{\lambda\nu} = \frac{1}{2} \ln \left| \frac{\sqrt{1 - (\hat{T}_c^0/\Omega)^2 + 1}}{\sqrt{1 - (\hat{T}_c^0/\Omega)^2 - 1}} \right|, \quad (2.85)$$

where $\hat{T}_c^0 = eEv_F\tau$ is finite, since the electric field $E \rightarrow 0$ to keep the product $E/\Gamma = E\tau$ finite. For $(\hat{T}_c^0/\Omega) \ll 1$, this equation yields the following condition for the boundary of the superconducting phase:

$$\hat{T}_c^0 = \Delta_0. \quad (2.86)$$

In a superconducting film the *depairing current density* is defined as that for which the kinetic energy of the current carriers exceeds the binding energy of the Cooper pairs. It is then energetically favorable for the electrons to separate and cease to be superconducting. This occurs when the energy balance $\delta E = 2\Delta_0 - 2mv_Dv_F$ becomes negative [37, 38]. The quantity v_D is the drift velocity and it can be easily verified that spontaneous *depairing* occurs at the critical drift velocity $v_D^c = \Delta_0/mv_F$. In our case, the drift velocity is given by $v_D = eE\tau/m$, such that, the condition $v_D^c = \Delta_0/mv_F$ implies $\hat{T}_c^0 = \Delta_0$ as obtained above. For current densities, such that, $(eEv_F\tau) > \Delta_0$, the superconducting order parameter vanishes[41]. Then, when $\Gamma \rightarrow 0$, and the film is decoupled from the substrate, it presents a *depairing transition* [38] from the superconducting to the normal state for $\hat{T}^0 > \Delta_0$, i.e., for a critical electric field $E_c^0 = \Delta_0/ev_F\tau$. This result relies on a correspondence, within the two fluid model, between a state with a finite normal but a zero superfluid one, and another state with a finite superfluid but zero normal component [37].

Let us now turn to the coupling Γ of the layer to the substrate. We get the linear order in Γ ($O(\Gamma)$), we get after performing the integrations and using that $1/\nu = \ln(2\Omega/\Delta_0)$,

$$\ln \frac{2\Omega}{\Delta_0} = \ln \frac{2\Omega}{\hat{T}_c} + \frac{2}{\pi} \frac{\Gamma/\Omega}{\sqrt{1 - (\hat{T}_c/\Omega)^2}}. \quad (2.87)$$

Neglecting the terms of $O[(\Gamma/\Omega)(\hat{T}_c^2/\Omega^2)]$, we get:

$$\hat{T}_c = \Delta_0 \exp\left(\frac{2\Gamma}{\pi\Omega}\right). \quad (2.88)$$

Then, the coupling of the layer to the metallic substrate *increases* the critical electric field to destroy superconductivity in the layer. The physical reason for this interesting phenomenon can be that the quantity Γ and consequently the lifetime τ are determined by the coupling t_z between the layer and the substrate (see the Hamiltonian – eq. (2.1)). This coupling is responsible for the proximity effect, which induces pairing in the metallic substrate reinforcing superconductivity in the whole system, at least for small t_z .

Finally, we consider Eq. (2.84) in the limit that $eEv_F\tau \rightarrow 0$ and for small Γ . After integration in k , we are left with the following angular integral:

$$\frac{1}{\lambda\nu} = \frac{1}{2\pi} \int_{-\pi}^{\pi} \ln \left[\frac{1 - y^2 \cos^2(\theta)}{(\Gamma/\Omega)^2} \right] d\theta, \quad (2.89)$$

where $y = (eEv_F\tau/\Omega)$. Performing the integral, we get

$$\frac{1}{\lambda\nu} = \ln \left(\frac{\frac{1}{4} \left[1 + \sqrt{1 - (\hat{T}_c/\Omega)^2} \right]^2}{\Gamma/\Omega} \right), \quad (2.90)$$

which yields,

$$\hat{T}_c = 2\Omega \left[\left(1 - \sqrt{\frac{\Gamma}{\Gamma_c}} \right) \sqrt{\frac{\Gamma}{\Gamma_c}} \right]^{1/2}, \quad (2.91)$$

for $\Gamma/\Gamma_c \geq 1/4$. The parameter $\Gamma_c = \Delta_0/2$ represents the critical value of dissipation for destroying superconductivity in the layer in the absence of the electric field. Then in mean-field we find a critical line $\hat{T}_c(\Gamma)$ separating the normal from the superconducting phase. If this line is to survive fluctuations, its non-mean-field forms, close to the dissipation, induced quantum critical point that can be obtained from a scaling approach using the properties of this QCP at $\hat{T}_c = 0$, $\Gamma = \Gamma_c$. We use the electric field (or \hat{T}) as a relevant perturbation at this QCP, together with standard renormalization group arguments to obtain, $\hat{T}_c \propto |\Gamma - \Gamma_c|^\psi$, where the shift exponent, $\psi = z/(d + z - 2)$ [55, 57]. For a nearly 2D system, using $z = 2$ as found before, we get $\psi = 1$ (see Fig. (2.2)). The crossover line between the quantum disordered and quantum critical regime, $\hat{T}_x \propto |\Gamma - \Gamma_c|^{\nu z}$ is also linear on the distance to the QCP, since $\nu z = 1$ (see Fig. (2.2)).

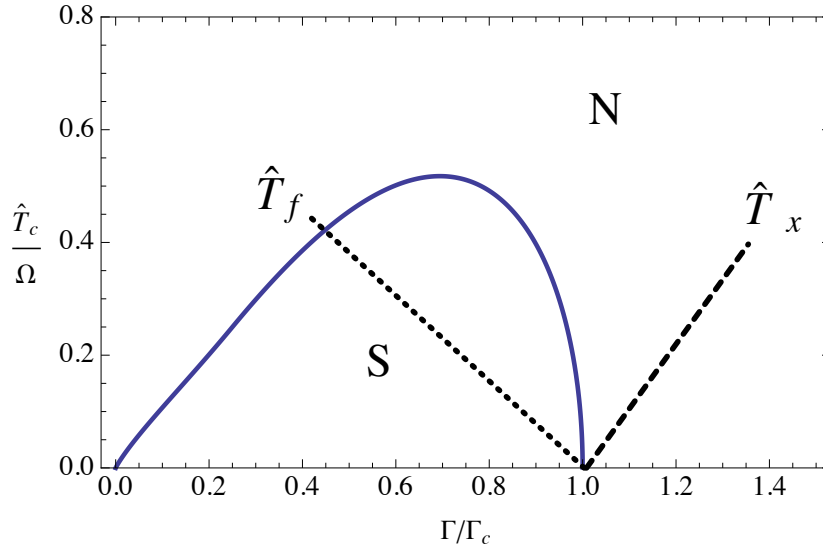


Figure 2.2: Mean-field critical line $\hat{T}_c(\Gamma)$ (full line) separating the normal and the superconducting phases, for $\lambda\nu = 0.25$. For convenience we used the variable $\hat{T} = eEv_F/\Gamma_c$ or $\hat{T} = (\Gamma/\Gamma_c)\hat{T}$. The dotted line, $\hat{T}_f \propto |g|^\psi$, with $\psi = 1$ for $\Gamma/\Gamma_c < 1$, represents the expected shape of the critical line when fluctuations are included. The dashed line, $\hat{T}_x \propto |g|^{\nu z}$, with $\nu z = 1$ is the crossover line separating the quantum critical from the quantum disordered, low field, regimes. The transition at $\Gamma = 0$, $\hat{T}_c = \Delta_0$ corresponding to the critical current in a dissipationless film (see text) appears in the variable \hat{T} at $\hat{T} = 0$.

A most relevant question concerns the nature of the quantum phase transition driven by the electric field along the line $\hat{T}_f(\Gamma)$ in Fig. (2.2). Since the electric field is a relevant perturbation close to the QCP at $\Gamma = \Gamma_c$, $\hat{T}_c = 0$, the critical behavior along this line is not governed by the dissipation induced QCP. Mitra et al. [58] argues that this transition is in the universality class of a thermal phase transition and, consequently, governed by 2D thermal exponents. Indeed, in the non-equilibrium Keldysh effective action approach of this problem, when frequency goes to zero, which is the relevant limit for the critical behavior, it can be neglected with respect to the effective temperature \hat{T} associated with the electric field and the problem becomes essentially classical [58].

In figure (2.2), we show the mean-field phase diagram $\hat{T}_c(\Gamma)$ as obtained in the present work. In the limit $\Gamma \rightarrow 0$, but with the product $E\Gamma$ finite, we recover the standard result for the critical current in a superconducting

film as discussed before. The phase transition in this limit is discontinuous [41] and the order parameter vanishes abruptly at the critical current. An interesting possibility is that the renormalization group (RG) flow, along the critical line of the electric field-driven phase transition in the presence of dissipation, is towards this point (in the variables of Fig. (2.2) this is located at $\hat{T}_c = 0, \Gamma = 0$). If this is the case, this point is a tri-critical point and the exponents along the line $\hat{T}_c(\Gamma)$ should be tri-critical (thermal) exponents.

2.5.2 Phase Diagram for $T \neq 0K$

Taking $\Delta_k^{(0)} = 0$ and $T \neq 0K$ we get

$$\begin{aligned} \mathcal{F}^{(1)<}(\omega, \bar{t}) = & -2\pi\Gamma\Delta_k^{(1)} \frac{f(\omega)[\omega + \epsilon_k(\bar{t})]^2\delta(\omega + \epsilon_k)}{[\Gamma^2 + (\omega - \epsilon_k(\bar{t}))^2][\Gamma^2 + (\omega + \epsilon_k(\bar{t}))^2]} + \\ & + 4i\Gamma\Delta_k^{(1)} \frac{f(\omega)\omega\delta(\omega + \epsilon_k)}{[\Gamma^2 + (\omega - \epsilon_k(\bar{t}))^2][\Gamma^2 + (\omega + \epsilon_k(\bar{t}))^2]} + \\ & + 2i\Delta_k^{(1)} \frac{f(\omega)[\omega - \epsilon_k(\bar{t})][\omega + \epsilon_k(\bar{t})]^2\delta(\omega + \epsilon_k)}{[\Gamma^2 + (\omega - \epsilon_k(\bar{t}))^2][\Gamma^2 + (\omega + \epsilon_k(\bar{t}))^2]}. \end{aligned} \quad (2.92)$$

Making use of the delta functions, the integral (2.80) simplifies and we get:

$$\Delta_k^{(1)} = \sum_k \frac{2\lambda\Gamma\Delta_k^{(1)}}{\pi} \int_{-\Omega_{BCS}}^0 d\omega f(\omega) \frac{\omega}{[\Gamma^2 + (\omega - \epsilon_k(\bar{t}))^2][\Gamma^2 + (\omega + \epsilon_k(\bar{t}))^2]} \quad (2.93)$$

or using that $k_F = 2\pi\nu v_F/A$ and considering $\Delta_k^{(1)}$ k -independent, i.e., $\Delta_k^{(1)} = \Delta^{(1)}$:

$$\frac{1}{\lambda\nu} = \frac{v_F\Gamma}{\pi^2} \int_{-\pi}^{+\pi} d\theta \int_{k_F-\delta}^{k_F+\delta} dk \int_{-\Omega_{BCS}}^0 d\omega f(\omega) \frac{\omega}{[\Gamma^2 + (\omega - \epsilon_k(\bar{t}))^2][\Gamma^2 + (\omega + \epsilon_k(\bar{t}))^2]}. \quad (2.94)$$

From the equation above, we can obtain the phase diagram of the system at finite temperatures as a function of the field and dissipation as shown in Fig. (2.3).

2.6 Conclusions

In this chapter we used the Keldysh formalism to treat many-body systems close to quantum criticality. We choose Keldysh approach because previously

Figure 2.3: Finite temperature phase diagram T/Ω_{BCS} versus $\hat{T}_c/\Omega_{BCS} = eE v_F \tau / \Omega_{BCS}$ for fixed $\Gamma/\Gamma_c = 0.7$ and $\lambda\nu = 0.25$.

use used it for time dependent impurity problems [49]. This approach allows us to obtain the time dependence of the order parameter for an arbitrary time dependence of the external parameter, if an adiabatic condition is satisfied. These expression was the first contributions of this work. We have used this method to study the normal to superconductor quantum phase transition in the presence of dissipation and time dependent perturbations. Specifically, we considered a superconducting layer, under the action of a time dependent vector potential and deposited over a metallic substrate with which it can interchange electrons through a momentum non-conserving process. This same system was study by Mitra [12]. So we could compare our results with Mitra results.

Initially, the dissipation induced quantum critical point was obtained in the mean field approximation yielding results in agreement with those obtained previously by Mitra [12]. Next, we used an alternative approach to include fluctuations close to the QCP using a Thouless criterion generalized to include dissipation. We were able to fully characterize the dissipa-

tion induced QCP, obtaining its dynamic exponent, effective dimension and universality class. This is the second contribution of this work. For the two-dimensional film, the quantum phase transition turns out to be at the upper critical dimension and the scaling behavior in its vicinity is expected to present logarithmic contributions.

After that, we treated the effect of an electric field, arising from a minimally coupled time dependent vector potential. Our approach yields the time dependence of the order parameter in the ordered phase. We proposed a phase diagram in the presence of the electric field and dissipation in the non-equilibrium stationary state and study it. Within the BCS and adiabatic approximations, we have obtained the full electric field versus temperature, versus dissipation phase diagram.

Here we study a paradigmatic problem in superconductivity. By using a powerful method to treat a time dependent problem, we revisit a problem studied by Mitra confirming their results and adding new pieces of information. This work was published in *Philosophical Magazine* [59], winning a honorable mention in “The James Clerk Maxwell Young Writers Prize” given by Taylor & Francis Group in 2013.

Chapter 3

Influence of an Odd-Parity Hybridization in the Superconducting State

Hybridization is an important concept in the physics of metallic multi-band systems. In these systems electrons arising from different atomic orbitals coexist at a common Fermi surface. In superconductors, for example, hybridization strongly affects the properties of a material. Since hybridization arises from the overlap of wave functions it can be controlled externally, by doping or applying pressure in the system. In this way it acts as an important control parameter which allows to explore the phase diagram of the material. It is well known that when hybridization is constant or has even-parity in k -space, it acts in detriment of superconductivity and can even destroy it at a superconducting quantum critical point (SQCP). This behavior was verified both, experimentally [17, 60, 61] and theoretically [62, 63]. However, anti-symmetric or odd-parity hybridization also can be considered. It occurs when the hybridization mixes orbitals with different parities in neighboring lattice sites. It turns out to be very important since it includes the cases of s-p, p-d and d-f orbitals relevant for semiconductors, oxide superconductors and metallic rare-earths as a few examples.

In the first section of this chapter we will discuss under which conditions hybridization has an anti-symmetric character. There are some interesting results when the hybridization is considered anti-symmetric [20, 64, 65]. The most remarkable one is the enhancement of superconductivity when the hybridization has odd-parity character. This result is presented in this chapter and was published in an important scientific magazine: *Annals of Physics* [66].

Another important topic that has recently attracted a lot of attention

is that of Majorana fermions [67, 68]. This interest is due to the fact that these quasi-particles are candidates to act as q-bits in quantum computers [69]. There are some necessary conditions to obtain these Majorana fermions, that in one-dimensional p-wave superconductors appear at the ends of a finite chain [23, 70, 71]. The possibility of achieving induced p-wave superconductivity in a normal superconductor has been demonstrated by considering the spin-orbit interaction [70, 71] in systems with broken inversion symmetry [70, 72].

In this chapter we show that a two-band metal with an attractive inter-band interaction has non-trivial superconducting properties if the hybridization is anti-symmetric. Our approach based on the equations of motion method [50] allows us to consider also the case of strong attractive interactions. We find among other results that anti-symmetric hybridization enhances superconductivity. We also show that it gives rise, via proximity effect, to an induced order parameter with p-wave symmetry.

A similar behavior was discussed in the literature [70] associated with a Rashba spin-orbit coupling (SOC) in semiconductors with a s-wave superconductor deposited on top. In this case, they consider a 2D layer and via proximity effect, an intra-band $p_x \pm ip_y$ pairing appears due to SOC. Here, we study a system without SOC that generates, also via proximity effect, a p -wave pairing. We can do a mapping between the problem with anti-symmetric hybridization studied in this thesis and that of material with Rashba type of SOC. The most remarkable proposition made in this chapter is that this system can produce a p -wave superconducting chain. It is known that in the ends of this chain exist Majorana fermions [23].

3.1 Origin of an Odd-Parity Hybridization

In this section, we will discuss the origin of an anti-symmetric hybridization. We will follow some assumptions used by M. Drzazga and E. Zipper in Ref. [19]. They assume that Wannier functions [73, 74] of the s , p , d or f electrons of the solid have the same parities as the corresponding atomic functions.

We consider that the hybridization is caused by a periodic lattice potential, called as $v(\vec{r})$. This lattice has inversion symmetry, i.e., $v(-\vec{r}) = v(\vec{r})$. The matrix elements of hybridization are written in the form of

$$V_{ll'}(\vec{r}_1 - \vec{r}_2) = \int_{-\infty}^{\infty} d\vec{r}' \psi_{lm}^*(\vec{r}' - \vec{r}_1) v(\vec{r}') \psi_{l'm'}(\vec{r}' - \vec{r}_2),$$

where $\psi_{lm(lm')}$ is the wave function of $lm(l'm')$ orbital. We can take $\vec{r}_1 = 0$

and $\vec{r}_2 = -\vec{r}$. So,

$$V_{ll'}(\vec{r}) = \int_{-\infty}^{\infty} d\vec{r}' \psi_{lm}^*(\vec{r}') v(\vec{r}') \psi_{l'm'}(\vec{r}' + \vec{r}). \quad (3.1)$$

The wave function ψ , in spherical coordinates, can be written as [75]:

$$\psi_{lm}(\vec{r}) = \psi_{lm}(r, \theta, \phi) = R(r) Y_l^m(\theta, \phi), \quad (3.2)$$

where $R(r)$ is the radial solution of Laplace's equation and $Y_l^m(\theta, \phi)$ is the angular solution, known as spherical harmonics. The indexes l and m are quantum numbers, such that $l > 0$ and $m = -l, \dots, 0, \dots, +l$.

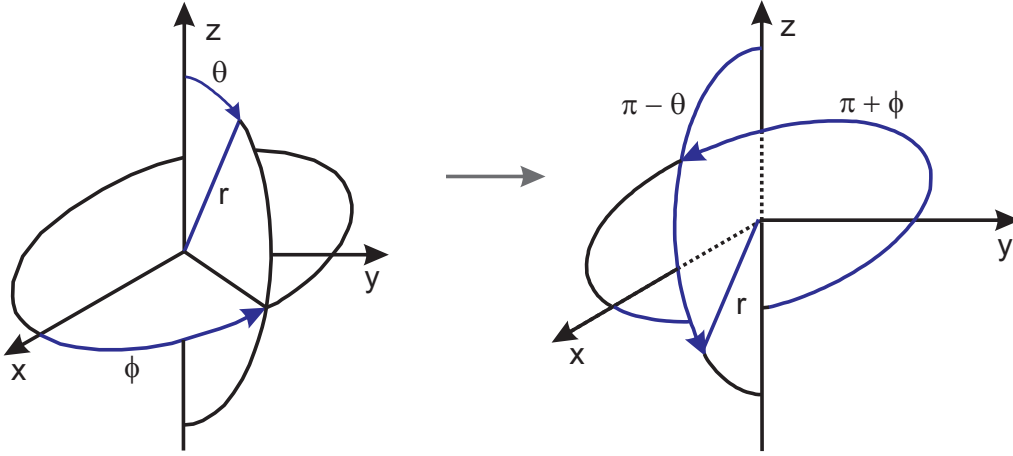


Figure 3.1: Schematic picture of an inversion of coordinates in spherical coordinates.

We want to investigate the parity of the equation (3.1). This is possible by doing an inversion of coordinates: $\vec{r} \rightarrow -\vec{r}$. In spherical coordinates, this is more complicated than in Cartesian coordinates. In Fig. (3.1) we show a schematic picture that help us to obtain the following relation

$$\begin{aligned} r &\longrightarrow r \\ \theta &\longrightarrow \pi - \theta \\ \phi &\longrightarrow \pi + \phi. \end{aligned} \quad (3.3)$$

Notice that: $\vec{r} = (x, y, z) \rightarrow \vec{r} = (r \sin \theta \cos \phi, r \sin \theta \sin \phi, r \cos \theta)$ with $|\vec{r}| = r \geq 0$, $\phi \in [0, 2\pi]$ and $\theta \in [0, \pi]$.

Doing an inversion of coordinates: $\vec{r} \rightarrow -\vec{r}$ in equation (3.2) we write

$$\psi_{lm}(-\vec{r}) = \psi_{lm}(r, \pi - \theta, \pi + \phi) = R(r) Y_l^m(\pi - \theta, \pi + \phi)$$

The parity of the Y_l^m , the spherical harmonics, depends of l by the following expression

$$Y_l^m(\pi - \theta, \pi + \phi) = (-1)^l Y_l^m(\theta, \phi). \quad (3.4)$$

So,

$$\begin{aligned} \psi_{lm}(-\vec{r}) &= \psi_{lm}(r, \pi - \theta, \pi + \phi) = (-1)^l R(r) Y_l^m(\theta, \phi) \\ &= (-1)^l \psi_{lm}(\vec{r}). \end{aligned} \quad (3.5)$$

Another important information that we will need is

$$\begin{aligned} \psi_{lm}^*(-\vec{r}) &= \psi_{lm}^*(r, \pi - \theta, \pi + \phi) = (-1)^{-l} R^*(r) Y_l^m(\theta, \phi) \\ &= (-1)^{-l} \psi_{lm}^*(\vec{r}). \end{aligned} \quad (3.6)$$

Now we are able to investigate the parity of the equation (3.1). Doing the following inversion $\vec{r} \rightarrow -\vec{r}$ we can write

$$V_{l'l'}(-\vec{r}) = \int_{-\infty}^{\infty} d\vec{r}' \psi_{lm}^*(\vec{r}') v(\vec{r}') \psi_{l'm'}(\vec{r}' - \vec{r}),$$

taking

$$\vec{r}' = -\vec{r}'' \quad \longrightarrow \quad d\vec{r}' = -d\vec{r}'' \quad \text{and} \quad \vec{r}'' \in [\infty, -\infty].$$

We get

$$\begin{aligned} V_{l'l'}(-\vec{r}) &= - \int_{\infty}^{-\infty} d\vec{r}'' \psi_{lm}^*(-\vec{r}'') v(-\vec{r}'') \psi_{l'm'}(-\vec{r}'' - \vec{r}) \\ &= \int_{-\infty}^{\infty} d\vec{r}'' \psi_{lm}^*(-\vec{r}'') v(\vec{r}'') \psi_{l'm'}(-[\vec{r}'' + \vec{r}]). \end{aligned}$$

Using equations (3.5) and (3.6), we finally write

$$\begin{aligned} V_{l'l'}(-\vec{r}) &= \int_{-\infty}^{\infty} d\vec{r}'' (-1)^{-l} \psi_{lm}^*(\vec{r}'') v(\vec{r}'') (-1)^{l'} \psi_{l'm'}(\vec{r}'' + \vec{r}) \\ &= (-1)^{l'-l} \int_{-\infty}^{\infty} d\vec{r}'' \psi_{lm}^*(\vec{r}'') v(\vec{r}'') \psi_{l'm'}(\vec{r}'' + \vec{r}) \\ &= (-1)^{l'-l} V_{l'l'}(\vec{r}). \end{aligned} \quad (3.7)$$

We can conclude that the parity of the hybridization depends on the difference $l' - l$. Remember that l is always positive, we have *even parity* of $V_{l'l'}$, if $l' - l$ is an even number and *odd parity* of $V_{l'l'}$ if $l' - l$ is a odd number. Further,

- If $l' = l + 1 \rightarrow l + 1 - l = 1$ is always an odd number;
- If $l' = l + 2 \rightarrow l + 2 - l = 2$ is always an even number;

Then every time we mix orbitals with different parities, like those with angular momentum l and $l + 1$ in neighboring sites, we need to consider odd-parity hybridization. Generically, every time we mix orbitals with angular momentum l and $l + n$, where n is a odd (even) number, the hybridization has odd (even)-parity. The anti-symmetric relation in real space is $V(-\vec{r}) = -V(\vec{r})$. We will show that in momentum space the anti-symmetry property of hybridization is given by: $V(-k) = -V(k)$. In one-dimension lattice, if the hybridization is anti-symmetric, one gets $V(k) \propto \sin ka$ with a the lattice spacing, for example.

Notice that the case of anti-symmetric $V(\vec{r})$ is of great relevance for condensed matter physics as it includes the $d - p$ type of mixing, relevant for the copper oxides, for example, and $d - f$ mixing that encompasses many rare-earth systems, the actinides and their compounds.

Another important property of the hybridization is the behavior at $k = 0$. This can be obtained by writing the hybridization in k -space:

$$\begin{aligned} V_{\vec{k}} &= \int_{-\infty}^{\infty} d\vec{r} V(\vec{r}) e^{i\vec{k}\cdot\vec{r}} \\ &= \int_{-\infty}^0 d\vec{r} V(\vec{r}) e^{i\vec{k}\cdot\vec{r}} + \int_0^{\infty} d\vec{r} V(\vec{r}) e^{i\vec{k}\cdot\vec{r}}. \end{aligned}$$

In the first integral on the right side, we take $\vec{r} \rightarrow -\vec{r}'$:

$$\begin{aligned} V_{\vec{k}} &= - \int_{\infty}^0 d\vec{r}' V(-\vec{r}') e^{-i\vec{k}\cdot\vec{r}'} + \int_0^{\infty} d\vec{r} V(\vec{r}) e^{i\vec{k}\cdot\vec{r}} \\ &= \int_0^{\infty} d\vec{r}' V(-\vec{r}') e^{-i\vec{k}\cdot\vec{r}'} + \int_0^{\infty} d\vec{r} V(\vec{r}) e^{i\vec{k}\cdot\vec{r}}. \end{aligned}$$

In the first integral on the right side, we now take $\vec{r}' \rightarrow \vec{r}$:

$$\begin{aligned} V_{\vec{k}} &= \int_0^{\infty} d\vec{r} V(-\vec{r}) e^{-i\vec{k}\cdot\vec{r}} + \int_0^{\infty} d\vec{r} V(\vec{r}) e^{i\vec{k}\cdot\vec{r}} \\ &= \int_0^{\infty} d\vec{r} \left(V(-\vec{r}) e^{-i\vec{k}\cdot\vec{r}} + V(\vec{r}) e^{i\vec{k}\cdot\vec{r}} \right). \end{aligned} \quad (3.8)$$

We must find when $V_{\vec{k}}$ has an odd parity. So, we take $\vec{k} \rightarrow -\vec{k}$:

$$V_{-\vec{k}} = \int_0^{\infty} d\vec{r} \left(V(-\vec{r}) e^{i\vec{k}\cdot\vec{r}} + V(\vec{r}) e^{-i\vec{k}\cdot\vec{r}} \right).$$

Consider $l' - l$ an odd number, thus the hybridization in real space is anti-symmetric: $V(-\vec{r}) = -V(\vec{r})$. We get,

$$\begin{aligned} V_{-\vec{k}} &= \int_0^\infty d\vec{r} \left(-V(\vec{r})e^{i\vec{k}\cdot\vec{r}} - V(-\vec{r})e^{-i\vec{k}\cdot\vec{r}} \right) \\ &= - \int_0^\infty d\vec{r} \left(V(-\vec{r})e^{-i\vec{k}\cdot\vec{r}} + V(\vec{r})e^{i\vec{k}\cdot\vec{r}} \right). \end{aligned}$$

So,

$$V_{-\vec{k}} = -V_{\vec{k}}, \quad (3.9)$$

when $l' - l$ is an odd number. A similar calculation can be done for $l' - l$ an even number and we find $V_{-\vec{k}} = V_{\vec{k}}$.

Now, taking $\vec{k} = 0$:

$$V_{\vec{k}=0} = \int_0^\infty d\vec{r} (V(-\vec{r}) + V(\vec{r})). \quad (3.10)$$

Notice that, if $V(-\vec{r})$ has odd-parity necessarily $V_{\vec{k}=0} = 0$. The same thing does not happen if $V(\vec{r})$ is symmetric in \vec{r} .

3.2 Model

We focus our study on a two-band system with an odd-parity hybridization between these bands, an attractive interaction between them, and also an attractive interaction in one of the bands. This hybridization is k -dependent since it mixes different orbitals in neighboring sites through the crystalline potential. It is anti-symmetric since we consider that it mixes orbitals with angular momentum l and $l + 1$, as we showed in section (3.1). In terms of symmetry, we can say that we will investigate a system with parity symmetry breaking.

The Hamiltonian of this problem can be written as

$$\begin{aligned} H &= \sum_{k,\sigma} \left(\epsilon_k^a a_{k\sigma}^\dagger a_{k\sigma} + \epsilon_k^b b_{k\sigma}^\dagger b_{k\sigma} \right) - \sum_{k\sigma} \left(\Delta_{ab} a_{k\sigma}^\dagger b_{-k-\sigma}^\dagger + \Delta_{ab}^* b_{-k-\sigma} a_{k\sigma} \right) - \\ &- \frac{1}{2} \sum_{k\sigma} \left(\Delta_{bb}(k, \sigma) b_{k\sigma}^\dagger b_{-k-\sigma}^\dagger + \Delta_{bb}^*(k, \sigma) b_{-k-\sigma} b_{k\sigma} \right) + \\ &+ \sum_{k\sigma} \left(V_k a_{k\sigma}^\dagger b_{k\sigma} + V_k^* b_{k\sigma}^\dagger a_{k\sigma} \right), \end{aligned} \quad (3.11)$$

where $\epsilon_k^{a,b}$ are the energies of the electron in the a and b bands. In an obvious notation, $a_{k\sigma}^{(\dagger)}$ and $b_{k\sigma}^{(\dagger)}$ annihilate (create) electrons in these bands respectively. As pointed out before, the hybridization has odd parity, so $V(-\vec{r}) = -V(\vec{r})$, in real space or in k -space, $V_{-k} = -V_k$.

The order parameters that characterizes the superconducting phase are given by,

$$\Delta_{ab} \equiv g_{ab} \sum_{k\sigma} \langle a_{k\sigma} b_{-k-\sigma} \rangle \quad (3.12)$$

is the inter-band superconducting order parameter and

$$\begin{aligned} \Delta_{bb}(k, \sigma) &\equiv g_{bb} \langle b_{k\sigma} b_{-k-\sigma} \rangle \\ \Delta_{bb} &= \sum_{k,\sigma} \Delta_{bb}(k, \sigma) \end{aligned} \quad (3.13)$$

is the intra-band superconducting order parameter. Since we will investigate the existence of induced superconductivity in the band a , we will also define the k -dependent anomalous correlation function in the a -band:

$$\Delta_{aa}(k, \sigma) = \langle a_{k\sigma} a_{-k-\sigma} \rangle. \quad (3.14)$$

This anomalous correlation function will appear because of the influence of hybridization and/or inter-band interactions, even in the absence of interactions in b -band.

It is important to find these three Green's functions:

$$\langle \langle b_{-k-\sigma}^\dagger | a_{k\sigma}^\dagger \rangle \rangle, \quad \langle \langle b_{-k-\sigma}^\dagger | b_{k\sigma}^\dagger \rangle \rangle, \quad \langle \langle a_{-k-\sigma}^\dagger | a_{k\sigma}^\dagger \rangle \rangle,$$

as they form a closed set of equations, which allow to calculate the order parameters defined above.

The expectation values of the operators can be calculated through the fluctuation dissipation theorem, which can be written as:

$$\langle a_{k\sigma}^\dagger b_{-k-\sigma}^\dagger \rangle = \frac{1}{\pi} \int d\omega f(\omega) \text{Im} \left(\langle \langle b_{-k-\sigma}^\dagger | a_{k\sigma}^\dagger \rangle \rangle^r \right), \quad (3.15)$$

when we want to find Δ_{ab} , for example. Notice that in our notation, the $\langle \langle \dots | \dots \rangle \rangle$ is the Green's function of two operators, like used in Re. [50]. Here, we have $f(\omega) = 1 / (e^{(\omega - E_F)/k_B T} + 1)$ is the Fermi-Dirac distribution, $\text{Im}(\dots)$ is the imaginary part of (\dots) , and the index r is the retarded component of the Green's function – defined in equation (2.7) when we consider that the function are $(t - t')$ -dependent.

In the next sections, we will show some calculations to determine the important parameters.

3.3 Calculations

In this section, we will calculate the Green's functions necessary to find the intra-band and inter-band order parameters, and the occupations in a and b bands. We will use the equation of motion method [50].

We start writing the equation of motion for the $\langle\langle b_{-k-\sigma}^\dagger | a_{k\sigma}^\dagger \rangle\rangle$ Green's function:

$$\omega \langle\langle b_{-k-\sigma}^\dagger | a_{k\sigma}^\dagger \rangle\rangle = \{b_{-k-\sigma}, a_{k\sigma}\} + \langle\langle [b_{-k-\sigma}^\dagger, H] | a_{k\sigma}^\dagger \rangle\rangle,$$

where a and b are fermionic operators, so the anti-commutation rules must be respected,

$$\begin{aligned} \{c_i^\dagger, c_j\} &= \delta_{ij} \\ \{c_i^{(\dagger)}, c_j^{(\dagger)}\} &= 0, \end{aligned}$$

where c is any fermionic operator. So, we get,

$$\begin{aligned} (\omega + \epsilon_{-k}^b) \langle\langle b_{-k-\sigma}^\dagger | a_{k\sigma}^\dagger \rangle\rangle + \Delta_{ab}^* \langle\langle a_{k\sigma} | a_{k\sigma}^\dagger \rangle\rangle + \\ + \frac{1}{2} \left(-\Delta_{bb}^*(-k, -\sigma) \langle\langle b_{k\sigma}^\dagger | a_{k\sigma}^\dagger \rangle\rangle + \Delta_{bb}^*(k, \sigma) \langle\langle b_{-k-\sigma}^\dagger | a_{k\sigma}^\dagger \rangle\rangle \right) + \\ + V_{-k} \langle\langle a_{-k-\sigma}^\dagger | a_{k\sigma}^\dagger \rangle\rangle = 0. \end{aligned}$$

Here, we need to use a property of the Hamiltonian (3.11). The b and $a - b$ bands are like singlet, that has symmetry in k -space: $\Delta_{bb}(-k) = \Delta_{bb}(k)$. However this decoupling is anti-symmetric in spin space: $\Delta_{bb}(-\sigma) = -\Delta_{bb}(\sigma)$, given a anti-symmetric total wave function for the electron pair ¹. Put all this information together, we get the following property for the order parameter

$$\Delta_{bb}(\pm k, -\sigma) = -\Delta_{bb}(\pm k, \sigma). \quad (3.16)$$

Using this relation, we can re-write the equation of motion

$$\begin{aligned} (\omega + \epsilon_{-k}^b) \langle\langle b_{-k-\sigma}^\dagger | a_{k\sigma}^\dagger \rangle\rangle + \Delta_{ab}^* \langle\langle a_{k\sigma} | a_{k\sigma}^\dagger \rangle\rangle + \Delta_{bb}^* \langle\langle b_{-k-\sigma}^\dagger | a_{-k\sigma}^\dagger \rangle\rangle + \\ + V_{-k} \langle\langle a_{-k-\sigma}^\dagger | a_{k\sigma}^\dagger \rangle\rangle = 0. \end{aligned}$$

We generate two new Green's functions for which we write the equations of motion

$$(\omega - \epsilon_k^a) \langle\langle a_{k\sigma} | a_{k\sigma}^\dagger \rangle\rangle + \Delta_{ab} \langle\langle b_{-k-\sigma}^\dagger | a_{k\sigma}^\dagger \rangle\rangle - V_k \langle\langle b_{k\sigma} | a_{k\sigma}^\dagger \rangle\rangle = 1$$

¹Notice that if our decoupling is a triplet one this relation should be different. In the triplet case the wave function is symmetric in spin but is anti-symmetric in k -space

$$\begin{aligned}
& (\omega - \epsilon_k^b) \langle \langle b_{k\sigma} | a_{k\sigma}^\dagger \rangle \rangle - \Delta_{ab} \langle \langle a_{-k-\sigma}^\dagger | a_{k\sigma}^\dagger \rangle \rangle + \\
& + \frac{1}{2} \left(-\Delta_{bb}(-k, -\sigma) \langle \langle b_{-k-\sigma}^\dagger | a_{k\sigma}^\dagger \rangle \rangle + \Delta_{bb}(k, \sigma) \langle \langle b_{-k-\sigma}^\dagger | a_{k\sigma}^\dagger \rangle \rangle \right) - \\
& - V_k^* \langle \langle a_{k\sigma} | a_{k\sigma}^\dagger \rangle \rangle = 0
\end{aligned}$$

or

$$\begin{aligned}
& (\omega - \epsilon_k^b) \langle \langle b_{k\sigma} | a_{k\sigma}^\dagger \rangle \rangle - \Delta_{ab} \langle \langle a_{-k-\sigma}^\dagger | a_{k\sigma}^\dagger \rangle \rangle + \Delta_{bb} \langle \langle b_{-k-\sigma}^\dagger | a_{k\sigma}^\dagger \rangle \rangle - \\
& - V_k^* \langle \langle a_{k\sigma} | a_{k\sigma}^\dagger \rangle \rangle = 0.
\end{aligned}$$

Again, we generate one new Green's function, $\langle \langle a_{-k-\sigma}^\dagger | a_{k\sigma}^\dagger \rangle \rangle$. It obeys the equation of motion

$$(\omega + \epsilon_{-k}^a) \langle \langle a_{-k-\sigma}^\dagger | a_{k\sigma}^\dagger \rangle \rangle - \Delta_{ab}^* \langle \langle b_{k\sigma} | a_{k\sigma}^\dagger \rangle \rangle + V_{-k}^* \langle \langle b_{-k-\sigma}^\dagger | a_{k\sigma}^\dagger \rangle \rangle.$$

Now, we have obtained a closed set of equation. It is helpful to write the system in matrix form,

$$\mathbf{D} \cdot \begin{pmatrix} x_1 = \langle \langle a_{k\sigma} | a_{k\sigma}^\dagger \rangle \rangle \\ y_1 = \langle \langle b_{-k-\sigma}^\dagger | a_{k\sigma}^\dagger \rangle \rangle \\ z_1 = \langle \langle b_{k\sigma} | a_{k\sigma}^\dagger \rangle \rangle \\ u_1 = \langle \langle a_{-k-\sigma}^\dagger | a_{k\sigma}^\dagger \rangle \rangle \end{pmatrix} = \begin{pmatrix} 1 \\ 0 \\ 0 \\ 0 \end{pmatrix} \quad (3.17)$$

where,

$$\mathbf{D} = \begin{pmatrix} (\omega - \epsilon_k^a) & \Delta_{ab} & -V_k & 0 \\ \Delta_{ab}^* & (\omega + \epsilon_{-k}^b) & \Delta_{bb}^* & V_{-k} \\ -V_k^* & \Delta_{bb} & (\omega - \epsilon_k^b) & -\Delta_{ab} \\ 0 & V_{-k}^* & -\Delta_{ab}^* & (\omega + \epsilon_{-k}^a) \end{pmatrix}. \quad (3.18)$$

Notice that, from this system of equations we can compute the correlation function initially desired. We could also calculate the Green's function related to the induced order parameter and the occupation number of the band a . It is interesting to know the occupation of a and b bands for future calculations.

We extract the results by calculating

$$x_1 = \frac{\det(\mathbf{D}_{\mathbf{x}_1})}{\det(\mathbf{D})},$$

related to the occupation number in a band (we will define this in subsection 3.3.4),

$$y_1 = \frac{\det(\mathbf{D}_{\mathbf{y}_1})}{\det(\mathbf{D})},$$

related to the inter-band order parameter, Δ_{ab} ,

$$u_1 = \frac{\det(\mathbf{D}_{\mathbf{u}_1})}{\det(\mathbf{D})},$$

related to the induced order parameter, Δ_{aa} . Where, we define

$$\mathbf{D}_{\mathbf{x}_1} = \begin{pmatrix} 1 & \Delta_{ab} & -V_k & 0 \\ 0 & (\omega + \epsilon_k^b) & \Delta_{bb}^* & V_{-k} \\ 0 & \Delta_{bb} & (\omega - \epsilon_k^b) & -\Delta_{ab} \\ 0 & V_{-k}^* & -\Delta_{ab}^* & (\omega + \epsilon_k^a) \end{pmatrix}, \quad (3.19)$$

$$\mathbf{D}_{\mathbf{y}_1} = \begin{pmatrix} (\omega - \epsilon_k^a) & 1 & -V_k & 0 \\ \Delta_{ab}^* & 0 & \Delta_{bb}^* & V_{-k} \\ -V_k^* & 0 & (\omega - \epsilon_k^b) & -\Delta_{ab} \\ 0 & 0 & -\Delta_{ab}^* & (\omega + \epsilon_k^a) \end{pmatrix}, \quad (3.20)$$

$$\mathbf{D}_{\mathbf{u}_1} = \begin{pmatrix} (\omega - \epsilon_k^a) & \Delta_{ab} & -V_k & 1 \\ \Delta_{ab}^* & (\omega + \epsilon_k^b) & \Delta_{bb}^* & 0 \\ -V_k^* & \Delta_{bb} & (\omega - \epsilon_k^b) & 0 \\ 0 & V_{-k}^* & -\Delta_{ab}^* & 0 \end{pmatrix}. \quad (3.21)$$

Notice that, as the electron energy is $\epsilon_k^i = (k^2/2m) - \mu_i$, we assume the following fact:

$$\epsilon_k^{a,b} = \epsilon_{-k}^{a,b}. \quad (3.22)$$

Now we will calculate the anomalous correlation function related to the intra-band order parameter, Δ_{bb} . Using the same method, we write

$$\omega \langle \langle b_{-k-\sigma}^\dagger | b_{k\sigma}^\dagger \rangle \rangle = \frac{1}{2\pi} \{ b_{-k-\sigma}^\dagger, b_{k\sigma} \} + \langle \langle [b_{-k-\sigma}^\dagger, H] | b_{k\sigma} \rangle \rangle.$$

Calculating the commutator and anti-commutator,

$$\begin{aligned} (\omega + \epsilon_{-k}^b) \langle \langle b_{-k-\sigma}^\dagger | b_{k\sigma}^\dagger \rangle \rangle + \Delta_{ab}^* \langle \langle a_{k\sigma}^\dagger | b_{k\sigma}^\dagger \rangle \rangle + \Delta_{bb}^* \langle \langle b_{k\sigma} | b_{k\sigma}^\dagger \rangle \rangle + \\ + V_{-k} \langle \langle a_{-k-\sigma}^\dagger | b_{k\sigma}^\dagger \rangle \rangle = 0. \end{aligned}$$

The equation of motion for the two new Green's functions are

$$(\omega - \epsilon_k^a) \langle \langle a_{k\sigma} | b_{k\sigma}^\dagger \rangle \rangle + \Delta_{ab} \langle \langle b_{-k-\sigma}^\dagger | b_{k\sigma}^\dagger \rangle \rangle - V_k \langle \langle b_{k\sigma} | b_{k\sigma}^\dagger \rangle \rangle = 0$$

$$\begin{aligned} (\omega - \epsilon_k^b) \langle \langle b_{k\sigma} | b_{k\sigma}^\dagger \rangle \rangle - \Delta_{ab} \langle \langle a_{-k-\sigma}^\dagger | b_{k\sigma}^\dagger \rangle \rangle + \Delta_{bb} \langle \langle b_{-k-\sigma}^\dagger | b_{k\sigma}^\dagger \rangle \rangle - \\ - V_k^* \langle \langle a_{k\sigma} | b_{k\sigma}^\dagger \rangle \rangle = 1. \end{aligned}$$

The last equation of motion is

$$(\omega + \epsilon_{-k}^a) \langle \langle a_{-k-\sigma}^\dagger | b_{k\sigma}^\dagger \rangle \rangle - \Delta_{ab}^* \langle \langle b_{k\sigma} | b_{k\sigma}^\dagger \rangle \rangle + V_{-k}^* \langle \langle b_{-k-\sigma}^\dagger | b_{k\sigma}^\dagger \rangle \rangle = 0.$$

Again, we can write the system of equations in matrix form

$$\mathbf{D} \cdot \begin{pmatrix} x_2 = \langle \langle a_{k\sigma} | b_{k\sigma}^\dagger \rangle \rangle \\ y_2 = \langle \langle b_{-k-\sigma}^\dagger | b_{k\sigma}^\dagger \rangle \rangle \\ z_2 = \langle \langle b_{k\sigma} | b_{k\sigma}^\dagger \rangle \rangle \\ u_2 = \langle \langle a_{-k-\sigma}^\dagger | b_{k\sigma}^\dagger \rangle \rangle \end{pmatrix} = \begin{pmatrix} 0 \\ 0 \\ 1 \\ 0 \end{pmatrix}. \quad (3.23)$$

This system of equations enables us to determine the correlation function related to the intra-band order parameter, Δ_{bb} , and to the occupation number in b band (we will also define this in subsection 3.3.4) given by

$$y_2 = \frac{\det(\mathbf{D}_{\mathbf{y}_2})}{\det(\mathbf{D})},$$

related to the intra-band order parameter,

$$z_2 = \frac{\det(\mathbf{D}_{\mathbf{z}_2})}{\det(\mathbf{D})},$$

associated with the occupation number. Where

$$\mathbf{D}_{\mathbf{y}_2} = \begin{pmatrix} (\omega - \epsilon_k^a) & 0 & -V_k & 0 \\ \Delta_{ab}^* & 0 & \Delta_{bb}^* & V_{-k} \\ -V_k^* & 1 & (\omega - \epsilon_k^b) & -\Delta_{ab} \\ 0 & 0 & -\Delta_{ab}^* & (\omega + \epsilon_k^a) \end{pmatrix}, \quad (3.24)$$

$$\mathbf{D}_{\mathbf{z}_2} = \begin{pmatrix} (\omega - \epsilon_k^a) & \Delta_{ab} & 0 & 0 \\ \Delta_{ab}^* & (\omega + \epsilon_k^b) & 0 & V_{-k} \\ -V_k^* & \Delta_{bb} & 1 & -\Delta_{ab} \\ 0 & V_{-k}^* & 0 & (\omega + \epsilon_k^a) \end{pmatrix}. \quad (3.25)$$

Until now the results presented are valid for odd or even-parity hybridization. The next results are specific to anti-symmetric hybridization. In the next subsections, we will calculate the relevant correlation functions and also the excitation energies of the system.

We will assume here that the order parameters Δ_{ab} and Δ_{bb} that appear in the Hamiltonian are real. The hybridization V_k that appears in this same Hamiltonian has to be purely imaginary to preserve time reversal symmetry.

3.3.1 Excitation Energies

The excitation energies of the system are given by the poles of the Green's functions. These poles are obtained from the equation $\det(\mathbf{D}) = 0$. So, we find the following fourth degree equation

$$\omega^4 - 2A_k\omega^2 + B_k = 0 \quad (3.26)$$

with

$$\begin{aligned} A_k &= \frac{\epsilon_k^{a2} + \epsilon_k^{b2} + \Delta_{bb}^2}{2} + \Delta_{ab}^2 + |V_k|^2 \\ B_k &= (\epsilon_k^a \epsilon_k^b + \Delta_{ab}^2 + |V_k|^2)^2 - 4\epsilon_k^a \epsilon_k^b |V_k|^2 + \epsilon_k^{a2} \Delta_{bb}^2 \end{aligned} \quad (3.27)$$

where we consider $V_{-k} = -V_k$ as mentioned before and $\epsilon_{-k}^{a,b} = \epsilon_k^{a,b}$.

The excitation energies are given by,

$$\begin{aligned} \omega_1 &= \sqrt{A_k + \sqrt{A_k^2 - B_k}} = -\omega_3 \\ \omega_2 &= \sqrt{A_k - \sqrt{A_k^2 - B_k}} = -\omega_4. \end{aligned} \quad (3.28)$$

We can write $\det(\mathbf{D})$ as

$$\det(\mathbf{D}) = (\omega + \omega_1)(\omega + \omega_2)(\omega + \omega_3)(\omega + \omega_4) = (\omega^2 - \omega_1^2)(\omega^2 - \omega_2^2).$$

In fact, it is interesting for future calculations to write $1/\det(\mathbf{D})$ as:

$$\frac{1}{\det(\mathbf{D})} = \frac{1}{(\omega_1^2 - \omega_2^2)} \left[\frac{1}{2\omega_1} \left(\frac{1}{\omega - \omega_1} - \frac{1}{\omega + \omega_1} \right) + \frac{1}{2\omega_2} \left(\frac{1}{\omega + \omega_2} - \frac{1}{\omega - \omega_2} \right) \right],$$

where $\omega = \omega \pm i\delta$ and $\delta \rightarrow 0$, with (+) for the retarded component of Green's function and (-) for the advanced. Considering the limit $\delta \rightarrow 0$, we can write

$$\begin{aligned} \frac{1}{\det(\mathbf{D})} &= Re \left(\frac{1}{\det(\mathbf{D})} \right) \mp \\ &\mp \frac{i\pi}{(\omega_1^2 - \omega_2^2)} \left[\frac{1}{2\omega_1} (\delta(\omega + \omega_1) - \delta(\omega - \omega_1)) + \frac{1}{2\omega_2} (\delta(\omega - \omega_2) - \delta(\omega + \omega_2)) \right]. \end{aligned} \quad (3.29)$$

Now, with (-) is for the retarded component and (+) is for the advanced component. We will use these results in next subsection.

3.3.2 Inter-band Order Parameter - Δ_{ab}

The inter-band order parameter defined by equation (3.12) is obtained using for:

$$\begin{aligned} \text{Im}(y_1^r) = & -\frac{\pi}{\omega_1^2 - \omega_2^2} \left[\frac{1}{2\omega_1} (\delta(\omega + \omega_1) - \delta(\omega - \omega_1)) + \frac{1}{2\omega_2} (\delta(\omega - \omega_2) - \delta(\omega + \omega_2)) \right] \\ & \times \left[-(\Delta_{ab}\omega^2 + (\epsilon_k^a \Delta_{ab} - \epsilon_k^b \Delta_{ab})\omega - \epsilon_k^a \epsilon_k^b \Delta_{ab} - |V_k|^2 \Delta_{ab} - \Delta_{ab}^3) \right]. \end{aligned}$$

We can use the fluctuation-dissipation theorem, written in a convenient way, to find the following relation

$$\Delta_{ab} = g_{ab} \sum_{k\sigma} \frac{1}{\pi} \int d\omega f(\omega) \text{Im}(y_1^r).$$

Using the properties of the delta function on the integral, we can perform the ω integral. Also, we will use the following properties of the Fermi-Dirac function

$$\begin{aligned} f(-x) - f(x) &= \tanh \beta x / 2 \\ f(-x) + f(x) &= 1. \end{aligned} \quad (3.30)$$

So

$$\begin{aligned} \Delta_{ab} = & \frac{g_{ab}}{2} \sum_{k\sigma} \left[\frac{\Delta_{ab} (\omega_1 \tanh(\beta\omega_1/2) - \omega_2 \tanh(\beta\omega_2/2))}{\omega_1^2 - \omega_2^2} + \right. \\ & \left. - \frac{(\Delta_{ab}\epsilon_k^a \epsilon_k^b + \Delta_{ab}|V_k|^2 + \Delta_{ab}^3)}{\omega_1^2 - \omega_2^2} \left(\frac{\tanh(\beta\omega_1/2)}{\omega_1} - \frac{\tanh(\beta\omega_2/2)}{\omega_2} \right) \right]. \end{aligned} \quad (3.31)$$

By considering $T = 0K$ in equation (3.31) and using the definition (3.12), we get

$$\Delta_{ab} = \frac{g_{ab}}{2} \sum_{k\sigma} \left[\frac{\Delta_{ab}}{\omega_1 + \omega_2} + \frac{(\Delta_{ab}\epsilon_k^a \epsilon_k^b + \Delta_{ab}|V_k|^2 + \Delta_{ab})}{\omega_1 \omega_2 (\omega_1 + \omega_2)} \right] \quad (3.32)$$

We want to be able to extend our calculations to the strong coupling regime. To do so, it is necessary to solve self-consistently three equations, namely those of the occupation number, inter-band order parameter and intra-band one. The equation for the inter-band order parameter is given by (3.32), but we must regulate the ultraviolet divergence in this equation. So

the definition of low energy limit of the two-body problem in the vacuum [78] for a three dimensional system must be used:

$$\frac{1}{g_{ab}} = -\frac{m^*}{4\pi a_s} + \sum_{k\sigma} [f_1(k) - f_1(k \rightarrow \infty)]. \quad (3.33)$$

where a_s are the s-wave scattering length. We assume that the bands are homothetic, so

$$\epsilon_k^a = \epsilon_k - \mu \quad \text{and} \quad (3.34)$$

$$\epsilon_k^b = \alpha\epsilon_k - \mu \quad (3.35)$$

where $\epsilon_k = k^2/2m_a$, and $m_a/m_b = \alpha$. Notice that $m^* = m_a/(1 + \alpha)$. The Fermi energy can be written as $E_F = k_{F,a(b)}^2/2m_{a(b)}$, where we can obtain the relation $k_{F,b} = k_{F,a}/\sqrt{\alpha}$

We define

$$f_1(k) = \left[\frac{1}{\omega_1 + \omega_2} + \frac{(\epsilon_k^a \epsilon_k^b + |V_k|^2 + \Delta_{ab}^2)}{\omega_1 \omega_2 (\omega_1 + \omega_2)} \right].$$

So,

$$-\frac{m^*}{4\pi a_s} = \frac{1}{2} \sum_{k\sigma} \left[\frac{1}{\omega_1 + \omega_2} + \frac{\epsilon_k^a \epsilon_k^b + |V_k|^2 + \Delta_{ab}^2}{\omega_1 \omega_2 (\omega_1 + \omega_2)} - f_1(k \rightarrow \infty) \right]$$

calculating the limit $f_1(k \rightarrow \infty) = 2/(1 + \alpha)\epsilon_k$.

The sum can be transformed in an integral using,

$$\sum_{k\sigma} \rightarrow \frac{1}{(2\pi)^3} k_{F,a}^3 \int_{-\infty}^{\infty} d\tilde{k}_x \int_{-\infty}^{\infty} d\tilde{k}_y \int_{-\infty}^{\infty} d\tilde{k}_z \quad (3.36)$$

due to the regulation procedure, where the limits now can be extended to infinity. The *tilde* means normalization by the Fermi energy. Finally, we get

$$\begin{aligned} -\frac{1}{k_{F,a} a_s} &= \frac{1 + \alpha}{(2\pi)^2} \int_{-\infty}^{\infty} d\tilde{k}_x \int_{-\infty}^{\infty} d\tilde{k}_y \int_{-\infty}^{\infty} d\tilde{k}_z \left[\frac{1}{(\tilde{\omega}_1 + \tilde{\omega}_2)} + \right. \\ &\quad \left. + \frac{(\tilde{\Delta}_{ab}^2 + \tilde{\epsilon}_k^a \tilde{\epsilon}_k^b + \tilde{V}_k^2)}{\tilde{\omega}_1 \tilde{\omega}_2 (\tilde{\omega}_1 + \tilde{\omega}_2)} - \frac{2}{(1 + \alpha)(\tilde{k}_x^2 + \tilde{k}_y^2 + \tilde{k}_z^2)} \right]. \end{aligned} \quad (3.37)$$

3.3.3 Intra-band Order Parameter - Δ_{bb}

Now we will find the intra-band order parameter. It is related to $Im(y_2^r)$:

$$Im(y_2^r) = -\frac{\pi}{\omega_1^2 - \omega_2^2} \times \\ \times \left[\frac{1}{2\omega_1} (\delta(\omega + \omega_1)\delta(\omega - \omega_1)) + \frac{1}{2\omega_2} (\delta(\omega - \omega_2) - \delta(\omega + \omega_2)) \right] \times \\ \times \left[-(\Delta_{bb}\omega^2 - \Delta_{bb}\epsilon_k^{a2}) \right].$$

We have

$$\Delta_{bb} = g_{bb} \sum_{k\sigma} \frac{1}{\pi} \int d\omega f(\omega) Im(y_2^r).$$

Using the properties of the delta function on the frequency integral, we can write the solution of the ω integral. Also using (3.30), we can write

$$\Delta_{bb} = \frac{g_{bb}}{2} \sum_{k\sigma} \left[\frac{\Delta_{bb} (\omega_1 \tanh(\beta\omega_1/2) \omega_2 \tanh(\beta\omega_2/2))}{\omega_1^2 - \omega_2^2} \right. \\ \left. - \frac{\Delta_{bb}\epsilon_k^{a2}}{\omega_1^2 - \omega_2^2} \left(\frac{\tanh(\beta\omega_1/2)}{\omega_1} - \frac{\tanh(\beta\omega_2/2)}{\omega_2} \right) \right]. \quad (3.38)$$

At $T = 0K$, we get

$$\Delta_{bb} = \frac{g_{bb}}{2} \sum_{k\sigma} \left[\frac{\Delta_{bb}}{\omega_1 + \omega_2} + \frac{\Delta_{bb}\epsilon_k^{a2}}{\omega_1\omega_2(\omega_1 + \omega_2)} \right] \quad (3.39)$$

We use again the following regularization relation

$$\frac{1}{g_{bb}} = -\frac{m_b}{4\pi a_{sb}} + \sum_{k\sigma} [f_2(k) - f_2(k \rightarrow \infty)] \quad (3.40)$$

where $m_b = m_a/\alpha$ and now a_{sb} is the s-wave scattering length in b -band. Being

$$f_2(k) = \left[\frac{1}{\omega_1 + \omega_2} + \frac{\epsilon_k^{a2}}{\omega_1\omega_2(\omega_1 + \omega_2)} \right].$$

So

$$-\frac{m_b}{4\pi a_{sb}} = \frac{1}{2} \sum_{k\sigma} \left[\frac{1}{\omega_1 + \omega_2} + \frac{\epsilon_k^{a2}}{\omega_1\omega_2(\omega_1 + \omega_2)} - f_2(k \rightarrow \infty) \right],$$

calculating the limit $f_2(k \rightarrow \infty) = 1/\alpha\epsilon_k$.

We used the transformation (3.36) and write

$$\begin{aligned}
-\frac{1}{k_F a_{sb}} &= \frac{\alpha}{(2\pi)^2} \int_{-\infty}^{\infty} d\tilde{k}_x \int_{-\infty}^{\infty} d\tilde{k}_y \int_{-\infty}^{\infty} d\tilde{k}_z \times \\
&\times \left[\frac{1}{(\tilde{\omega}_1 + \tilde{\omega}_2)} + \frac{\tilde{\epsilon}_k^{a2}}{\tilde{\omega}_1 \tilde{\omega}_2 (\tilde{\omega}_1 + \tilde{\omega}_2)} - \frac{1}{\alpha(\tilde{k}_x^2 + \tilde{k}_y^2 + k_z^2)} \right].
\end{aligned} \tag{3.41}$$

3.3.4 Occupation Number

In this section, the total occupation number will be calculated. This information is crucial to find the order parameter specially in strong coupling regime. The total occupation number, intra-band order parameter and inter-band order parameter expressions form a closed set of equations that should be solved self-consistently.

The total occupation number is given by the sum of occupation numbers in a and b bands:

$$\begin{aligned}
n_a &= \sum_{k\sigma} \langle a_{k\sigma}^\dagger a_{k\sigma} \rangle \\
n_b &= \sum_{k\sigma} \langle b_{k\sigma}^\dagger b_{k\sigma} \rangle.
\end{aligned} \tag{3.42}$$

Therefore, the total occupation number is

$$\begin{aligned}
n &= n_a + n_b \\
n &= \sum_{k\sigma} \left(\langle a_{k\sigma}^\dagger a_{k\sigma} \rangle + \langle b_{k\sigma}^\dagger b_{k\sigma} \rangle \right).
\end{aligned} \tag{3.43}$$

We will start by calculating n_a . The occupation in a band is related to the imaginary part of x_1 given by

$$\begin{aligned}
Im(x_1^r) &= -\frac{\pi}{\omega_1^2 - \omega_2^2} \left[\frac{1}{2\omega_1} (\delta(\omega + \omega_1) - \delta(\omega - \omega_1)) + \frac{1}{2\omega_2} (\delta(\omega - \omega_2) - \delta(\omega + \omega_2)) \right] \\
&\times (\omega^3 + \epsilon_k^a \omega^2 - (\epsilon_k^{b2} + |V_k|^2 + \Delta_{bb}^2 + \Delta_{ab}^2) \omega - \epsilon_k^a \epsilon_k^{b2} + \epsilon_k^b |V_k|^2 - \epsilon_k^a \Delta_{bb}^2 + \epsilon_k^b \Delta_{ab}^2).
\end{aligned}$$

We can use the following relation

$$n_a = \sum_{k\sigma} \frac{1}{\pi} \int d\omega f(\omega) Im(x_1^r)$$

and find the occupation number in a band. Using the properties of the delta function on integral, we can write the solution of ω integral. Also using (3.30), we can write

$$n_a = -\frac{1}{2} \sum_{k\sigma} \left\{ -1 + (\omega_1^2 - \omega_2^2) + \frac{\epsilon_k^a}{\omega_1^2 - \omega_2^2} \left(\omega_1 \tanh\left(\frac{\beta\omega_1}{2}\right) - \omega_2 \tanh\left(\frac{\beta\omega_2}{2}\right) \right) - \left[\frac{\epsilon_k^a \epsilon_k^{b2} - \epsilon_k^b |V_k|^2 + \epsilon_k^a \Delta_{bb}^2 - \epsilon_k^b \Delta_{ab}^2}{\omega_1^2 - \omega_2^2} \right] \left(\frac{\tanh(\beta\omega_1/2)}{\omega_1} - \frac{\tanh(\beta\omega_2/2)}{\omega_2} \right) \right\}. \quad (3.44)$$

At $T = 0K$, we get

$$n_a = \frac{1}{2} \sum_{k\sigma} \left\{ 1 + \frac{\epsilon_k^a}{\omega_1 + \omega_2} + \frac{\epsilon_k^a \epsilon_k^{b2} - \epsilon_k^b |V_k|^2 + \epsilon_k^a \Delta_{bb}^2 - \epsilon_k^b \Delta_{ab}^2}{\omega_1 \omega_2 (\omega_1 + \omega_2)} \right\}. \quad (3.45)$$

Now, we will repeat the same procedure done before to find the occupation number in the b band. First we find the imaginary part of z_2 :

$$Im(z_2^r) = -\frac{\pi}{\omega_1^2 - \omega_2^2} \left[\frac{1}{2\omega_1} (\delta(\omega + \omega_1) - \delta(\omega - \omega_1)) + \frac{1}{2\omega_2} (\delta(\omega - \omega_2) - \delta(\omega + \omega_2)) \right] \times (\omega^3 + \epsilon_k^b \omega^2 - (\epsilon_k^{b2} + |V_k|^2 + \Delta_{ab}^2) \omega - \epsilon_k^{a2} \epsilon_k^b + \epsilon_k^a |V_k|^2 - \epsilon_k^a \Delta_{ab}^2).$$

Then, we use the following expression

$$n_b = \sum_{k\sigma} \frac{1}{\pi} \int d\omega f(\omega) Im(z_2^r),$$

to find n_b . Again, using the properties of the delta function on integral, we can perform the ω integral. Also, by using (3.30), we can write

$$n_b = \sum_{k\sigma} \frac{1}{2} \left\{ 1 + \frac{\epsilon_k^b}{\omega_1^2 - \omega_2^2} \left(\omega_1 \tanh\left(\frac{\beta\omega_1}{2}\right) - \omega_2 \tanh\left(\frac{\beta\omega_2}{2}\right) \right) + \frac{\epsilon_k^{a2} \epsilon_k^b - \epsilon_k^a |V_k|^2 + \epsilon_k^a \Delta_{ab}^2}{\omega_1^2 - \omega_2^2} \left(\frac{\tanh(\beta\omega_1/2)}{\omega_1} - \frac{\tanh(\beta\omega_2/2)}{\omega_2} \right) \right\}. \quad (3.46)$$

At $T = 0K$, we get

$$n_b = \sum_{k\sigma} \frac{1}{2} \left\{ 1 + \frac{\epsilon_k^b}{\omega_1 + \omega_2} + \frac{\epsilon_k^{a2} \epsilon_k^b - \epsilon_k^a |V_k|^2 + \epsilon_k^a \Delta_{ab}^2}{\omega_1 \omega_2 (\omega_1^2 + \omega_2^2)} \right\}. \quad (3.47)$$

Once we know n_a and n_b we can use equation (3.43) to write the total occupation number for $T = 0K$,

$$n = \frac{1}{2} \sum_{k\sigma} \left[2 - \frac{\epsilon_k^a + \epsilon_k^b}{\omega_1 + \omega_2} - \frac{(\epsilon_k^a + \epsilon_k^b) (\epsilon_k^a \epsilon_k^b - |V_k|^2 + \Delta_{ab}^2) + \epsilon_k^a \Delta_{bb}^2}{\omega_1 \omega_2 (\omega_1 + \omega_2)} \right] \quad (3.48)$$

Using the transformation (3.36) and the relation:

$$\begin{aligned} n &= \frac{1}{(2\pi)^3} \frac{4}{3} \pi k_{F,a}^3 + \frac{1}{(2\pi)^3} \frac{4}{3} \pi k_{F,b}^3 \\ n &= \frac{k_{F,a}^3}{6\pi^2} \left(\frac{\alpha^{3/2} + 1}{\alpha^{3/2}} \right), \end{aligned} \quad (3.49)$$

we write

$$\begin{aligned} 1 &= \frac{3}{8\pi} \frac{\alpha^{3/2}}{\alpha^{3/2} + 1} \int_{-\infty}^{\infty} d\tilde{k}_x \int_{-\infty}^{\infty} d\tilde{k}_y \int_{-\infty}^{\infty} d\tilde{k}_z \times \\ &\quad \left[2 - \frac{\tilde{\epsilon}_k^a + \tilde{\epsilon}_k^b}{\tilde{\omega}_1 + \tilde{\omega}_2} - \frac{(\tilde{\epsilon}_k^a + \tilde{\epsilon}_k^b) (\tilde{\epsilon}_k^a \tilde{\epsilon}_k^b - |\tilde{V}_k|^2 + \tilde{\Delta}_{ab}^2) + \tilde{\epsilon}_k^a \tilde{\Delta}_{bb}^2}{\tilde{\omega}_1 \tilde{\omega}_2 (\tilde{\omega}_1 + \tilde{\omega}_2)} \right]. \end{aligned} \quad (3.50)$$

3.3.5 Induced Order Parameter - Δ_{aa}

The anomalous correlation function Δ_{aa} is a new feature in the problem. It is induced by hybridization and inter-band interactions since there are no interactions in a -band. Here we will investigate if Δ_{aa} is different from zero for this anti-symmetric hybridization case. We will also indicate what is essential to induce this correlation.

The induced order parameter is calculated by the expression

$$\Delta_{aa}^*(k, \sigma) = \frac{1}{\pi} \int d\omega f(\omega) (u_1^r - u_1^a),$$

where

$$u_1^r = \frac{\Delta_{bb} (\Delta_{ab}^2 - V_k^{*2}) + 2\epsilon_k^b \Delta_{ab} V_k^*}{((\omega + i\delta)^2 - \omega_1^2) ((\omega + i\delta)^2 - \omega_2^2)} \quad (3.51)$$

and

$$u_1^a = \frac{\Delta_{bb} (\Delta_{ab}^2 - V_k^{*2}) + 2\epsilon_k^b \Delta_{ab} V_k^*}{((\omega - i\delta)^2 - \omega_1^2) ((\omega - i\delta)^2 - \omega_2^2)}, \quad (3.52)$$

where $\delta \rightarrow \infty$.

Solving the integral, we can write

$$\Delta_{aa}^*(k) = -\frac{1}{2} \left[\frac{2\epsilon_k^b V_k^* \Delta_{ab} - \Delta_{bb} (V_k^{*2} - \Delta_{ab}^2)}{\omega_1^2 - \omega_2^2} \times \left(\frac{\tanh(\beta\omega_1/2)}{\omega_1} - \frac{\tanh(\beta\omega_2/2)}{\omega_2} \right) \right]. \quad (3.53)$$

At $T = 0K$, we get

$$\Delta_{aa}^*(k, \sigma) = \frac{1}{4\pi} \left[\frac{2\epsilon_k^b V_k^* \Delta_{ab} - \Delta_{bb} (V_k^{*2} - \Delta_{ab}^{*2})}{\omega_1 \omega_2 (\omega_1 + \omega_2)} \right]. \quad (3.54)$$

or

$$\Delta_{aa}(k, \sigma) = \frac{1}{4\pi} \left[\frac{2\epsilon_k^b V_k \Delta_{ab} - \Delta_{bb}(k, \sigma) (V_k^2 - \Delta_{ab}^2)}{\omega_1 \omega_2 (\omega_1 + \omega_2)} \right]. \quad (3.55)$$

Notice that this anomalous correlation function appears due to the influence of hybridization and/or inter-band interactions even in the absence of attractive interactions in a -band.

There is an special behavior when the second term in the right side of equation (3.55) is neglected, i.e., when $2\epsilon_k^b V_k \Delta_{ab} \gg \Delta_{bb}(k, \sigma) (V_k^2 - \Delta_{ab}^2)$. If it is true, we can write

$$\Delta_{aa}(k, \sigma) \approx \frac{1}{2\pi} \left[\frac{\epsilon_k^b V_k \Delta_{ab}}{\omega_1 \omega_2 (\omega_1 + \omega_2)} \right]. \quad (3.56)$$

Equation (3.56) give to us an interesting information about the induced parameter: Δ_{aa} follows the parity of V_k . In this thesis we assume that V_k is anti-symmetric in k -space, thus Δ_{aa} has odd-parity in k -space.

The induced order parameter Δ_{aa} should be anti-symmetric. This can be written as a product of a spin part and a spatial part (Fourier transformed) as,

$$\Delta_{aa} = R(k)S(\sigma). \quad (3.57)$$

If the spacial contribution is anti-symmetric and the total function is necessarily anti-symmetric due to the fermionic character of the pair, the spin contributions must be symmetric. This indicates that the induced order parameter has triplet character. In fact, since Δ_{aa} relates σ and $-\sigma$, we conclude that this induced order parameter is related with the momentum angular component $l = 1$ and $m = 0$: $(|\uparrow\downarrow\rangle + |\downarrow\uparrow\rangle)/2$.

This anti-symmetric spacial behavior of Δ_{aa} is expected in p -wave superconductors. One of most remarkable work using p -wave superconductors was done by Kitaev [23], he shows that Majorana fermions exist in the ends of p -wave superconductor chain. The Kitaev Hamiltonian is written as

$$H_K = \sum_{i,j} t_{ij} c_i^\dagger c_j + \sum_{i,j} \Delta_{ij} (c_i^\dagger c_j^\dagger + c_i c_j), \quad (3.58)$$

where the order parameter has the important characteristic: $\Delta_{ji} = -\Delta_{ij}$ or $\Delta_{-k} = -\Delta_k$, the same property of Δ_{aa} .

So, in the limit $2\epsilon_k^b V_k \Delta_{ab} \gg \Delta_{bb}(k, \sigma) (V_k^2 - \Delta_{ab}^2)$, we can propose that this block of a metal superconductor with a p -metal superconductor studied here produces, via proximity effects, a Kitaev's chain. This system is very interesting because we do not need any external magnetic field, as in Alicea [70], to produce this anti-symmetric behavior in the induced order parameter.

3.4 Self Consistent Equations

Now we can summarize the results obtained in the last subsection – equations (3.37), (3.41) and (3.50). These equations should be solved together in the self-consistent way, using numerical methods. In order to implement these numerical methods we need write:

$$\begin{aligned} \epsilon_k^a &= \epsilon_k - \mu \quad \text{and} \quad \epsilon_k^b = \alpha \epsilon_k - \mu \\ \tilde{\epsilon}_k &= E_F \left(\tilde{k}_z^2 + \tilde{k}_\perp^2 \right) \\ \tilde{V}_k &= i\tilde{\gamma} (k_x + k_y). \end{aligned} \quad (3.59)$$

We assumed that the bands are homotetic, i.e., the dispersion relations for the a and b quasi-particles differ only in their effective masses, with their ratio, $m_a/m_b = \alpha$. Also, it was assumed here that the hybridization is mostly effective in a plane xy as for tetragonal systems. This allows us to write the a and b energies as above. Remember that we consider $E_F = k_{F,a(b)}^2/2m_{a(b)}$ the Fermi energy.

The complete case considers attractive interactions in the b band and between the $a - b$ band, and also anti-symmetric hybridization between a and b bands. Solve it is numerically costly, so we will study some particular cases in the next section.

3.5 Particular Case

3.5.1 Special Case I - $g_{bb} = 0$

In this section we will study a special case of our problem. If we “turn off” the attractive interaction in b -band, consider only inter-band attractive interactions, we recover results found by Alicea and shown in appendix C.

If we consider $g_{bb} = 0$ in equation (3.11) we get a new simplified Hamiltonian:

$$H = \sum_{k,\sigma} \left(\epsilon_k^a a_{k\sigma}^\dagger a_{k\sigma} + \epsilon_k^b b_{k\sigma}^\dagger b_{k\sigma} \right) - \sum_{k\sigma} \left(\Delta_{ab} a_{k\sigma}^\dagger b_{-k-\sigma}^\dagger + \Delta_{ab}^* b_{-k-\sigma} a_{k\sigma} \right) + \sum_{k\sigma} \left(V_k a_{k\sigma}^\dagger b_{k\sigma} + V_k^* b_{k\sigma}^\dagger a_{k\sigma} \right), \quad (3.60)$$

where we can define the inter-band order parameter, Δ_{ab} , as in equation (3.12) and the induced parameter, Δ_{aa} , as in equation (3.14), but there will be one more induced parameter that we define as

$$\Delta'_{bb}(k, \sigma) = \langle b_{k\sigma} b_{-k-\sigma} \rangle. \quad (3.61)$$

Using results previously calculated we can write

$$\Delta_{ab} = \frac{g_{ab}}{4\pi} \sum_{k\sigma} \left[\frac{\Delta_{ab}}{\omega'_1 + \omega'_2} + \frac{(\Delta_{ab} \epsilon_k^a \epsilon_k^b + \Delta_{ab} |V_k|^2 + \Delta_{ab} |\Delta_{ab}|^2)}{\omega'_1 \omega'_2 (\omega'_1 + \omega'_2)} \right], \quad (3.62)$$

$$\Delta'_{bb}(k, \sigma) = -\frac{1}{2\pi} \left[\frac{\epsilon_k^a V_k^* \Delta_{ab}}{\omega'_1 \omega'_2 (\omega'_1 + \omega'_2)} \right], \quad (3.63)$$

and

$$\Delta_{aa}(k, \sigma) = \frac{1}{2\pi} \left[\frac{\epsilon_k^b V_k \Delta_{ab}}{\omega'_1 \omega'_2 (\omega'_1 + \omega'_2)} \right]. \quad (3.64)$$

Where ω'_1 and ω'_2 are the energies (3.29) with $g_{bb} = 0$.

Notice that the inter-band order parameter, Δ_{ab} , is symmetric even if V_k is anti-symmetric, that is equivalent to expression (C.28). We also generate, via proximity effect, two “order parameters” Δ_{aa} and Δ'_{bb} that have $p_x \pm ip_y$ pairing with opposite chirality for upper/lower bands, like equations (C.26) and (C.27). So, putting $g_{bb} = 0$, we find the same results from Alicea [70].

In this limit, $g_{bb} = 0$, our problem maps onto that of spinless fermions with Spin Orbit Coupling (SOC) and $p_x + ip_y$ pairing. This mapping can be easily seen when we make the following associations:

$$\begin{aligned}\epsilon_k^a &\equiv \xi_{k\uparrow} = \epsilon_k - \mu_\uparrow \\ \epsilon_k^b &\equiv \xi_{k\downarrow} = \epsilon_k - \mu_\downarrow \\ V_k &\equiv \lambda k_\perp e^{-i\phi_k},\end{aligned}\tag{3.65}$$

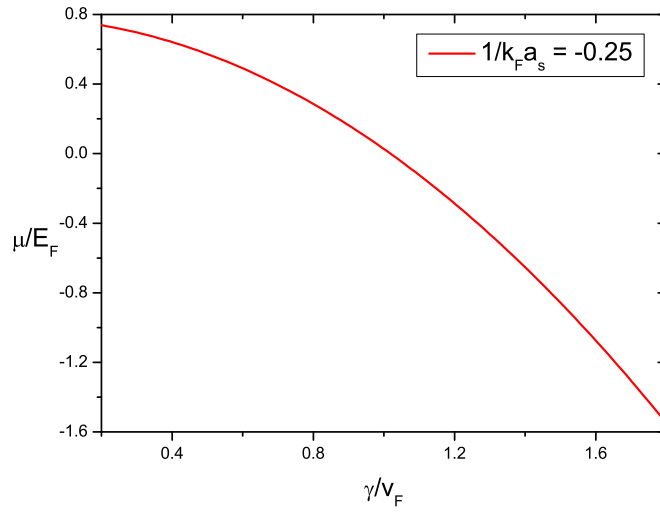
where $\epsilon_k = k^2/2m$, $\mu_{\uparrow(\downarrow)}$ is the chemical potential of *up* (*down*) spin band, λ is the strength of Rashba spin-orbit coupling and $\phi_k = \arg(k_x + ik_y)$. We can write (3.60) as

$$\begin{aligned}H &= \sum_k \left(\xi_{k\uparrow} a_k^\dagger a_k + \xi_{k\downarrow} b_k^\dagger b_k \right) - \sum_k \left(\Delta_{ab} a_k^\dagger b_{-k}^\dagger + \Delta_{ab}^* b_{-k} a_k \right) + \\ &+ \sum_k \lambda k_\perp \left(e^{-i\phi_k} a_k^\dagger b_{k\sigma} + e^{i\phi_k} b_k^\dagger a_{k\sigma} \right).\end{aligned}\tag{3.66}$$

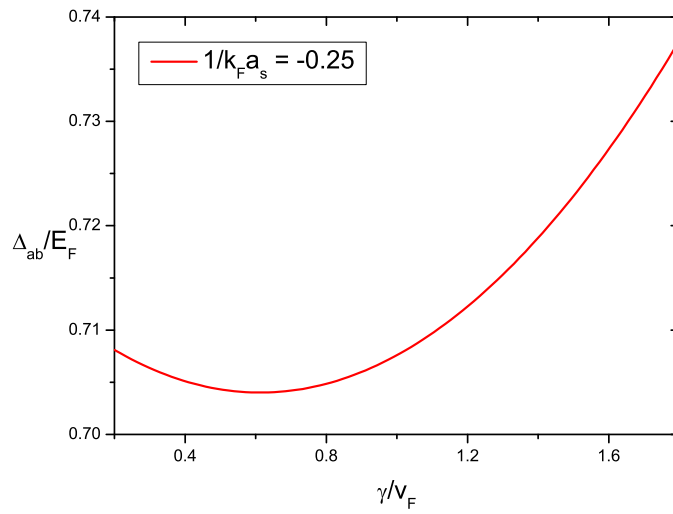
It is easy to see that the *a* band represents the *up* spin band while the *b* band represent the *down* spin band.

This mapping is interesting because this spinless fermions with $p_x + ip_y$ pairing problem is the canonical example of a topological superconductor supporting a single Majorana bound state [79, 80]. This is a 2-D interesting system, but here we focus only in an 1-D problem.

We present in the Figure (3.2) the self-consistent solution for the chemical potential and the inter-band order parameter. This figure show us an interesting property of this type of system with odd-parity hybridization: the hybridization *enhances* the superconductivity.



(a) Chemical potential



(b) Inter-band Order Parameter

Figure 3.2: We present here the solution of the two self-consistent equations for $\alpha = 0.5$ and $1/k_F a_s = -0.25$.

3.5.2 Special Case II - $g_{ab} = 0$

Considering $g_{ab} = 0$ we find a “new” Hamiltonian:

$$\begin{aligned}
H = & \sum_{k,\sigma} \left(\epsilon_k^a a_{k\sigma}^\dagger a_{k\sigma} + \epsilon_k^b b_{k\sigma}^\dagger b_{k\sigma} \right) - \\
& - \frac{1}{2} \sum_{k\sigma} \left(\Delta_{bb}(k) b_{k\sigma}^\dagger b_{-k-\sigma}^\dagger + \Delta_{bb}^*(k) b_{-k-\sigma} b_{k\sigma} \right) + \sum_{k\sigma} \left(V_k a_{k\sigma}^\dagger b_{k\sigma} + V_k^* b_{k\sigma} a_{k\sigma} \right).
\end{aligned} \tag{3.67}$$

The order parameter that characterizes the superconductivity in the b-band is the intra-band order parameter Δ_{bb} , that is defined in equation (3.13).

Our intention is to find the intra-band superconductivity order parameter and the occupation number. We can use the results previously calculated putting $g_{ab} = 0$, i.e., $\Delta_{ab} = 0$. The intra-band order parameter is given by the equation (3.39):

$$\Delta_{bb} = \sum_{k\sigma} \left[\frac{\Delta_{bb}}{\omega_1 + \omega_2} + \frac{\Delta_{bb} \epsilon_k^{a2}}{\omega_1 \omega_2 (\omega_1 + \omega_2)} \right],$$

with $g_{ab} = 0$. Or we can use equation (3.41), with $\Delta_{ab} = 0$, and find the equation for intra-band order parameter when we consider strong coupling

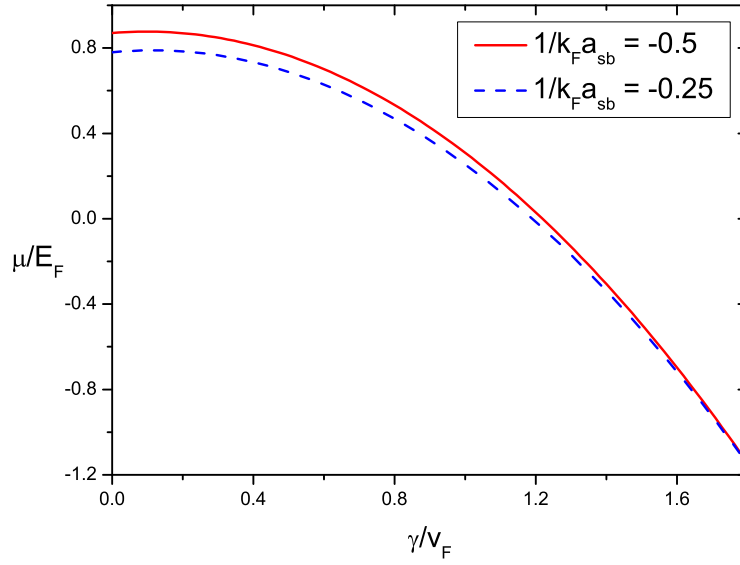
$$\begin{aligned}
-\frac{1}{k_F a_{sb}} = & \\
= & \frac{\alpha}{(2\pi)^2} \int_0^\infty d\tilde{k}_z \int_0^\infty d\tilde{d}_\perp \tilde{k}_\perp \left[\frac{1}{\tilde{\omega}_1 + \tilde{\omega}_2} + \frac{\tilde{\epsilon}_k^{a2}}{\tilde{\omega}_1 \tilde{\omega}_2 (\tilde{\omega}_1 + \tilde{\omega}_2)} - \frac{1}{\alpha (\tilde{k}_z^2 + \tilde{k}_\perp^2)} \right].
\end{aligned} \tag{3.68}$$

Now, from equation (3.50), we can write

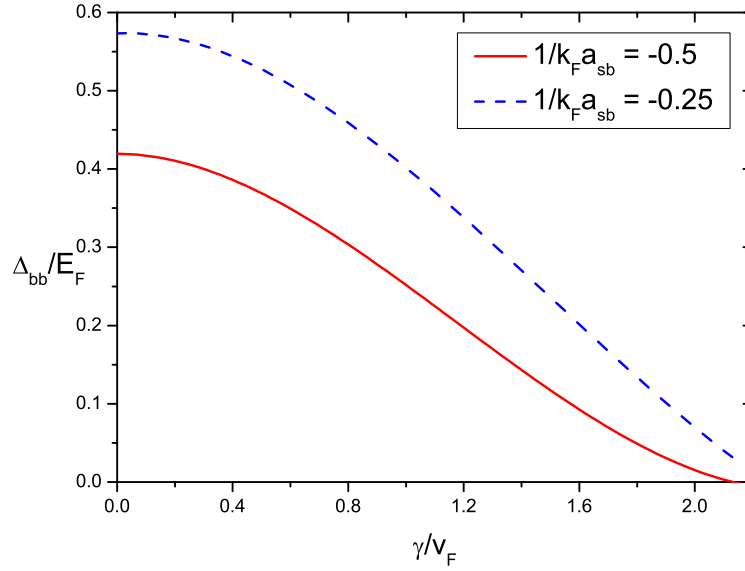
$$\begin{aligned}
1 = & \frac{3}{8\pi} \frac{\alpha^{3/2}}{\alpha^{3/2} + 1} \int_0^\infty d\tilde{k}_z \int_0^\infty d\tilde{k}_\perp \tilde{k}_\perp \times \\
& \times \left[2 - \frac{\tilde{\epsilon}_k^a + \tilde{\epsilon}_k^b}{\tilde{\omega}_1 + \tilde{\omega}_2} - \frac{(\tilde{\epsilon}_k^a + \tilde{\epsilon}_k^b) (\tilde{\epsilon}_k^a \tilde{\epsilon}_k^b - |\tilde{V}_k|^2) + \tilde{\epsilon}_k^a |\tilde{\Delta}_{bb}|^2}{\tilde{\omega}_1 \tilde{\omega}_2 (\tilde{\omega}_1 + \tilde{\omega}_2)} \right].
\end{aligned} \tag{3.69}$$

Again, we have a self-consistent system with only two equations, that must be solved numerically. We present the self-consistent solution for the chemical potential in terms of $\gamma/v_F = \tilde{\gamma}$ in Fig. (3.3).

You can notice that the behavior of Δ_{bb} is the same both for even or odd parity, i.e., the hybridization destroy the superconductivity.



(a) The chemical potential.



(b) The intra-band order parameter.

Figure 3.3: We present here the solution of the two self-consistent equations for $\alpha = 0.5$ and two values of $1/k_F a_{sb}$: $1/k_F a_{sb} = -0.5$ and $1/k_F a_{sb} = -0.25$.

3.6 Conclusion

In this chapter, we studied the influence of an odd-parity hybridization in the superconducting state. First, when discussing the origin of an odd-parity hybridization, we showed that the anti-symmetric hybridization appears when it mixes orbitals with angular momentum differing by an odd number as for l and $l + 1$.

Next, we studied a two-band model with an odd-parity hybridization between the two bands and an attractive interaction in one of the bands. We solved this problem using the Green's function formalism. We found the intra-band order parameter, the inter-band order parameter and the occupation number equations and we solved them self-consistently. We saw that an induced order parameter appears due proximity effect. We can conclude that this induced order parameter has an anti-symmetric character in k -space allowing us to propose that the mechanism studied here is one possible way to produce a Kitaev's chain [23] without the necessity of spin orbit coupling or any external parameters, such as an external magnetic field. This is very interesting because in the ends of a Kitaev chain there are exist Majorana [23, 77]. This conclusion is one of most remarkable result os this thesis because the Majorana fermions are promising candidates to acts as a q-bits in quantum computers.

We also studied two special cases. In the first, we turned off the intra-band attractive interaction. First we noticed that we recover the results from Alicea [70] using a different formalism. We find two induced parameters with opposite chirality for a and b bands. We also saw that in this case it is possible to map our problem onto that of spinless fermions with SOC, where the a band is the \uparrow band and the b band is the \downarrow band.

The second special case studied is when we only consider intra-band attractive interactions. This case is simpler than the complete problem and gives a surprising behavior of the superconductivity parameter. Unlike when hybridization is symmetric, if we consider odd-parity hybridization we conclude that the hybridization enhances superconductivity [66].

Chapter 4

Spin Current in the Presence of Dzyaloshinskii-Moriya Interaction

Magnetic properties of low dimensional metallic magnets in general is understood by the competition of three main interactions: the exchange interaction designed by Heisenberg model (ferro- or antiferromagnetic, long or short range), the magneto-crystalline anisotropy (which induces easy axes or easy planes for the magnetic moments) and the dipole-dipole interaction which plays a big role in nanostructures [81]. However, for a correct description of these materials, it is also necessary to consider other types of interactions, like Spin-Orbit Coupling (SOC).

The spin orbit coupling is not only the origin of the magnetocrystalline anisotropy in bulk systems, but it also has large effects in nanostructures. The SOC is known to play an important role in nanostructures since inversion symmetry is broken near surfaces and interfaces. It is a small effect but with important consequences both on the magnetic arrangement near a surface and on transport properties. Concerning magnetic arrangement, it was shown that magneto-crystalline anisotropy can be different at surfaces and in the volume, inducing some possible reorientation of the magnetic moments. Another consequence of SOC is the existence of anti-symmetric Dzyaloshinskii-Moriya exchange near the surface [29].

In this chapter we will discuss about the Dzyaloshinskii-Moriya (DM) interaction. It is driven by SOC and only appears in structures that lack inversion symmetry. This interaction has important consequences on magnetic structures both in bulk systems and nanomaterials where it can lead to non-collinear chiral magnetic structures [82, 83] or to the stabilization of skyrmions [84].

Concerning transport, SOC has also important consequences, e. g. anomalous Hall effect in bulk systems [85]. In nanostructures, the effect of SOC is usually introduced through Rashba coupling at interfaces [86]. However there is no study of the influence of DM coupling on transport in nanostructures. So, in this chapter we will propose a simple model to study this influence. After introducing a possible mechanism responsible for this DM interaction, we study its effect using a toy model which has the advantage of providing a simple solution.

4.1 Introduction: Spin-Orbit Coupling (SOC)

An important part of the technology developed today in the field of sensors or data storage is based on the control of the spin degree of freedom. The most important spin-dependent effect in metallic systems is the giant magnetoresistance (GMR) effect [25, 26], discovered in 1988. After this discovery, appeared a new interesting field that aims at identifying, understanding, controlling and utilizing spin-dependent phenomena, known as *Spintronics*.

A very important interaction influencing magnetism in nanostructures is the spin-orbit coupling. The spin-orbit coupling plays an important role in magnetic nanostructures, both on the magnetic arrangement and on transport. In fact SOC was shown by Dirac to result from the relativistic generalization of Schrödinger equation for electrons [87]. It can be written as

$$H_{SOC} = \frac{e\hbar}{2(mc)^2} (\vec{p} \times \nabla V(r)) \cdot \vec{s}, \quad (4.1)$$

where \vec{p} is the momentum of the electron, $V(r)$ is the potential and \vec{s} is the spin operator. In atomic physics, $V(r)$ is the atomic potential seen by one electron and it has spherical symmetry. In this case the expression of spin-orbit Hamiltonian can easily be transformed into the following expression:

$$H_{SOC} = \lambda (\vec{l} \cdot \vec{s}), \quad (4.2)$$

where \vec{l} is the orbital momentum of the electron and λ is known as spin-orbit constant.

The consequences of SOC in magnetic systems are several. In a bulk material, even if the spin-orbit energy is very small, the atomic SOC gives rise to important effects such as Hund's rule, magnetic anisotropy or Hall effect. Even in a bulk system it is also necessary to consider other contributions since the potential $V(r)$ has no longer spherical symmetry. In particular in solids without inversion symmetry, SOC leads to the Bychkov-Rashba effect

[88] and Dresselhaus effect [89]. In 2D systems, inversion symmetry is always broken and the Rashba interaction can be written as :

$$H_R = \alpha \left(\vec{s} \times \vec{k} \right) \cdot \vec{n}, \quad (4.3)$$

where α is the Rashba coupling constant, \vec{k} is the wave-vector of the conduction electron and \vec{n} is a unit vector perpendicular to the 2D system. In magnetic nanostructures, Rashba effect is expected to be present at surfaces or interfaces [86], since symmetry is always broken.

The SOC has consequences on spin transport in nanostructures, the study of this consequences is the subject of this chapter. Obviously, spin-orbit interaction also influences the magnetic arrangement in magnetic systems mainly through two different mechanisms:

- Magnetic Anisotropy: in presence of SOC, rotational invariance is destroyed and the “atomic” spin-orbit interaction, Equation (4.2), gives rise to magnetic anisotropy [90, 91, 92]. This magnetic anisotropy corresponds to the direction dependence of magnetization (existence of easy axis or easy plane).
- Dzyaloshinskii-Moriya (DM) interaction: this interaction is described in more detail in the next section. It is an interaction between spins which exists if there is no inversion center between these two spins [30, 31]. This type of interaction is always present at surfaces and interfaces.

Spin-orbit coupling plays also an important role in transport properties : anomalous Hall effect is a consequence of spin-orbit coupling [85], in magnetic bulk materials and nanostructures. Rashba effect also affects transport in nanostructures [93].

In the thesis I have studied the effect of DM interactions on spin transport properties. In the next sections we will further study the origin of Dzyaloshinskii-Moriya Interaction and its effect on spin transport .

4.2 Dzyaloshinskii-Moriya Interaction

Dzyaloshinskii and Moriya observed that, beyond the bilinear exchange between magnetic moments, an anti-symmetric interaction might be present in crystals with low symmetry. In 1958, Dzyaloshinskii [30] predicted, based on symmetry arguments, that this interaction can be written as $\vec{D} \cdot (\vec{S}_1 \times \vec{S}_2)$. Two

years later, in 1960, Moriya [31] proposed a microscopic mechanism based on superexchange in presence of SOC, which allowed him to calculate explicitly the vector \vec{D} . Nowadays this phenomenon is known as anti-symmetric exchange or Dzyaloshinskii-Moriya interaction (DM).

This interaction gives a contribution to the total magnetic exchange interaction between two magnetic spins, \vec{S}_i and \vec{S}_j . DM interaction is a relativistic effect, because spin-orbit coupling (SOC) – meaning that the intrinsic spin degree of freedom of an electron is coupled to its orbital motion – is crucial for its occurrence. We can write the Dzyaloshinskii-Moriya interaction mathematically as

$$H_{DM} = \vec{D}_{ij} \cdot (\vec{S}_i \times \vec{S}_j), \quad (4.4)$$

where \vec{D}_{ij} is the DM vector between magnetic spins at sites i and j . One should notice that this DM vector obeys the relation: $\vec{D}_{ij} = -\vec{D}_{ji}$. The DM interaction occurs between two spins and it is mediated by the DM vector. Figure (4.1) shows schematically the DM interaction. This will be described in more details in the next section. Notice that DM interaction promotes canted spin structures because it favors perpendicular configuration of \vec{S}_i and \vec{S}_j , while ordinary bilinear exchange favors collinear structures.

A DM interaction can only occur when spin-orbit coupling is taken into account. In the absence of SOC, the spin space is not coupled to the real space, and a rotation of all spins in real space can be made without changing the energy of the system, i.e., the Hamiltonian of the system is invariant under unitary rotation transformation such as $U^\dagger H U = H$, where U is a unitary matrix rotation in real space. Not only SOC is crucial for the existence of Dzyaloshinskii-Moriya interaction, but also is needed an inversion anti-symmetric environment (e. g. anti-symmetry introduced by a surface) to obtain an interaction of the form of equation (4.4).

Notice that symmetry breaking is always present when we treat interfaces problems, as for example, in magnetic multi-layers. However when we are dealing with bulk material this inversion symmetry breaking occurs only when the material has some peculiar crystal structure, or contains some impurities.

Both the value and direction of the DM vector have to be determined. Of course they depend on the microscopic mechanism, but the direction can be partly determined by symmetry considerations. In bulk material, the symmetry can be broken by several factors as crystal structure or presence of impurities. Moriya [31] gives in his paper some rules to find the direction of the DM vector. We summarize this rules below.

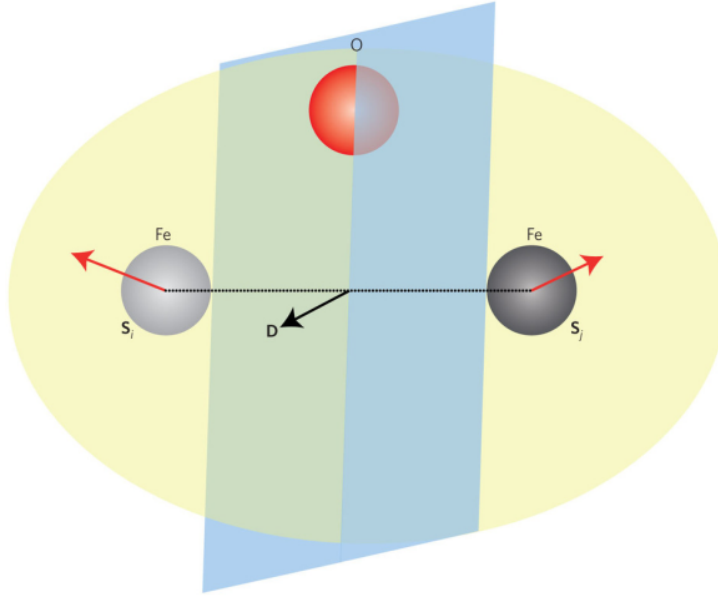


Figure 4.1: DM interaction between two Fe (dark and light grey) ions mediated by a nearby oxygen ion (red). Red arrows represent two adjacent spins \vec{S}_i and \vec{S}_j lying in a plane (yellow). The DM coupling vector \vec{D} lies a different plane (blue), the orientation of which depends on local symmetry.

Consider two spins located at \vec{R}_1 and \vec{R}_2 ; the middle is labeled as $\vec{R} = (\vec{R}_1 + \vec{R}_2)/2$:

- If a center of inversion is located at \vec{R} , then $\vec{D} = 0$.
- If a mirror plane perpendicular to $(\vec{R}_1 - \vec{R}_2)$ includes \vec{R} , then \vec{D} is perpendicular to $(\vec{R}_1 - \vec{R}_2)$.
- If a mirror plane includes \vec{R}_1 and \vec{R}_2 , then \vec{D} is perpendicular to this mirror plane.
- If a two-fold rotation axis perpendicular to $(\vec{R}_1 - \vec{R}_2)$ includes \vec{R} , then \vec{D} is perpendicular to the rotation axis.

- If a n -fold rotation axis ($n \geq 2$) includes \vec{R}_1 and \vec{R}_2 then \vec{D} is parallel to $(\vec{R}_1 - \vec{R}_2)$.

We presented in this section the main properties of DM interaction. Equation (4.4) gives the general expression of the DM interaction, between \vec{S}_i and \vec{S}_j . In magnetic nanostructures such interaction is expected to be present: for example Ref. [94] studies the DM interaction between magnetic moments both located at a surface or interface, or between magnetic moment at a surface and a moment on the 1st layer below the surface. Interlayer DM interaction can also exist when the two layers are made with a different materials. Besides Moriya's mechanism (superexchange with SOC) other mechanisms have been proposed, more adapted for metallic systems [95, 96, 97] and DM interaction can also be induced by Rashba interaction [98].

Such intra or interlayer DM interaction may affect magnetic arrangements. However rearrangement of magnetic structure will not be considered here. In the thesis we are interested by looking at transport in a 3-layer system made of 2 ferromagnetic layers FL and FR separated by a non-magnetic layer NM . We will not consider the effect of DM interaction on the magnetic arrangements (either inside each layer or possible global reorientation of magnetizations of the layers), but since we are interested by transport, we will study the influence on transport of DM interaction between magnetic ions in one of the ferromagnetic layers and spin of conduction electrons located near the interface (either in the ferromagnetic layer, or in the paramagnetic one). Such an interaction can be written as: $\vec{D} \cdot (\vec{S} \times \vec{s})$ [33]. We will first show that such an interaction exists and describe a possible mechanism for it. Then we will study the influence of this interaction on transport in a simplified model. In other words, we will study the effect of DM interaction on the conduction electron states, and how this interaction modifies the spin current.

4.3 DM Interaction between Magnetic Ions and Conduction Electrons

In this section we derive a possible mechanism for DM interaction between magnetic ions at the surface of a ferromagnetic layer and spin of conduction electrons located near this surface (or interface). Moriya's rules cannot help in this case, since the 2 magnetic moments involved in the interaction are of different type. We generalize to our case the Moriya's mechanism based on superexchange, using a formulation derived by Herzog and Wegewijs (2010)

[99] that gives an analytical expression of the DM's vector between two ions which may have a different nature.

The case considered here is the following: we have one 'magnetic' ion located at the surface. We suppose that this ion has one localized d-electron in a t_{2g} orbital (these t_{2g} orbitals are threefold degenerate in cubic symmetry) and the surface is parallel to the x-z plane. At the surface, the crystal field has no longer cubic symmetry and the orbital degeneracy is partially lifted in the following way:

- $1 \rightarrow |1\rangle = -\frac{1}{\sqrt{2}} (|2, 1\rangle - |2, -1\rangle)$ corresponds to the d_{xz} level with energy ϵ . This level is supposed to be the ground state.
- $1' \rightarrow |1'\rangle = \frac{i}{\sqrt{2}} (|2, 1\rangle - |2, -1\rangle)$ corresponds to the d_{yz} level with energy δ .
- $1'' \rightarrow |1''\rangle = -\frac{i}{\sqrt{2}} (|2, 2\rangle - |2, -2\rangle)$ corresponds to the d_{xy} level with energy δ .

Notice that d_{yz} and d_{xy} are still degenerate. In these expressions the notation $|l, m\rangle$ corresponds for the t_{2g} electrons to the orbitals with $l = 2$.

The 2nd site that we consider is a site with one s-electron (conduction electron), in the vicinity of the 1st one. This situation is shown schematically on figure (4.2). Adapting the calculation of Herzog *et al.* [99] to our case leads to the following expression for \vec{D} :

$$\vec{D} = 2 \frac{i\lambda_1 \vec{l}_{1'1}}{\epsilon_{1'} - \epsilon_1} \left(\frac{t_{12}t_{21'}}{U} + v_{1221'} \right) + 2 \frac{i\lambda_1 \vec{l}_{1''1}}{\epsilon_{1''} - \epsilon_1} \left(\frac{t_{12}t_{21''}}{U} + v_{1221''} \right) \quad (4.5)$$

where $\vec{l}_{ab} = \langle a | \vec{l} | b \rangle$, is the matrix element of the angular momentum operator \vec{l} between 2 states a and b , (a and b are the states 1, 1' and 1''), λ_1 is the spin-orbit amplitude of the t_{2g} electrons, the ϵ_i are the crystal field energies on the magnetic site (site 1), U is the Coulomb repulsion between d -electrons on the magnetic site, t_{a2} is the hopping integral between a orbital (a can be 1 or 1'') on 1st site and s-orbital on 2nd site and v_{122a} (a can be 1 or 1'') is an exchange energy corresponding to an effective orbital excitation associated to spin flip as explained by Herzog [99].

The direction of \vec{D} depends on the matrix elements $\vec{l}_{1'1}$ and $\vec{l}_{1''1}$. Calculation of these matrix elements is performed using the following relations for the angular momentum :

$$L_{\pm} |l, m\rangle = \hbar \sqrt{l(l+1) - m(m \pm 1)} |l, m \pm 1\rangle$$

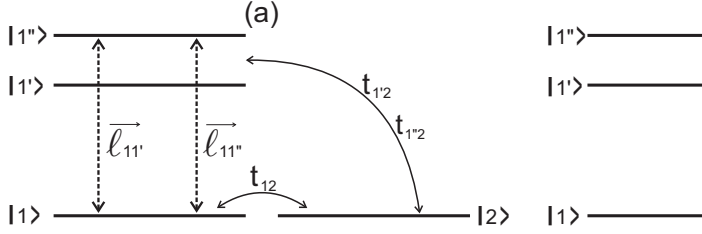


Figure 4.2: Site 1 is the magnetic site, site 2 corresponds to the conduction electron. In (a) is shown the superexchange process and in (b) the direct exchange one.

and

$$L_z|l, m\rangle = \hbar m|l, m\rangle.$$

For our case, we get the following expressions:

$$\begin{aligned} (l_{1'1})_x &= \left[-\frac{i}{\sqrt{2}} (\langle 2, 1| - \langle 2, -1|) \right] \left[\frac{1}{2} (L_+ + L_-) \right] \left[-\frac{1}{\sqrt{2}} (|2, 1\rangle - |2, -1\rangle) \right] \\ &= \frac{i}{2} (\langle 1, 2| - \langle -1, 2|) \left(2\hbar|2, 2\rangle - \sqrt{6}\hbar|2, 0\rangle + \sqrt{6}\hbar|2, 0\rangle - 2\hbar|2, -2\rangle \right) \\ &= 0, \end{aligned}$$

$$\begin{aligned} (l_{1'1})_y &= \left[-\frac{i}{\sqrt{2}} (\langle 2, 1| - \langle 2, -1|) \right] \left[\frac{1}{2i} (L_+ - L_-) \right] \left[-\frac{1}{\sqrt{2}} (|2, 1\rangle - |2, -1\rangle) \right] \\ &= \frac{1}{4} (\langle 1, 2| - \langle -1, 2|) \left(2\hbar|2, 2\rangle - \sqrt{6}\hbar|2, 0\rangle - \sqrt{6}\hbar|2, 0\rangle + 2\hbar|2, -2\rangle \right) \\ &= 0, \end{aligned}$$

$$\begin{aligned} (l_{1'1})_z &= \left[-\frac{i}{\sqrt{2}} (\langle 2, 1| - \langle 2, -1|) \right] L_z \left[-\frac{1}{\sqrt{2}} (|2, 1\rangle - |2, -1\rangle) \right] \\ &= \frac{i}{2} (\langle 1, 2| - \langle -1, 2|) (\hbar|2, 1\rangle - \hbar|2, -1\rangle) = \frac{i\hbar}{2} + \frac{i\hbar}{2} \\ &= i\hbar, \end{aligned}$$

$$\begin{aligned} (l_{1''1})_x &= \left[\frac{i}{\sqrt{2}} (\langle 2, 2| - \langle -2, 2|) \right] \left[\frac{1}{2} (L_+ + L_-) \right] \left[-\frac{1}{\sqrt{2}} (|2, 1\rangle - |2, -1\rangle) \right] \\ &= -\frac{i}{4} (\langle 2, 2| - \langle -2, 2|) \left(2\hbar|2, 2\rangle - \sqrt{6}\hbar|2, 0\rangle + \sqrt{6}\hbar|2, 0\rangle - 2\hbar|2, -2\rangle \right) \\ &= -i\hbar, \end{aligned}$$

$$\begin{aligned}
(l_{1''1})_y &= \left[\frac{i}{\sqrt{2}} (\langle 2, 2 | - \langle -2, 2 |) \right] \left[\frac{1}{2i} (L_+ - L_-) \right] \left[-\frac{1}{\sqrt{2}} (|2, 1\rangle - |2, -1\rangle) \right] \\
&= -\frac{i}{4} (\langle 2, 2 | - \langle -2, 2 |) \left(2\hbar|2, 2\rangle - \sqrt{6}\hbar|2, 0\rangle - \sqrt{6}\hbar|2, 0\rangle + 2\hbar|2, -2\rangle \right) \\
&= -\frac{1}{4} (2\hbar - 2\hbar) = 0, \\
(l_{1''1})_z &= \left[\frac{i}{\sqrt{2}} (\langle 2, 2 | - \langle -2, 2 |) \right] L_z \left[-\frac{1}{\sqrt{2}} (|2, 1\rangle - |2, -1\rangle) \right] \\
&= -\frac{i}{2} (\langle 2, 2 | - \langle -2, 2 |) (\hbar|2, 1\rangle + \hbar|2, -1\rangle) \\
&= 0.
\end{aligned} \tag{4.6}$$

Using these results – (4.6) – we arrive to the following expression for \vec{D} :

$$\vec{D} = \frac{\lambda_1 A}{\Delta} \hat{x} + \frac{\lambda_1 B}{\Delta} \hat{z}, \tag{4.7}$$

where $A \equiv 2\hbar \left(\frac{t_{12}t_{21'}}{U} + v_{1221'} \right)$ and $B \equiv 2\hbar \left(\frac{t_{12}t_{21''}}{U} + v_{1221''} \right)$ and $\Delta = \delta - \epsilon$, where δ and ϵ are the crystal field energies of the t_{2g} as explained above. It is clear from equation (4.7) that the DM vector is pointing in the x-z plane, i.e. it is parallel to the surface. In the following, we will write the DM vector in spherical coordinates as follows

$$\vec{D} = \left(|\vec{D}| \sin \theta_D, 0, |\vec{D}| \cos \theta_D \right), \tag{4.8}$$

where $|\vec{D}|$ is the intensity of vector \vec{D} and θ_D is the angle between the vector and the coordinate axis.

Thus we have shown that DM interaction between a magnetic moment and the spin of conduction electron may occur near the surface, when crystal field is modified due to the symmetry change. This interaction occurs with all conduction electrons which are in the vicinity of this magnetic ion; A and B should be non zero, .if the hopping integrals t_{12} or the the exchange energy v in eq. (4.7) are different from zero.

Finally it is interesting to remark that the same kind of DM interaction between a magnetic impurity and conduction electrons was derived by Zarea *et al.* [33] in the context of the Kondo effect in presence of Rashba interaction. They show in their paper that this DM interaction writes as:

$$H_{DM}^{Zarea} = i\lambda k_F C (\vec{k} - \vec{k}'). \left(\vec{s}_{\vec{k}\vec{k}'} \times \vec{S} \right), \tag{4.9}$$

where

$$\vec{S}_{\vec{k}\vec{k}'} = \frac{1}{2} \left(c_{\vec{k}s}^\dagger \vec{\sigma}^{ss'} c_{\vec{k}'s'} \right),$$

where $\vec{\sigma}$ is the Pauli matrices. \vec{S} is the impurity spin vector, $C(\vec{k} - \vec{k}')$ is a function that was calculated in Ref. [33], k_F is the Fermi wave vector and λ is the spin-orbit constant. Thus using a completely different model, they obtained the same kind of interaction when spin-orbit is present in a 2-dimensional system (notice that this was obtained in the context of Kondo effect, but remains valid for any magnetic impurity).

4.4 Model

In this section we will introduce the two “toy models” that we have studied. These toy models can be viewed as simplified description of a three layers nanostructure consisting of two ferromagnetic (FM) layers, FL and FR , separated by a paramagnetic layer, NM , as shown in Figure (4.3).

We suppose that the magnetization of the FM layers is uniform, and we neglect any interlayer coupling between magnetizations on the R and L layers. Since magnetization is uniform, we will consider a simple toy model where each layer is replaced by a site on 1-D chain. We show below that, despite this model is simple, one can get interesting results. Bruno [90] introduced a similar 2 sites toy model to study the effect of inhomogeneous magnetization on spin current.

Within this approximation the three layers nanostructure will be described by 3-sites: L and R for the magnetic “layers” and NM for the intermediate non-magnetic “layer”. The magnetization of FR and FL layers will be represented by classical vectors \vec{S}_L and \vec{S}_R on the sites R and L , see Fig. (4.4). There are also conduction electrons propagating both in ferromagnetic and in non-magnetic layers. In the real system there is a DM interaction between magnetic moments and conduction electrons spins located both in the magnetic layer and in the NM layer (close enough to the interface).

In the absence of spin-orbit interaction, the Hamiltonian of this model is

$$H_0 = H_{TB} + H_{s-d}, \quad (4.10)$$

where H_{TB} describes the conduction electrons in tight binding approxima-

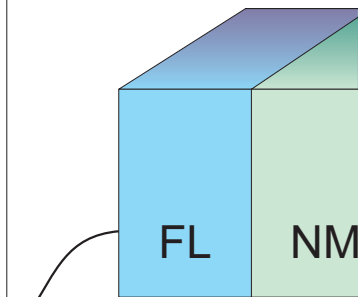


Figure 4.3: A physical system with three layers: two ferromagnetic layers (FL and FR) and a non-magnetic one (NM). Dzyaloshinskii-Moriya interaction is considered at both interfaces FL/NM and FR/NM .

tion:

$$\begin{aligned}
H_{TB} = & t_{RL} \left(c_{L\uparrow}^\dagger c_{R\uparrow} + c_{L\downarrow}^\dagger c_{R\downarrow} + c_{R\uparrow}^\dagger c_{L\uparrow} + c_{R\downarrow}^\dagger c_{L\downarrow} \right) + \\
& + \tau \left(c_{L\uparrow}^\dagger c_{NM\uparrow} + c_{L\downarrow}^\dagger c_{NM\downarrow} + c_{NM\uparrow}^\dagger c_{L\uparrow} + c_{NM\downarrow}^\dagger c_{L\downarrow} \right) + \\
& + \tau \left(c_{R\uparrow}^\dagger c_{NM\uparrow} + c_{R\downarrow}^\dagger c_{NM\downarrow} + c_{NM\uparrow}^\dagger c_{R\uparrow} + c_{NM\downarrow}^\dagger c_{R\downarrow} \right) + \\
& + V \left(c_{NM\uparrow}^\dagger c_{NM\uparrow} + c_{NM\downarrow}^\dagger c_{NM\downarrow} \right)
\end{aligned} \tag{4.11}$$

where $c^{(\dagger)}$ are the annihilation (creation) operators that represent the conduction electron in left (L), middle (NM) and right (R) sites, t_{LR} is a direct hopping between L and R sites, τ is the hopping integral between magnetic (L and R) sites and non-magnetic (NM) site, and V is a potential on the non-magnetic site. H_{s-d} is the usual $s-d$ interaction:

$$H_{s-d} = -J_0 \left(\vec{S}_L \cdot \vec{s}_L + \vec{S}_R \cdot \vec{s}_R \right), \tag{4.12}$$

where J_0 is the exchange parameter and \vec{s}_i is written in terms of the operators

$c^{(\dagger)}$ as follows

$$s_{i;x} = \frac{1}{2} \left(c_{i\uparrow}^\dagger c_{i\downarrow} + c_{i\downarrow}^\dagger c_{i\uparrow} \right), \quad (4.13)$$

$$s_{i;y} = \frac{1}{2i} \left(c_{i\uparrow}^\dagger c_{i\downarrow} - c_{i\downarrow}^\dagger c_{i\uparrow} \right), \quad (4.14)$$

$$s_{i;z} = \frac{1}{2} \left(c_{i\uparrow}^\dagger c_{i\uparrow} + c_{i\downarrow}^\dagger c_{i\downarrow} \right), \quad (4.15)$$

where $i = L, R$ and NM . Here we assume that the two magnetic layers are made of the same material, thus \vec{S}_L and \vec{S}_R have the same length, the exchange parameter, J_0 , is the same on both layers and the hopping between $L - NM$ and $NM - R$ are equal, $t_{L-NM} = t_{NM-R} = \tau$.

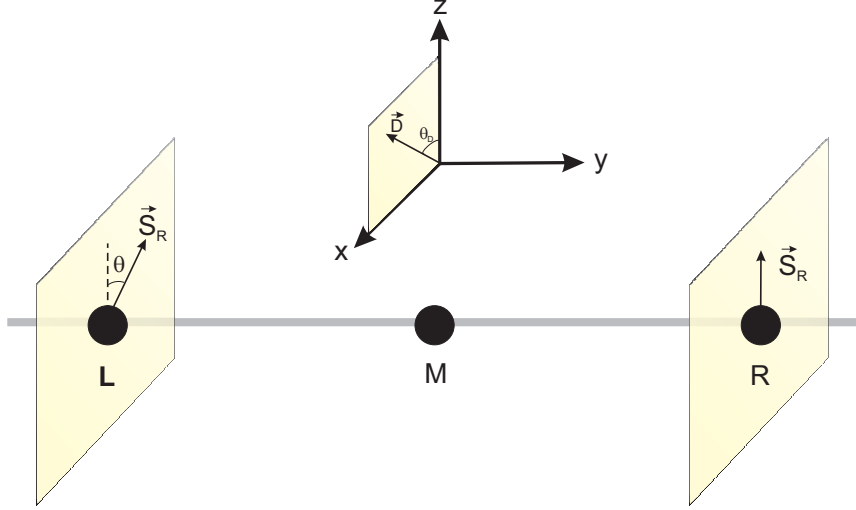


Figure 4.4: A schematic picture of the three sites approximation. \vec{S}_L represents the left (FL) and \vec{S}_R the right (FR) ferromagnetic layer. A non-magnetic layer is represented by the central site NM . Conduction electrons can travel on all sites.

Now we will discuss how the DM interaction will be incorporated in the 3-sites approximation. Notice that in our toy model Rashba effect cannot be included since conduction electrons can only move in the perpendicular direction. Thus conduction electrons do not move in the magnetic site. However, we have shown in the previous section that SOC gives rise to DM interaction between magnetic sites and conduction electrons. In our 3 sites model, there can be two kind of DM interactions:

(i) between local spin, \vec{S}_L and \vec{S}_R , and spin of conduction electrons in the NM site, \vec{s}_{NM} ;

(ii) between local spins \vec{S}_L and \vec{S}_R and conduction electrons inside the ferromagnetic layers, i.e., \vec{s}_L and \vec{s}_R .

In our case, this last interaction will be local, which of course is not possible for real DM interaction. DM interaction needs in principle 2 different sites, but this description allows us to describe and compare both DM interactions in the toy model.

In this model the DM Hamiltonian is written as:

$$H_{DM} = \vec{D} \cdot (\vec{S}_L \times \vec{s}_{NM}) + \vec{D} \cdot (\vec{S}_R \times \vec{s}_{NM}) + \vec{D}' \cdot (\vec{S}_L \times \vec{s}_L) + \vec{D}' \cdot (\vec{S}_R \times \vec{s}_R). \quad (4.16)$$

where \vec{D}' and \vec{D} are different vectors, both lying in the x-z plane (y-direction is chosen as the L-R direction as shown on the figure 4.4). \vec{D}' is the ‘intralayer’ DM coupling, while \vec{D} is the ‘interlayer’ DM coupling. Notice that in this model, DM interaction between \vec{S}_L and \vec{S}_R vanishes since the site NM is an inversion center for this toy model.

Our aim in this work is to study how the DM interaction can influence the spin transport for different configurations of the local spins \vec{S}_L and \vec{S}_R . We will perform this study by calculating the spin current which is given by the following expression:

$$\begin{aligned} \hat{j}_{x,i \rightarrow j} &= \frac{i\tau_{ij}}{2} \left(c_{i\uparrow}^\dagger c_{j\downarrow} + c_{i\downarrow}^\dagger c_{j\uparrow} - c_{j\downarrow}^\dagger c_{i\uparrow} - c_{j\uparrow}^\dagger c_{i\downarrow} \right) \\ \hat{j}_{y,i \rightarrow j} &= \frac{\tau_{ij}}{2} \left(c_{i\uparrow}^\dagger c_{j\downarrow} - c_{i\downarrow}^\dagger c_{j\uparrow} + c_{j\downarrow}^\dagger c_{i\uparrow} - c_{j\uparrow}^\dagger c_{i\downarrow} \right) \\ \hat{j}_{z,i \rightarrow j} &= \frac{i\tau_{ij}}{2} \left(c_{i\uparrow}^\dagger c_{j\uparrow} - c_{i\downarrow}^\dagger c_{j\downarrow} - c_{j\uparrow}^\dagger c_{i\uparrow} + c_{j\downarrow}^\dagger c_{i\downarrow} \right), \end{aligned} \quad (4.17)$$

where τ_{ij} is the hopping between i and j sites. It is important to point out that, in these expressions, x , y and z refer to the spin space. In general, the spin current operator is a tensor in both real space and spin space. In our case, the current (spin or charge) can only flow along the y -direction in real space, but all spin components participate to the spin current.

This is a very simple system that can be solved in any mathematical software. We use the software *Wolfram Mathematica* to discover the eigenvalues and eigenvectors of the model. In order to discover which is the lowest energy state, we plot a graphic with the all eigenvalues and choose the eigenvector with respect to the lowest eigenvalue.

Once all parameters are well defined, we can start the calculation. The effect of \vec{D} and \vec{D}' will be studied separately using two different models that we briefly describe below.

4.4.1 Model I: Three Sites Problem for the study of interlayer DM

We first study the interlayer DM alone (\vec{D} in eq. (4.16)). The total Hamiltonian that we consider is

$$H_1 = H_{TB} + H_{s-d} + H_{DM}, \quad (4.18)$$

where H_{TB} is given by equation (4.11). Notice that the potential V on the non-magnetic site can be positive or negative. When V is large and positive, the central site represents a situation where the electrons can only flow by tunneling (potential barrier). When V is positive the layer behaves as a potential well. The term H_{s-d} are given in Equation (4.12). We only consider here the \vec{D} term ('interlayer' DM coupling) in DM Hamiltonian (4.16).

In this work we use Schrödinger formalism to solve the problem, but other methods are also possible. In fact in non-equilibrium situation, we should use Heisenberg equation for the temporal evolution of the operators¹. The local spins \vec{S}_L and \vec{S}_R are supposed to be fixed in some direction. In this three sites case the system is described by three spin operators: \vec{s}_L , \vec{s}_{NM} and \vec{s}_R . Writing the Heisenberg equation for each of these operators we can find three "continuity equations":

$$\begin{aligned} \hbar \frac{\partial}{\partial t} \vec{s}_L &= -\vec{j}_{L \rightarrow R} - \vec{j}_{L \rightarrow NM} + J_0 \left(\vec{s}_L \times \vec{S}_L \right) \\ \hbar \frac{\partial}{\partial t} \vec{s}_R &= \vec{j}_{L \rightarrow R} + \vec{j}_{NM \rightarrow R} + J_0 \left(\vec{s}_R \times \vec{S}_R \right) \\ \hbar \frac{\partial}{\partial t} \vec{s}_{NM} &= - \left(\vec{j}_{L \rightarrow NM} + \vec{j}_{NM \rightarrow R} \right) + \vec{s}_{NM} \times \left(\vec{S}_L \times \vec{D} \right) + \vec{s}_{NM} \times \left(\vec{S}_R \times \vec{D} \right), \end{aligned} \quad (4.19)$$

One can notice that $\vec{j}_{L \rightarrow NM} + \vec{j}_{NM \rightarrow R} \neq \vec{j}_{L \rightarrow R}$ indicating that there can be direct current from L to R sites: the current flowing from left to central site and from central to right, is proportional to τ , while the current flowing

¹The Heisenberg equation for operator is

$$\frac{d}{dt} A(t) = \frac{i}{\hbar} [H, A(t)],$$

where $A(t)$ is the operator evolves in time

directly from the left to the right site is proportional to t_{LR} . We will show how to calculate each of this spin current.

We consider only the steady states, thus the time derivatives on the left hand side of the equations (4.19) vanish. Then it is convenient to calculate the spin current using the Schrödinger formalism. What we need to know are the eigenfunctions of the Hamiltonian. In this 3-sites problem, up to 6 conduction electrons can be injected in the system, according to Pauli's principle. For one conduction electron the wave function can be written as a combination of the 6 possible states of this electron:

$$|\psi\rangle = d_1 c_{L\uparrow}^\dagger |0\rangle + d_2 c_{L\downarrow}^\dagger |0\rangle + d_3 c_{R\uparrow}^\dagger |0\rangle + d_4 c_{R\downarrow}^\dagger |0\rangle + d_5 c_{NM\uparrow}^\dagger |0\rangle + d_6 c_{NM\downarrow}^\dagger |0\rangle, \quad (4.20)$$

where $|0\rangle$ is the vacuum state.

The Schrödinger equation in a matrix form is

$$\hat{H} |\psi\rangle = \hat{E} |\psi\rangle,$$

where \hat{E} is the diagonal matrix of the eigenvalues and

$$\hat{H} = \begin{pmatrix} -\frac{J_0}{2} S_{Lz} & F_1^* & t_{LR} & 0 & \tau & 0 \\ F_1 & \frac{J_0}{2} S_{Lz} & 0 & t_{LR} & 0 & \tau \\ t_{LR} & 0 & -\frac{J_0}{2} S_{Rz} & F_2^* & \tau & 0 \\ 0 & t_{LR} & F_2 & \frac{J_0}{2} S_{Rz} & 0 & \tau \\ \tau & 0 & \tau & 0 & V + \chi & F_3 \\ 0 & \tau & 0 & \tau & F_3^* & V - \chi \end{pmatrix} \quad (4.21)$$

where

$$\begin{aligned} \chi &= \frac{D_x}{2} S_{Ly} - \frac{D_y}{2} S_{Lx} + \frac{D_x}{2} S_{Ry} - \frac{D_y}{2} S_{Rx}, \\ F_1 &= -\frac{J_0}{2} (S_{Lx} + iS_{Ly}), \\ F_2 &= -\frac{J_0}{2} (S_{Rx} + iS_{Ry}), \\ F_3 &= \frac{S_{Lz}}{2} (D_y - iD_x) - \frac{D_z}{2} (S_{Ly} - iS_{Lx}) - \\ &\quad - \frac{S_{Rz}}{2} (D_y - iD_x) - \frac{D_z}{2} (S_{Ry} - iS_{Rx}). \end{aligned}$$

In principle a similar calculation can be done for other occupation numbers: for 2 electrons, there are 15 possible states, and it is necessary to solve a 15×15 matrix.

In the following calculation we will specify more precisely the components of the local spins and the DM vector. As we discussed before in this three sites case there will be three spin currents. The way to calculate the three components is: first we find the lowest eigenvalue and corresponding eigenvector using Schrödinger equation and this will give the ground state wave function. Once we know the ground state wave function, we calculate the average value of spin current operator: $\langle \psi | \vec{j}_{ij} | \psi \rangle$. The results of this calculation will be presented in section (4.5).

4.4.2 Model II: Two Sites Problem

In this section we introduce a further simplification : we do not consider the central site, but only the two magnetic sites. This model is well adapted for studying the ‘intra-layer’ DM coupling (D’ term in eq. (4.16)). Furthermore, since it is simpler, we can also study the spin current for different occupation numbers.

In this case the tight-binding Hamiltonian is also simpler (there is no potential V in NM site and no τ hopping) and is given by:

$$H'_{TB} = t_{RL} \left(c_{L\uparrow}^\dagger c_{R\uparrow} + c_{L\downarrow}^\dagger c_{R\downarrow} + c_{R\uparrow}^\dagger c_{L\uparrow} + c_{R\downarrow}^\dagger c_{L\downarrow} \right). \quad (4.22)$$

The total Hamiltonian that describes this two sites problem is

$$H_2 = H'_{TB} + H_{s-d} + H_{DM} \quad (4.23)$$

where H_{s-d} is given by Equation (4.12) and H_{DM} by Equation (4.16) now with $\vec{D} = 0$.

We will solve the problem using Schrödinger formalism as before. Again we need to know the wave function to do the calculations. This wave function is written using properties of quantum mechanics: we can occupy two sites with, at maximum, four electrons respecting the Pauli’s exclusion principle. Here we will study the case with occupation numbers equal to one or two electrons. The case of 3 (4) electrons is similar to 1 (2) electron, due to electron-hole symmetry

First we write the wave function for one electron in the 2-sites model:

$$|\psi\rangle = a_1 c_{L\uparrow}^\dagger |0\rangle + a_2 c_{L\downarrow}^\dagger |0\rangle + a_3 c_{R\uparrow}^\dagger |0\rangle + a_4 c_{R\downarrow}^\dagger |0\rangle, \quad (4.24)$$

where $|0\rangle$ is the vacuum state. The coefficients a ’s will be determined by solving the Schrödinger equation:

$$H_2 |\psi\rangle = E |\psi\rangle,$$

where H_2 is the Hamiltonian determined above (eq. (4.23)) and E is the eigenvalue of the system. Solving this equation, we get

$$\begin{pmatrix} \beta_1 & B_1 & t_{LR} & 0 \\ B_1^* & -\beta_1 & 0 & t_{LR} \\ t_{LR} & 0 & \beta_2 & B_2 \\ 0 & t_{LR} & B_2^* & -\beta_2 \end{pmatrix} \begin{pmatrix} a_1 \\ a_2 \\ a_3 \\ a_4 \end{pmatrix} = E \begin{pmatrix} a_1 \\ a_2 \\ a_3 \\ a_4 \end{pmatrix} \quad (4.25)$$

where

$$\begin{aligned} \beta_1 &= -\frac{J_0}{2} S_{Lz} + \frac{D'_x}{2} S_{Ly} - \frac{D'_y}{2} S_{Lx} \\ \beta_2 &= -\frac{J_0}{2} S_{Rz} + \frac{D'_x}{2} S_{Ry} - \frac{D'_y}{2} S_{Rx} \\ B_1 &= -\frac{J_0}{2} (S_{Lx} - iS_{Ly}) + \frac{S_{Lz}}{2} (D'_y + iD'_x) - \frac{D'_z}{2} (S_{Ly} + iS_{Lx}) \\ B_2 &= -\frac{J_0}{2} (S_{Rx} - iS_{Ry}) + \frac{S_{Rz}}{2} (D'_y + iD'_x) - \frac{D'_z}{2} (S_{Ry} + iS_{Rx}) . \end{aligned}$$

In Figure (4.5) we show an example which indicates the 4 energy levels for one specific value of $|\vec{D}'|$ and θ_D . We choose the lowest one that represents the fundamental energy level.

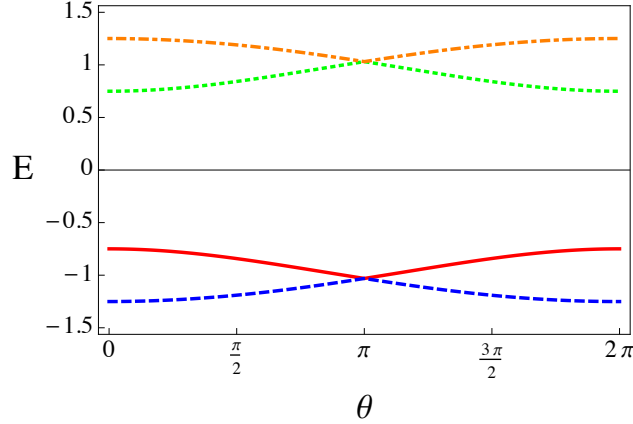


Figure 4.5: This graphic shows the 4 energy levels in model II, the lowest one is represented by the blue curve. θ is the angle between the 2 spins \vec{S}_L and \vec{S}_R . Here, $J_0/t_{LR} = 0.5$, $|\vec{D}'|/t_{LR} = 0.05$ and $\theta_D = \pi/4$.

For two electrons we can use the same procedure. There are 6 possible states, thus it is necessary to diagonalize a 6×6 matrix. The wave function

is written as:

$$|\psi\rangle = b_1 c_{L\uparrow}^\dagger c_{R\uparrow}^\dagger |0\rangle + b_2 c_{L\uparrow}^\dagger c_{R\downarrow}^\dagger |0\rangle + b_3 c_{L\downarrow}^\dagger c_{R\uparrow}^\dagger |0\rangle + b_4 c_{L\downarrow}^\dagger c_{R\downarrow}^\dagger |0\rangle + b_5 c_{L\uparrow}^\dagger c_{L\downarrow}^\dagger |0\rangle + b_6 c_{R\uparrow}^\dagger c_{R\downarrow}^\dagger |0\rangle, \quad (4.26)$$

where $|0\rangle$ is the vacuum state.

The coefficients b 's are determined by solving the Schrödinger equation $H|\psi\rangle = E|\psi\rangle$. In a matrix form, we can write

$$\begin{pmatrix} \delta_1 & D_2 & D_1 & 0 & 0 & 0 \\ D_2^* & \delta_2 & 0 & D_1 & t_{LR} & t_{LR} \\ D_1^* & 0 & -\delta_2 & D_2 & -t_{LR} & -t_{LR} \\ 0 & D_1^* & D_2^* & -\delta_1 & 0 & 0 \\ 0 & t_{LR} & t_{LR} & 0 & 0 & 0 \\ 0 & t_{LR} & t_{LR} & 0 & 0 & 0 \end{pmatrix} \begin{pmatrix} b_1 \\ b_2 \\ b_3 \\ b_4 \\ b_5 \\ b_6 \end{pmatrix} = E \begin{pmatrix} b_1 \\ b_2 \\ b_3 \\ b_4 \\ b_5 \\ b_6 \end{pmatrix}, \quad (4.27)$$

where

$$\begin{aligned} \delta_1 &= -\frac{J_0}{2} S_{Lz} - \frac{J_0}{2} S_{Rz} + \frac{D'_x}{2} S_{Ly} - \frac{D'_y}{2} S_{Lx} + \frac{D'_x}{2} S_{Ry} - \frac{D'_y}{2} S_{Rx} \\ \delta_2 &= -\frac{J_0}{2} S_{Lz} + \frac{J_0}{2} S_{Rz} + \frac{D'_x}{2} S_{Ly} - \frac{D'_y}{2} S_{Lx} - \frac{D'_x}{2} S_{Ry} + \frac{D'_y}{2} S_{Rx} \\ D_1 &= -\frac{J_0}{2} (S_{Lx} - iS_{Ly}) + \frac{S_{Lz}}{2} (D'_y + iD'_x) - \frac{D'_z}{2} (S_{Ly} + iS_{Lx}) \\ D_2 &= -\frac{J_0}{2} (S_{Rx} - iS_{Ry}) + \frac{S_{Rz}}{2} (D'_y + iD'_x) - \frac{D'_z}{2} (S_{Ry} + iS_{Rx}). \end{aligned}$$

We can plot the same type of graphic as in the 1-electron case – Fig. (4.5) –, but now there are 6 eigenvalues. We choose the lowest one and find the corresponding eigenvector. This eigenvector has six components, determining the b 's coefficients. Once the coefficients of the wave function are determined, we calculate the spin current.

In this case we can also write a continuity equation using Heisenberg formalism:

$$\begin{aligned} \hbar \frac{\partial \vec{s}_L}{\partial t} &= -\vec{j}_{L \rightarrow R} + J_0 (\vec{s}_L \times \vec{S}_L) + \vec{s}_L \times (\vec{S}_L \times \vec{D}') \\ \hbar \frac{\partial \vec{s}_R}{\partial t} &= \vec{j}_{L \rightarrow R} + J_0 (\vec{s}_R \times \vec{S}_R) + \vec{s}_R \times (\vec{S}_R \times \vec{D}'), \end{aligned} \quad (4.28)$$

where the term $\vec{j}_{L \rightarrow R}$ is the spin current flowing from the left to the right site, proportional to t_{LR} . The problem is time independent, so the left side vanishes. This equation gives another way for calculating the spin current.

4.5 Results and Discussion

In this section we present the results obtained for the spin currents for both models. In all the following, we considered that \vec{S}_R is fixed along the z -axis

$$\vec{S}_R = (0, 0, 1), \quad (4.29)$$

\vec{D} is making an angle of θ_D , written as in equation (4.7), and the spin current will be calculated as a function of the angle θ of the spin \vec{S}_L , which can be rotated in the z - x plane

$$\vec{S}_L = (\sin \theta, 0, \cos \theta). \quad (4.30)$$

First we present the results for the three sites model, model I, and then the results for the two sites model, model II.

4.5.1 Model I

We calculate the three components of the spin current, following the method described in section IV-4 . These components are shown on figures (4.6), (4.7) and (4.8) as a function of the angle θ between the 2 spins \vec{S}_L and \vec{S}_R .

In Fig. (4.6) we show the current flowing from the left to right site. This component is smaller than the others because it is proportional to the second neighbor hopping, t_{LR} . Notice that DM interaction has a different effect on the y component compared to the x and z components: while increasing the interaction, the y component decreases. For the x and z components the behavior is opposite: when $\vec{D} = 0$ there is no transverse component of the spin current, only a longitudinal one when \vec{S}_L and \vec{S}_R are non-collinear. j_y vanishes only when $\theta = 0$ or π . However if DM interaction increases, the transverse components of the spin current increase. We can also see that both transverse components j_x and j_z vanish when $\theta = 0$ or π . All components of spin current vary with the angle θ between \vec{S}_L and \vec{S}_R . Thus, if DM interaction is considered, the three components of the spin current are different from zero, and they vary with angle θ between spins \vec{S}_L and \vec{S}_R . The variation of the x and z components are far from a sinusoidal behavior, they are even not symmetric around $\theta = \pi$. This is due to the fact that \vec{D} is making an angle of $\pi/4$ with \vec{S}_R . For other geometries, different variation of the spin current components would be obtained.

Figures (4.7) and (4.8) show the spin current flowing from left to central site and from the central to right site, respectively. The magnitude of this two currents is bigger since it is proportional to first neighboring hopping, τ . The component y in both Figs. (4.7 - b) and (4.8 - b) has the same behavior,

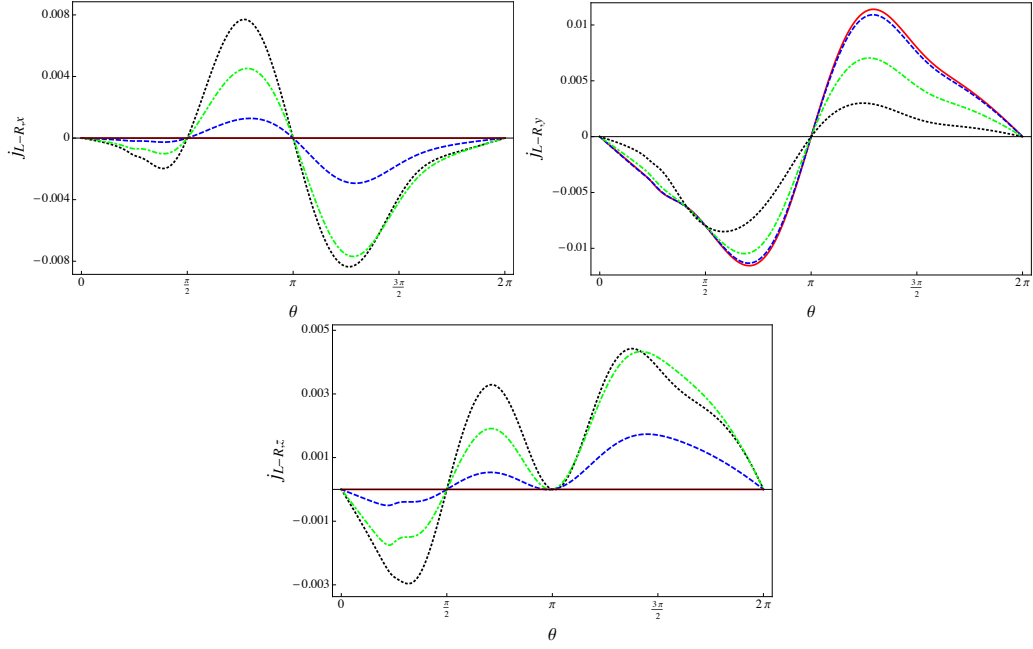


Figure 4.6: Model I: The x , y and z components of the spin current flowing from the left (L) to the right (R) site for occupation number of one electron. Parameters are: $J_0/\tau = 0.5$, $t_{LR}/\tau = 0.1$, $\theta_D = \pi/4$ and $V/\tau = 1$. Here, each line represents one value of $|\vec{D}|/\tau$: Red thick line is $|\vec{D}|/\tau = 0$, Blue dotted line is $|\vec{D}|/\tau = 0.1$, Green dot dashed line is $|\vec{D}|/\tau = 0.4$ and Black dotted line is $|\vec{D}|/\tau = 1.0$.

DM interaction almost does not affect it. The qualitative behavior of the x and z components of the two spin currents is the same, when there is no DM interaction these components are zero. When DM interaction increases, the x and z components of spin current appear.

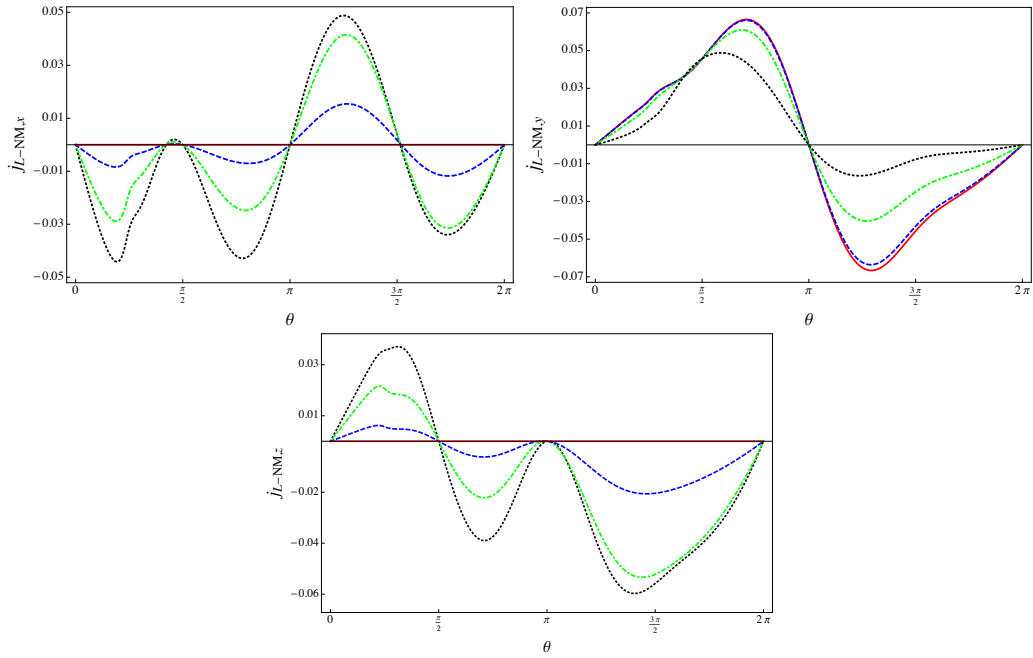


Figure 4.7: Model I: The x , y and z components of the spin current flowing from the left (L) to the central non-magnetic (NM) site for occupation number of one electron. Parameters are: $J_0/\tau = 0.5$, $t_{LR}/\tau = 0.1$, $\theta_D = \pi/4$ and $V/\tau = 1$. Here, each line represents one value of $|\vec{D}|/\tau$: Red thick line is $|\vec{D}|/\tau = 0$, Blue dotted line is $|\vec{D}|/\tau = 0.1$, Green dot dashed line is $|\vec{D}|/\tau = 0.4$ and Black dotted line is $|\vec{D}|/\tau = 1.0$

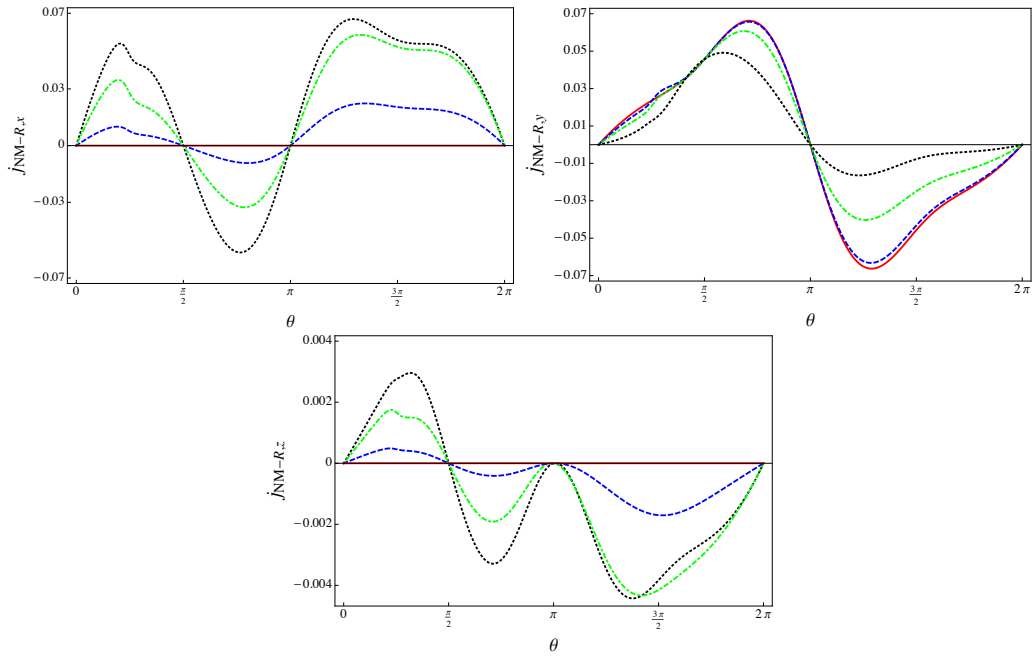


Figure 4.8: Model I: The x , y and z components of the spin current flowing from the central non-magnetic (NM) to right (R) site for occupation number of one electron. Parameters are: $J_0/\tau = 0.5$, $t_{LR}/\tau = 0.1$, $\theta_D = \pi/4$ and $V/\tau = 1$. Here, each line represents one value of $|\vec{D}|/\tau$: Red thick line is $|\vec{D}|/\tau = 0$, Blue dotted line is $|\vec{D}|/\tau = 0.1$, Green dot dashed line is $|\vec{D}|/\tau = 0.4$ and Black dotted line is $|\vec{D}|/\tau = 1.0$.

We also can study the effect of V on spin current. In Fig. (4.9) we calculate again the spin current flowing from left to right site with a fixed value of $|\vec{D}|/J_0 = 1$ (we choose the largest DM value to better see the effect of V) and varied V considering a large negative or positive and zero value. We can see that V affects mainly the magnitude of spin current, not the shape. But we can notice that all components are reduced if the potential V is negative. This is a consequence of the localization of the charge on the NM site in this case. On the contrary, a positive V enhances the current: in the case of a large potential barrier, electrons are localized mainly on the magnetic sites, and they can tunnel from one site to the other.

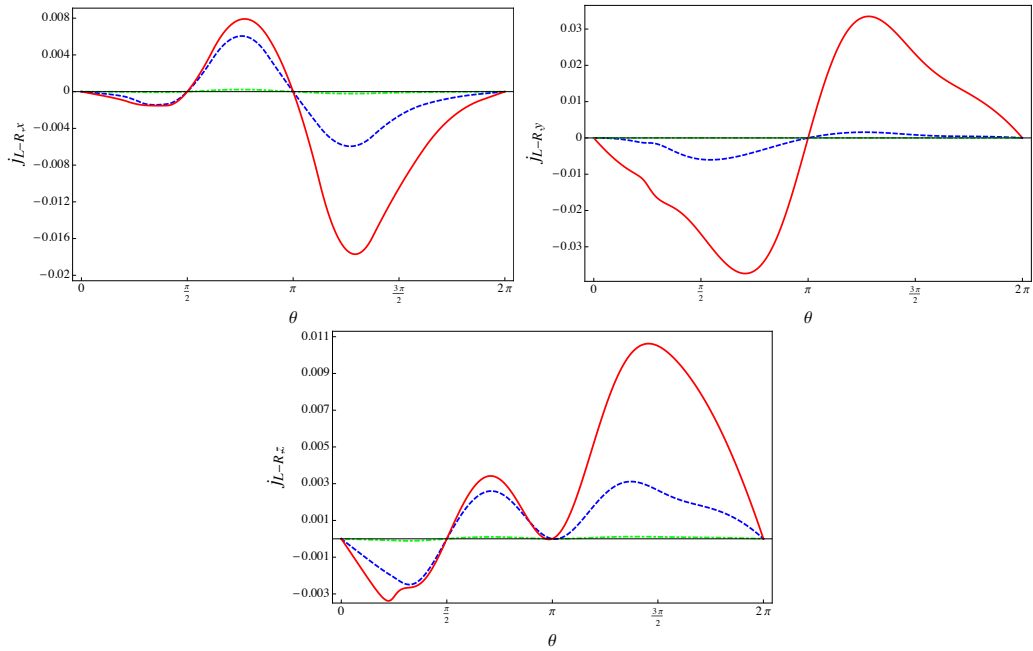


Figure 4.9: Model I: The three components of spin current flowing from the left (L) to the right (R) site when the occupation is one electron. Parameters are: $J_0/\tau = 0.5$, $t_{LR}/\tau = 0.1$, $\theta_D = \pi/4$ and $|\vec{D}|/J_0 = 1$. Here, each line represents one value of V/τ : Red line is $V/\tau = 5.0$, Blue dashed lines $V/\tau = 0$ and Green dot dashed line is $V/\tau = -5.0$

We have only studied the case of 1 electron in this model I, the effect of a different band filling has been studied within model II.

4.5.2 Model II

Now we present the results for the case where we represent the three layers system by two sites, as shown in section IV (model II). The number of possible states is smaller and this allows us to find the solution for different occupation numbers. So we can compare how the band filling influences the spin current when we consider DM interaction. We present our results for occupation equal to one or two electrons.

One Electron

First we present the case where the ‘band’ contains only one electron. In Figure (4.10) we present the three figures that represent the 3 components of the spin current. These figures are done for a fixed angle (θ_D) of \vec{D} , and a fixed exchange parameter, J_0 , as a function of the angle θ between \vec{S}_L and \vec{S}_R . We present, for each component, five curves corresponding to different values of $|\vec{D}'|$.

One can see that the DM interaction changes the behavior of all components of the spin current, as in model I. Also with this model, we can see that when DM interaction is absent, spin current appears only in the y direction [Fig. (4.10-b)]. When DM increases, the y component slightly decreases and spin current in x and z direction appear. The angle at which the y component vanishes changes significantly with $|\vec{D}'|$.

Analyzing Figures (4.10-a) and (4.10-c) we observe the same qualitative behavior as for the three sites case [Fig. (4.6 - a and c)]. We notice that the DM interaction causes an increase in these two components. The θ angle where j_x and j_z are zero, is well defined for both components it is exactly in π .

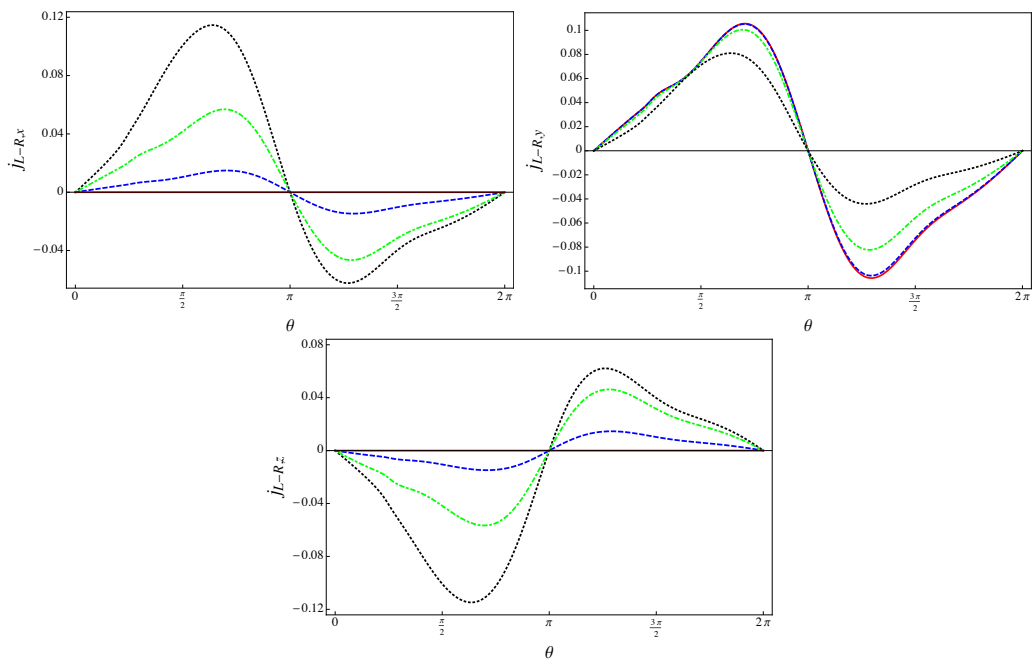


Figure 4.10: Model II - One Electron Occupation: The three components of the spin current. Parameters are: $J_0/t_{LR} = 0.5$ and $\theta_D = \pi/4$. Here, each line represents one value of $|\vec{D}|/\tau$: Red thick line is $|\vec{D}|/\tau = 0$, Blue dotted line is $|\vec{D}|/\tau = 0.1$, Green dot dashed line is $|\vec{D}|/\tau = 0.4$ and Black dotted line is $|\vec{D}|/\tau = 1.0$.

Two Electrons

Now we present in Fig. (4.11) the results for two electrons. Here again x and z components of spin current increase with the DM interaction. However if we compare the x (z) components for the one electron case with the two electrons case, we see that the sign of the x and z components is opposite, and most importantly, the absolute value is much smaller when there are 2 electrons (in our case, it is smaller by a factor 3 approximatively). This indicates that the ‘band filling’ plays an important role on the transverse components of spin current. On the other hand the longitudinal component (Fig. (4.11-b)) is almost not affected by DM interaction.

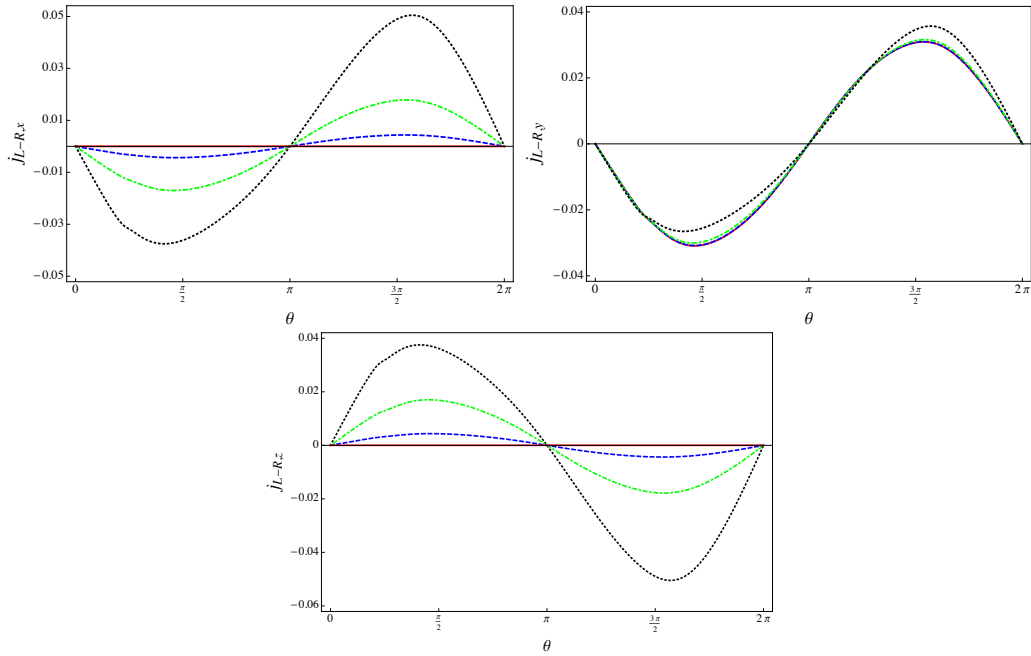


Figure 4.11: Model II - Two Electrons Occupation: The x , y and z components of spin current. Where $J_0/t_{LR} = 0.5$ and $\theta_D = \pi/4$. Here, each line represents one value of $|\vec{D}|/\tau$: Red thick line is $|\vec{D}|/\tau = 0$, Blue dotted line is $|\vec{D}|/\tau = 0.1$, Green dot dashed line is $|\vec{D}|/\tau = 0.4$ and Black dotted line is $|\vec{D}|/\tau = 1.0$.

Our results allow to conclude :

- in the presence of DM interaction, transverse spin components appear, while the longitudinal component is modified;

- the behavior of spin current as a function of the angle between the 2 local spins, θ , is far from sinusoidal;
- the absolute value of the transverse components depends on many factors as : the value of the potential of the intermediate layer (V), the occupation number and all other parameters of the model (hopping integral, s-d exchange, etc.);
- All components vanish at $\theta = \pi$, but on the current is not symmetric for $\theta = \pi$; this is due to the fact that the angle θ_D is $\pi/4$.

4.5.3 Spin Accumulation

In this section we will discuss the spin accumulation in each site. We will define the spin accumulation on site i only by the average value of spin in site i $\langle \vec{s}_i \rangle$, i.e., $\langle \vec{s}_i \rangle$ is the average value of the \vec{s}_i (the three components are given by equations (4.13), (4.14) and (4.15)). We calculate the spin accumulation only in Model I. The results are presented in figures (4.12), (4.13) and (4.14). Spin accumulation can be related to spin current by the continuity equations – eqs. (4.19) in the 3-sites description or eqs. (4.28) in the 2-sites model – and we can check that a calculation of this spin accumulation through the continuity equations would give the same results as the direct calculation that can be done from the electron wave function. In this model spin accumulation is rather large, but a more realistic model would certainly give smaller values.

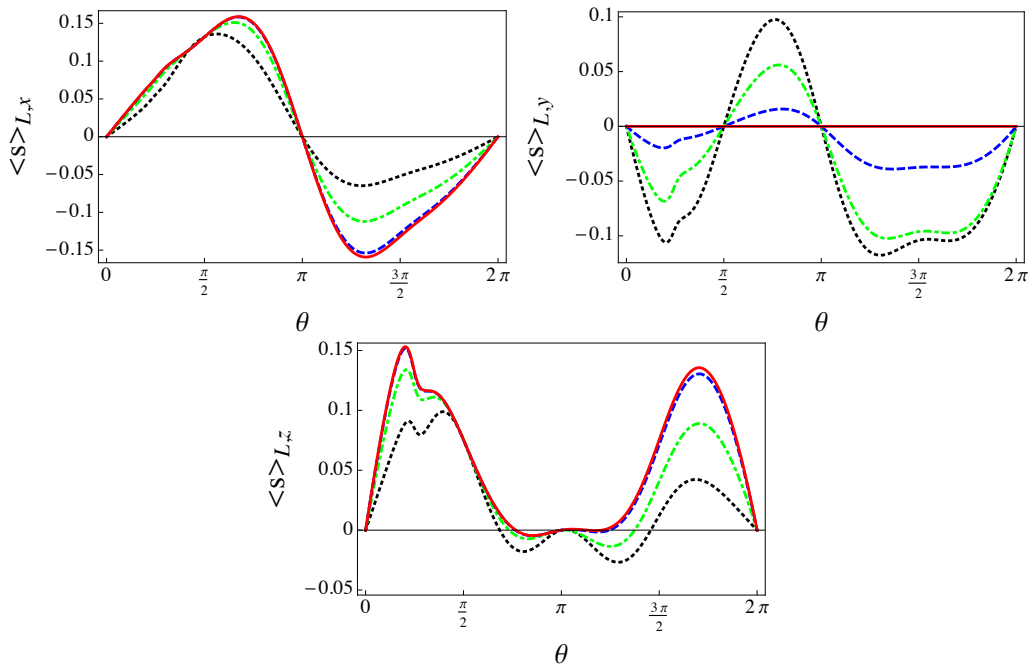


Figure 4.12: Model I - This figure shows the spin accumulation in site L. Parameters are: $J_0/\tau = 0.5$, $t_{LR}/\tau = 0.1$, $\theta_D = \pi/4$ and $V/\tau = 1$. Here, each line represents one value of $|\vec{D}|/\tau$: Red thick line is $|\vec{D}|/\tau = 0$, Blue dotted line is $|\vec{D}|/\tau = 0.1$, Green dot dashed line is $|\vec{D}|/\tau = 0.4$ and Black dotted line is $|\vec{D}|/\tau = 1.0$

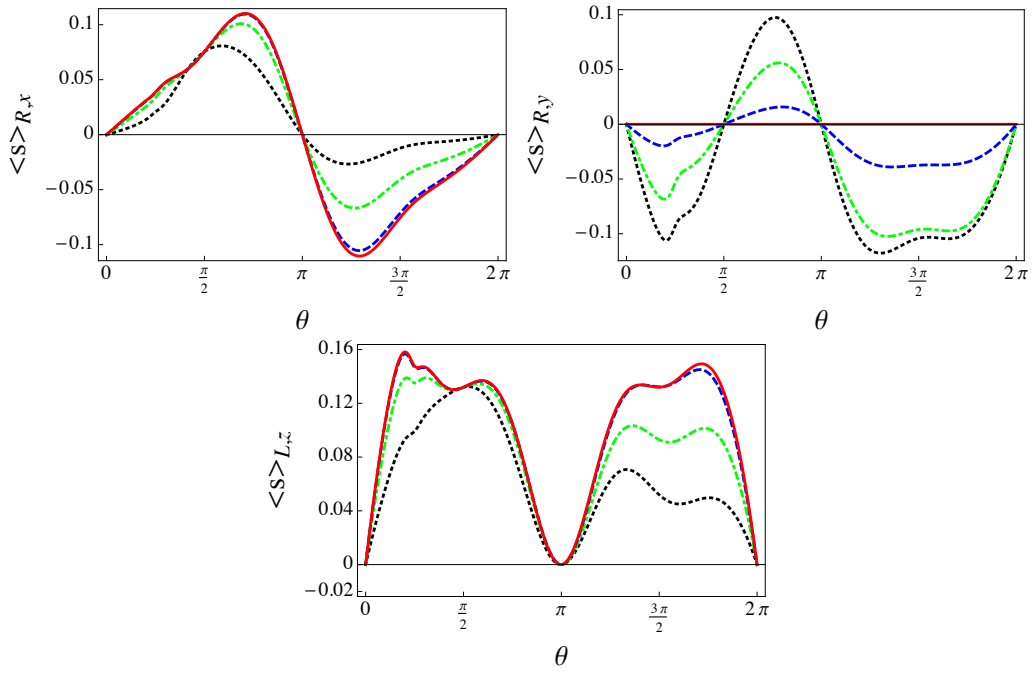


Figure 4.13: Model I - The spin accumulation in site R. Parameters are: $J_0/\tau = 0.5$, $t_{LR}/\tau = 0.1$, $\theta_D = \pi/4$ and $V/\tau = 1$. Here, each line represents one value of $|\vec{D}|/\tau$: Red thick line is $|\vec{D}|/\tau = 0$, Blue dotted line is $|\vec{D}|/\tau = 0.1$, Green dot dashed line is $|\vec{D}|/\tau = 0.4$ and Black dotted line is $|\vec{D}|/\tau = 1.0$.

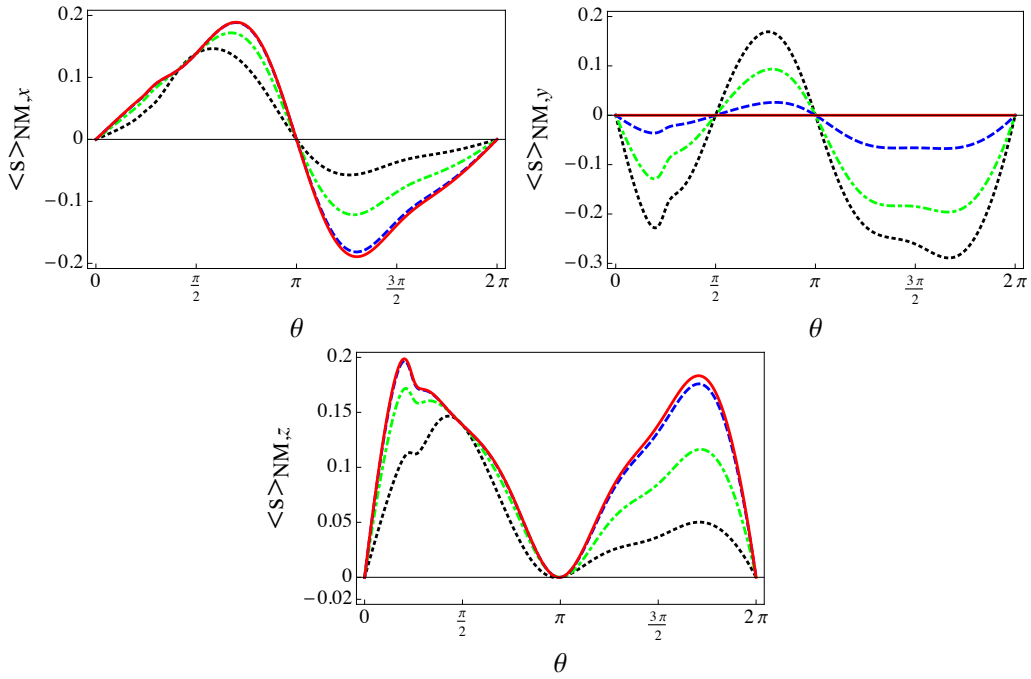


Figure 4.14: Model I - This figure shows the spin accumulation in site R. Parameters are: $J_0/\tau = 0.5$, $t_{LR}/\tau = 0.1$, $\theta_D = \pi/4$ and $V/\tau = 1$. Here, each line represents one value of $|\vec{D}|/\tau$: Red thick line is $|\vec{D}|/\tau = 0$, Blue dotted line is $|\vec{D}|/\tau = 0.1$, Green dot dashed line is $|\vec{D}|/\tau = 0.4$ and Black dotted line is $|\vec{D}|/\tau = 1.0$.

4.6 Perspective: A More Realistic Description

Throughout the last section we present several results for the 3-layers problem in two very simple approximation. Our goal was discovery if the DM interaction could influences the spin current. Even in these simple models we can verify that the Dzyaloshinskii-Moriya interaction induces some spin current. However we know that this a limited description, we cannot compare the results obtained in this thesis with experimental ones. So, in this section we present the idea of a more sophisticated theoretical model that incorporates some new elements in the model.

A more realistic description of the system can be performed where magnetic layers will be represented as semi-infinite chains, each point of the chain representing an atomic plane while the non-magnetic layer will be represented by n sites on this chain, n measuring the width of this intermediate layer.

The spin current between 2 sites A and B is now given by

$$\vec{I}_{AB} = Tr \left[\int d\omega (G_{AB}^<(\omega) - G_{BA}^<(\omega)) \bar{\sigma} \right] \quad (4.31)$$

Here $G_{ij}^<$ is the Green's function between sites i and j and $\bar{\sigma}$ are the Pauli matrices. We choose to write Dyson equations and solve the set of equations that close a system. In 1 dimension, the model can be solved following the technique developed for spin transfer torque [100].

We started do some investigation in this path, but this description request a mathematical and computational apparatus much more complex than the one we used here. In future work we will present this new description of the problem.

Chapter 5

Conclusions and Perspectives

First we investigated the dissipative and non - equilibrium effects near a superconductor - metal quantum critical point. We considered a superconducting layer, submitted to a time dependent vector potential and deposited over a metallic substrate. The superconducting layer and the substrate can exchange electrons through a momentum non-conserving process. First we found that a dissipation induced quantum critical point appears. Next, we treated the effect of an electric field. We have shown that the phase diagram is modified both by the electric field and dissipation in a non-equilibrium stationary state. We also included fluctuations close to this quantum critical point (QCP), and we were able to fully characterize the dissipation induced QCP, obtaining its dynamic exponent, effective dimension and universality class. We proposed that the quantum normal-to-superconductor phase transition in the layer when its coupling to the metallic substrate has mean-field critical behavior.

The microscopic mechanism for the dissipation is the transfer of electrons between the two systems. This is the same type of coupling that gives rise to the proximity effect. So, as a future step, we want investigate how this proximity effect can affect the metallic bath. Maybe an induced superconductivity will appear in the substrate.

Next we studied the influence of an odd-parity hybridization on a superconducting state. The specific system was a two-band metal with an attractive interaction between quasi-particles in different bands and an attractive intra-band interaction in one of these bands. The hybridization between the two bands is assumed to be anti-symmetric. We noticed that, when we consider anti-symmetric hybridization, it enhances the superconducting properties. This behavior is unexpected if we compare to the case of symmetric hybridization. Another important result was that, in this problem, an induced order parameter appears that has an anti-symmetric spatial part.

Due this property we can propose a new mechanism to produce a Kitaev's chain without introducing spin orbit coupling or any external parameters, such as magnetic field. This is an important result since this Kitaev's chain presents a non-trivial topological phase with Majorana fermions at its ends.

The last problem discussed was related to the effect of Dzyaloshinskii-Moriya interactions on the spin current. We studied a 3-layer system composed by a non-magnetic layer between two ferromagnetic layers. In order to investigate this problem we proposed a simple toy model where each layer was described by one site. We concluded that the DM interaction affects the spin current and should be taken into account in the description of magnetic nanostructures. To continue this work we proposed to study a more realistic 1-dimensional model that can describe this 3-layer system.

Appendix A

Adiabatic Expansion of Green's Function

In this appendix we show explicitly the adiabatic expansion of terms similar to those that appear in the equations (2.26) and (2.27).

$$\begin{aligned} F\left(t-t_1, \frac{t+t_1}{2}\right) &= F(t-t_1, \bar{t}) + \left(\frac{t+t_1}{2} - \frac{t+t'}{2}\right) \frac{\partial F}{\partial \bar{t}}(t-t_1, \bar{t}) \\ &= F(t-t_1, \bar{t}) + \left(\frac{t_1-t'}{2}\right) \frac{\partial F}{\partial \bar{t}}(t-t_1, \bar{t}). \end{aligned} \tag{A.1}$$

$$\begin{aligned} g_L\left(t-t_1, \frac{t+t_1}{2}\right) &= g_L(t-t_1, \bar{t}) + \left(\frac{t+t_1}{2} - \frac{t+t'}{2}\right) \frac{\partial g_L}{\partial \bar{t}}(t-t_1, \bar{t}) \\ &= g_L(t-t_1, \bar{t}) + \left(\frac{t_1-t'}{2}\right) \frac{\partial g_L}{\partial \bar{t}}(t-t_1, \bar{t}). \end{aligned} \tag{A.2}$$

$$\begin{aligned} \Delta_k(t_1) &= \Delta_k(\bar{t}) + (t_1 - \bar{t}) \frac{\partial \Delta_k}{\partial \bar{t}}(\bar{t}) \\ &= \Delta_k(\bar{t}) + \left(\frac{t_1-t}{2} + \frac{t_1-t'}{2}\right) \frac{\partial \Delta_k}{\partial \bar{t}}(\bar{t}) \end{aligned} \tag{A.3}$$

$$\begin{aligned} \mathcal{F}\left(t_1-t', \frac{t_1+t'}{2}\right) &= \mathcal{F}(t_1-t', \bar{t}) + \left(\frac{t_1+t'}{2} - \frac{t+t'}{2}\right) \frac{\partial \mathcal{F}}{\partial \bar{t}}(t_1-t', \bar{t}) \\ &= \mathcal{F}(t_1-t', \bar{t}) + \left(\frac{t_1-t}{2}\right) \frac{\partial \mathcal{F}}{\partial \bar{t}}(t_1-t', \bar{t}). \end{aligned} \tag{A.4}$$

$$\begin{aligned}
G_L \left(t_1 - t', \frac{t_1 + t'}{2} \right) &= G_L(t_1 - t', \bar{t}) + \left(\frac{t_1 + t'}{2} - \frac{t + t'}{2} \right) \frac{\partial G_L}{\partial \bar{t}}(t_1 - t', \bar{t}) \\
&= G_L(t_1 - t', \bar{t}) + \left(\frac{t_1 - t}{2} \right) \frac{\partial G_L}{\partial \bar{t}}(t_1 - t', \bar{t}).
\end{aligned} \tag{A.5}$$

$$\begin{aligned}
\Sigma \left(t_1 - t_2, \frac{t_1 + t'}{2} \right) &= \Sigma(t_1 - t_2, \bar{t}) + \left(\frac{t_1 + t_2}{2} - \frac{t + t'}{2} \right) \frac{\partial \Sigma}{\partial \bar{t}}(t_1 - t_2, \bar{t}) \\
&= \Sigma(t_1 - t_2, \bar{t}) + \left(\frac{t_1 - t}{2} + \frac{t_2 - t'}{2} \right) \frac{\partial \Sigma}{\partial \bar{t}}(t_1 - t_2, \bar{t}).
\end{aligned} \tag{A.6}$$

$$\begin{aligned}
\mathcal{F} \left(t_2 - t', \frac{t_2 + t'}{2} \right) &= \mathcal{F}(t_2 - t', \bar{t}) + \left(\frac{t_2 + t'}{2} - \frac{t + t'}{2} \right) \frac{\partial \mathcal{F}}{\partial \bar{t}}(t_2 - t', \bar{t}) \\
&= \mathcal{F}(t_2 - t', \bar{t}) + \left(\frac{t_2 - t}{2} \right) \frac{\partial \mathcal{F}}{\partial \bar{t}}(t_2 - t', \bar{t}).
\end{aligned} \tag{A.7}$$

$$\begin{aligned}
G_L \left(t_2 - t', \frac{t_2 + t'}{2} \right) &= G_L(t_2 - t', \bar{t}) + \left(\frac{t_2 + t'}{2} - \frac{t + t'}{2} \right) \frac{\partial G_L}{\partial \bar{t}}(t_2 - t', \bar{t}) \\
&= G_L(t_2 - t', \bar{t}) + \left(\frac{t_2 - t}{2} \right) \frac{\partial G_L}{\partial \bar{t}}(t_2 - t', \bar{t}).
\end{aligned} \tag{A.8}$$

Multiplying the terms and neglecting terms above first order with $t - t'$ we got the equations (2.30) and (2.31).

Appendix B

Retarded Green's Function

Solving the system composed by equations (2.69) and (2.70) we find

$$\begin{aligned}
G_L^{(1)r(a)} = & \frac{1 - F^{(0)r(a)\Sigma r(a)}}{\left(1 - g_L^{(0)r(a)\Sigma r(a)}\right) \left(1 - F^{(0)r(a)\Sigma r(a)}\right) - F^{(0)r(a)\Delta_k^{(0)}}} \left\{ \right. \\
& - g_L^{(0)r(a)\Delta_k^{(1)}} \mathcal{F}^{(0)r(a)} - \\
& + \frac{i\Sigma}{2} \left[\frac{\partial g_L^{(0)r(a)}}{\partial \bar{t}} \frac{\partial G_L^{(0)r(a)}}{\partial \omega} - \frac{\partial g_L^{(0)r(a)}}{\partial \omega} \frac{\partial G_L^{(0)r(a)}}{\partial \bar{t}} \right] + \\
& + \frac{i}{2} \left[\frac{\partial g_L^{(0)r(a)}}{\partial \omega} \frac{\partial}{\partial \bar{t}} \left(\Delta_k^{(0)} \mathcal{F}^{(0)r(a)} \right) - \frac{\partial}{\partial \bar{t}} \left(g_L^{(0)r(a)} \Delta_k^{(0)} \right) \frac{\partial \mathcal{F}^{(0)r(a)}}{\partial \omega} \right] - \\
& - \frac{g_L^{(0)r(a)\Delta_k^{(0)}}}{1 - F^{(0)r(a)\Sigma r(a)}} \left\{ - F^{(0)r(a)\Delta_k^{(1)}} G_L^{(0)r(a)} + \right. \\
& + \frac{i\Sigma}{2} \left[\frac{\partial F^{(0)r(a)}}{\partial \bar{t}} \frac{\partial \mathcal{F}^{(0)r(a)}}{\partial \omega} - \frac{\partial F^{(0)r(a)}}{\partial \omega} \frac{\partial \mathcal{F}^{(0)r(a)}}{\partial \bar{t}} \right] + \\
& \left. \left. + \frac{i}{2} \left[\frac{\partial F^{(0)r(a)}}{\partial \omega} \frac{\partial}{\partial \bar{t}} \left(\Delta_k^{(0)} G_L^{(0)r(a)} \right) - \frac{\partial}{\partial \bar{t}} \left(F^{(0)r(a)} \Delta_k^{(0)} \right) \frac{\partial \mathcal{F}^{(0)r(a)}}{\partial \omega} \right] \right\} \right\} \\
& \tag{B.1}
\end{aligned}$$

$$\begin{aligned}
\mathcal{F}^{(1)r(a)} = & \frac{1}{1 - F^{(0)r(a)\Sigma^{r(a)}}} \left\{ -F^{(0)r(a)} \Delta_k^{(1)}(\bar{t}) G_L^{(0)r(a)} + \right. \\
& + \frac{i\Sigma}{2} \left[\frac{\partial F^{(0)r(a)}}{\partial \bar{t}} \frac{\partial \mathcal{F}^{(0)r(a)}}{\partial \omega} - \frac{\partial F^{(0)r(a)}}{\partial \omega} \frac{\partial \mathcal{F}^{(0)r(a)}}{\partial \bar{t}} \right] + \\
& \left. + \frac{i}{2} \left[\frac{\partial F^{(0)r(a)}}{\partial \omega} \frac{\partial}{\partial \bar{t}} \left(\Delta_k^{(0)} G_L^{(0)r(a)} \right) - \frac{\partial}{\partial \bar{t}} \left(F^{(0)r(a)} \Delta_k^{(0)} \right) \frac{\partial \mathcal{F}^{(0)r(a)}}{\partial \omega} \right] \right\} + \\
& \frac{F^{(0)r(a)}}{\left(1 - g_L^{(0)r(a)\Sigma^{r(a)}} \right) \left(1 - F^{(0)r(a)\Sigma^{r(a)}} \right) - F^{(0)r(a)} \Delta_k^{(0)}} \left\{ -g_L^{(0)r(a)} \Delta_k^{(1)} \mathcal{F}^{(0)r(a)} - \right. \\
& + \frac{i\Sigma}{2} \left[\frac{\partial g_L^{(0)r(a)}}{\partial \bar{t}} \frac{\partial G_L^{(0)r(a)}}{\partial \omega} - \frac{\partial g_L^{(0)r(a)}}{\partial \omega} \frac{\partial G_L^{(0)r(a)}}{\partial \bar{t}} \right] + \\
& + \frac{i}{2} \left[\frac{\partial g_L^{(0)r(a)}}{\partial \omega} \frac{\partial}{\partial \bar{t}} \left(\Delta_k^{(0)} \mathcal{F}^{(0)r(a)} \right) - \frac{\partial}{\partial \bar{t}} \left(g_L^{(0)r(a)} \Delta_k^{(0)} \right) \frac{\partial \mathcal{F}^{(0)r(a)}}{\partial \omega} \right] - \\
& - \frac{g_L^{(0)r(a)} \Delta_k^{(0)}}{1 - F^{(0)r(a)\Sigma^{r(a)}}} \left\{ -F^{(0)r(a)} \Delta_k^{(1)} G_L^{(0)r(a)} + \right. \\
& + \frac{i\Sigma}{2} \left[\frac{\partial F^{(0)r(a)}}{\partial \bar{t}} \frac{\partial \mathcal{F}^{(0)r(a)}}{\partial \omega} - \frac{\partial F^{(0)r(a)}}{\partial \omega} \frac{\partial \mathcal{F}^{(0)r(a)}}{\partial \bar{t}} \right] + \\
& \left. \left. + \frac{i}{2} \left[\frac{\partial F^{(0)r(a)}}{\partial \omega} \frac{\partial}{\partial \bar{t}} \left(\Delta_k^{(0)} G_L^{(0)r(a)} \right) - \frac{\partial}{\partial \bar{t}} \left(F^{(0)r(a)} \Delta_k^{(0)} \right) \frac{\partial \mathcal{F}^{(0)r(a)}}{\partial \omega} \right] \right\} \right\} \\
\end{aligned} \tag{B.2}$$

Appendix C

Spin Orbit Coupling Induces p-wave Superconductors

Here we will follow the paper from Alicea [70] to show the existence of $p_x \pm ip_y$ pairing with opposite chirality for upper/lower bands.

The model considers an isolated zinc-blende semiconductor quantum well grown along the (100) direction. Coupled to a ferromagnetic insulator whose magnetization points perpendicular to the two-dimensional layer, that induces a Zeeman interaction. We can summarize this problem in the following Hamiltonian:

$$H = H_0 + H_{Zeeman} + H_{SOC}, \quad (C.1)$$

with

$$H_0 = \sum_{\vec{k}} \left(\epsilon_k c_{\vec{k}\uparrow}^\dagger c_{\vec{k}\uparrow} + \epsilon_k c_{\vec{k}\downarrow}^\dagger c_{\vec{k}\downarrow} \right), \quad (C.2)$$

where $\vec{k} = (k_x, k_y)$ and $k = \sqrt{k_x^2 + k_y^2}$, $\epsilon_k = \frac{k^2}{2m} - \mu$ is the energy of an electron and $c_{ij}^{(\dagger)}$ creates (annihilates) an electron with momentum i and spin j .

$$H_{Zeeman} = \sum_{\vec{k}} h \left(c_{\vec{k}\uparrow}^\dagger c_{\vec{k}\uparrow} - c_{\vec{k}\downarrow}^\dagger c_{\vec{k}\downarrow} \right), \quad (C.3)$$

where h is a magnetic field.

$$H_{SOC} = \sum_{\vec{k}} \left(V_{\vec{k}} c_{\vec{k}\uparrow}^\dagger c_{\vec{k}\downarrow} + V_{\vec{k}}^* c_{\vec{k}\downarrow}^\dagger c_{\vec{k}\uparrow} \right), \quad (C.4)$$

where $V_{\vec{k}} = \lambda k e^{-i\phi_{\vec{k}}}$ and $\phi_{\vec{k}} = \arctan(k_x/k_y)$.

We can write Schrödinger equation for this problem in a matrix way

$$\begin{pmatrix} \epsilon_{k\uparrow} & V_{\vec{k}} \\ V_{\vec{k}}^* & \epsilon_{k\downarrow} \end{pmatrix} \vec{\psi} = \mathbf{E}\vec{\psi}, \quad (\text{C.5})$$

where $\epsilon_{k\uparrow,\downarrow} = \epsilon_k \pm h$. We can calculate the eigenvalues \mathbf{E} through the equation $\det(H - \mathbf{E}I) = 0$, where I is the identity matrix. Doing this calculation we find the excitation energies:

$$E_{\pm} = \epsilon_k \pm \sqrt{h^2 + |V_{\vec{k}}|^2}. \quad (\text{C.6})$$

This same result is shown by Alicea [70] in equation (9).

Once we calculate the eigenvalues, it is also possible to find the eigenvectors:

$$\vec{v}_1 = \frac{|V_{\vec{k}}|}{\sqrt{(h + \sqrt{h^2 + |V_{\vec{k}}|^2})^2 + |V_{\vec{k}}|^2}} \begin{pmatrix} \frac{h + \sqrt{h^2 + |V_{\vec{k}}|^2}}{V_{\vec{k}}^*} \\ 1 \end{pmatrix} \quad (\text{C.7})$$

and

$$\vec{v}_2 = \frac{|V_{\vec{k}}|}{\sqrt{(h + \sqrt{h^2 + |V_{\vec{k}}|^2})^2 + |V_{\vec{k}}|^2}} \begin{pmatrix} 1 \\ -\frac{h + \sqrt{h^2 + |V_{\vec{k}}|^2}}{V_{\vec{k}}} \end{pmatrix}. \quad (\text{C.8})$$

And this two eigenvectors constitute the matrix:

$$p = \frac{|V_{\vec{k}}|}{\sqrt{(h + \sqrt{h^2 + |V_{\vec{k}}|^2})^2 + |V_{\vec{k}}|^2}} \begin{pmatrix} 1 & \frac{h + \sqrt{h^2 + |V_{\vec{k}}|^2}}{V_{\vec{k}}^*} \\ -\frac{h + \sqrt{h^2 + |V_{\vec{k}}|^2}}{V_{\vec{k}}} & 1 \end{pmatrix}. \quad (\text{C.9})$$

The procedure done is necessary to find a set of basis that diagonalize the Hamiltonian $H_0 + H_{Zeeman}$. The last step is calculate:

$$\begin{pmatrix} \psi_+(\vec{k}) \\ \psi_-(\vec{k}) \end{pmatrix} = p^{-1} \begin{pmatrix} c_{\vec{k}\uparrow} \\ c_{\vec{k}\downarrow} \end{pmatrix}, \quad (\text{C.10})$$

where

$$\psi_+(\vec{k}) = f_+(\vec{k}) \begin{pmatrix} 1 \\ 0 \end{pmatrix}, \quad (\text{C.11})$$

$$\psi_-(\vec{k}) = f_-(\vec{k}) \begin{pmatrix} 0 \\ 1 \end{pmatrix} \quad (\text{C.12})$$

and p^{-1} is the matrix inverse of p , such as,

$$p^{-1} = \begin{pmatrix} a_{\vec{k}} & -b_{\vec{k}}^* \\ b_{\vec{k}} & a_{\vec{k}} \end{pmatrix}, \quad (\text{C.13})$$

with

$$a_{\vec{k}} \equiv \frac{|V_{\vec{k}}|}{\sqrt{(h + \sqrt{h^2 + |V_{\vec{k}}|^2})^2 + |V_{\vec{k}}|^2}} \quad (\text{C.14})$$

and

$$b_{\vec{k}} \equiv \frac{|V_{\vec{k}}| (h + \sqrt{h^2 + |V_{\vec{k}}|^2})}{V_{\vec{k}} \sqrt{(h + \sqrt{h^2 + |V_{\vec{k}}|^2})^2 + |V_{\vec{k}}|^2}}. \quad (\text{C.15})$$

Equation (C.10) can be write now as

$$\begin{pmatrix} \psi_+(\vec{k}) \\ \psi_-(\vec{k}) \end{pmatrix} = \begin{pmatrix} a_{\vec{k}} & -b_{\vec{k}}^* \\ b_{\vec{k}} & a_{\vec{k}} \end{pmatrix} \begin{pmatrix} c_{\vec{k}\uparrow} \\ c_{\vec{k}\downarrow} \end{pmatrix}. \quad (\text{C.16})$$

Thus

$$c_{k\uparrow} = \frac{a_{\vec{k}}}{a_{\vec{k}}^2 + |b_{\vec{k}}|^2} \psi_+(\vec{k}) + \frac{b_{\vec{k}}^*}{a_{\vec{k}}^2 + |b_{\vec{k}}|^2} \psi_-(\vec{k})$$

$$c_{k\downarrow} = \frac{a_{\vec{k}}}{a_{\vec{k}}^2 + |b_{\vec{k}}|^2} \psi_-(\vec{k}) - \frac{b_{\vec{k}}}{a_{\vec{k}}^2 + |b_{\vec{k}}|^2} \psi_+(\vec{k}).$$

Notice that,

$$a_{\vec{k}}^2 + |b_{\vec{k}}|^2 = \frac{|V_{\vec{k}}|^2}{(h + \sqrt{h^2 + |V_{\vec{k}}|^2})^2 + |V_{\vec{k}}|^2} + \frac{|V_{\vec{k}}|^2 (h + \sqrt{h^2 + |V_{\vec{k}}|^2})}{|V_{\vec{k}}|^2 [(h + \sqrt{h^2 + |V_{\vec{k}}|^2})^2 + |V_{\vec{k}}|^2]}$$

$$= 1.$$

So

$$c_{k\uparrow} = a_{\vec{k}} \psi_+(\vec{k}) + b_{\vec{k}}^* \psi_-(\vec{k})$$

$$c_{k\downarrow} = a_{\vec{k}} \psi_-(\vec{k}) - b_{\vec{k}} \psi_+(\vec{k}). \quad (\text{C.17})$$

Alicea considers that the semiconductor comes into contact with an s-wave superconductor. Now the Hamiltonian is

$$H' = H_0 + H_{Zeeman} + H_{SC}, \quad (\text{C.18})$$

where

$$H_{SC} = \sum_k \Delta (c_{-k\downarrow} c_{k\uparrow} + H.c.). \quad (\text{C.19})$$

We can write the Hamiltonian of the superconductor using (C.17):

$$\begin{aligned} & \Delta \left(a_{-\vec{k}} \psi_{-}(-\vec{k}) - b_{-\vec{k}} \psi_{+}(-\vec{k}) \right) \left(a_{\vec{k}} \psi_{+}(\vec{k}) + b_{\vec{k}}^* \psi_{-}(\vec{k}) \right) = \\ & \Delta \left(a_{-\vec{k}} a_{\vec{k}} \psi_{-}(-\vec{k}) \psi_{+}(\vec{k}) - b_{-\vec{k}} a_{\vec{k}} \psi_{+}(-\vec{k}) \psi_{+}(\vec{k}) - b_{-\vec{k}} b_{\vec{k}}^* \psi_{+}(-\vec{k}) \psi_{-}(\vec{k}) + a_{-\vec{k}} b_{\vec{k}}^* \psi_{-}(-\vec{k}) \psi_{-}(\vec{k}) \right). \end{aligned} \quad (\text{C.20})$$

Consider $\vec{k} \rightarrow -\vec{k}$

$$\Delta \left(-b_{\vec{k}} a_{-\vec{k}} \psi_{+}(\vec{k}) \psi_{+}(-\vec{k}) + a_{\vec{k}} b_{-\vec{k}}^* \psi_{-}(\vec{k}) \psi_{-}(-\vec{k}) - \left(a_{-\vec{k}} a_{\vec{k}} + b_{\vec{k}} b_{-\vec{k}}^* \right) \psi_{+}(\vec{k}) \psi_{-}(-\vec{k}) \right), \quad (\text{C.21})$$

where we use the property: $\psi_{-}(-\vec{k}) \psi_{+}(\vec{k}) = -\psi_{+}(\vec{k}) \psi_{-}(-\vec{k})$.

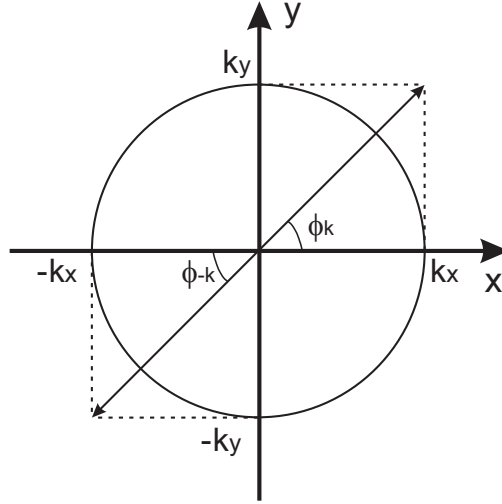


Figure C.1: Schematic picture of how k -inversion affects ϕ .

Before calculating the coefficients in the new base, we analyze V_k . Look at Figure (C.1), we can conclude that $\phi_{-\vec{k}} = \phi_{\vec{k}}$. However when we do $\vec{k} \rightarrow -\vec{k}$ the system acquires a π -phase difference. So $V_{\vec{k}}$ has a character anti-symmetric, such as, $V_{-\vec{k}} = -V_{\vec{k}}$.

Returning to the calculation we can write

$$-b_{\vec{k}} a_{-\vec{k}} = -\frac{V_{\vec{k}}^*}{2\sqrt{\hbar^2 + |V_{\vec{k}}|^2}} = -\frac{\lambda k}{2\sqrt{\hbar^2 + (\lambda k)^2}} e^{i\phi_{\vec{k}}} \quad (\text{C.22})$$

$$a_{\vec{k}} b_{-\vec{k}}^* = \frac{V_{-\vec{k}}}{2\sqrt{h^2 + |V_{\vec{k}}|^2}} = -\frac{\lambda k}{2\sqrt{h^2 + (\lambda k)^2}} e^{-i\phi_{\vec{k}}}. \quad (\text{C.23})$$

The last coefficient is

$$-\left(a_{-\vec{k}} a_{\vec{k}} + b_{\vec{k}} b_{-\vec{k}}^*\right) = \frac{h}{\sqrt{h^2 + |V_{\vec{k}}|^2}} = \frac{h}{\sqrt{h^2 + (\lambda k)^2}} \quad (\text{C.24})$$

Using the notation from Alicea:

$$f_p(k) \equiv -\frac{\lambda k}{2\sqrt{h^2 + (\lambda k)^2}} \quad (\text{C.25})$$

and

$$f_s(k) \equiv \frac{h}{\sqrt{h^2 + (\lambda k)^2}}, \quad (\text{C.26})$$

that only depends of $k = \sqrt{k_x^2 + k_y^2}$.

Finally, equation (C.19) can be written as

$$H_{SC} = \sum_k \left(\Delta_{++}(\vec{k}) \psi_+(\vec{k}) \psi_+(-\vec{k}) + \Delta_{--}(\vec{k}) \psi_-(\vec{k}) \psi_-(-\vec{k}) + \Delta_{+-}(k) \psi_+(\vec{k}) \psi_-(-\vec{k}) + H.c. \right), \quad (\text{C.27})$$

where

$$\Delta_{++}(\vec{k}) = f_p(k) \Delta e^{i\phi_{\vec{k}}} \quad (\text{C.28})$$

$$\Delta_{--}(\vec{k}) = f_p(k) \Delta e^{-i\phi_{\vec{k}}} \quad (\text{C.29})$$

$$\Delta_{+-}(k) = f_s(k) \Delta. \quad (\text{C.30})$$

The $\Delta_{++}(\vec{k})$ and $\Delta_{--}(\vec{k})$ are generated via proximity effect and have $p_x \pm ip_y$ pairing with opposite chirality for upper/lower bands.

Appendix D

List of Publications

- **Fernanda Deus**, Alexis R. Hernández and Mucio A. Continentino, *Adiabatic charge and spin pumping through interacting quantum dots*, J. Phys.: Condens. Matter **24**, 356001 (2012).
- **Fernanda Deus** and Mucio A. Continentino, *Superconductor-normal metal quantum phase transition in dissipative and non-equilibrium systems*, Philosophical Magazine **93**, 3062-3080 (2013).
- Mucio A. Continentino, **Fernanda Deus**, Igor T. Padilha and Heron Caldas, *Topological transitions in multi-band superconductors*, Annals of Physics **348**, 1-14 (2014).
- Mucio A. Continentino, **Fernanda Deus** and Heron Caldas, *Renormalization group approach to a p-wave superconducting model*, Physics Letters A **378**, 1561-1565 (2014).

Bibliography

- [1] H. Bruuns and K. Flensberg, *Many-Body Quantum Theory in Condensed Matter Physics* (Oxford University Press, Oxford, 2004).
- [2] L. P. Kadanoff and G. Baym, *Quantum Statistical Mechanics* (Benjamin, New York, 1962).
- [3] L. V. Keldysh, Sov. Phys. JETP **20**, 1018 (1965).
- [4] W. Kohn, Rev. Mod. Phys **71**, 1253 (1998).
R. O. Jones and O. Gunnarsson, Rev. Mod. Phys **61**, 689 (1989).
- [5] A. L. Fetter and J. D. Walecka, *Quantum Theory of Many-Particle System, 1st Ed.* (New York: Mc Graw-Hill, New York, 1971).
- [6] H. Kamerlingh Onnes, Leiden Comm. **120b**, **122b**, **124c**, (1911).
- [7] V. L. Ginzburg and L. D. Landau, Zh. Eksperim. i Teor. Fiz. **20**, 1064 (1950).
- [8] J. Bardeen, L. N. Cooper and J. R. Schrieffer, Phys. Rev. **106**, 162 (1957).
- [9] G. Bednorz and K. A. Müller, Z. Phys. B **64**, 189 (1986).
- [10] D. Dalidovich and P. Phillips, Phys. Rev. Lett. **93**, 027004 (2004).
- [11] A. G. Green and S. L. Sondhi, Phys. Rev. Lett. **95**, 267001 (2005).
- [12] A. Mitra, Phys. Rev. B, **78**, 214512 (2008).
- [13] A. Ramires and M. A. Continentino, J. Phys.: Condens. Matter **22**, 485701 (2010).
- [14] C. Petrovic *et al.*, J. Phys.: Condens. Matter **13**, L337 (2001).
- [15] S. M. Ramos *et al.*, Physica B: Cond. Matt. **359-361**, 398-400 (2005).

- [16] M. Núñez-Regueiro, D. C. Freitas, R. Brusetti and J. Marcus, Sol. Sta. Comm. **159**, 26 (2013).
- [17] E. D. Bauer *et al.*, Phys. Rev. B **73**, 245109 (2006).
- [18] M. Daniel *et al.*, Phys. Rev. Lett **95**, 016406 (2005).
- [19] M. Drzazga and E. Zipper, Sol. Stat. Comm. **68**, 605 (1998).
- [20] H. Takagi, S. Ishibashi, T. Ido and S. Uchida, Phys. Rev. B **41**, 11657 (1990).
- [21] A. H. Nevidomskyy and P. Coleman, Phys. Rev. Lett. **102**, 077202 (2009).
- [22] A. P. Mackenzie and Y. Manero, Physica B: Cond. Matt. **280**, 148-153 (2000).
- [23] A. Kitaev, Ann. Phys. **303**, 2 (2003).
A. Kitaev, Phys. Usp. **44**, 131 (2001).
- [24] M. Johnson and H. R. Silsbee, Phys. Rev. Lett. **55**, 17 (1985).
- [25] M. N. Baibich, J. M. Broto, A. Fert, F. Nguyen van Dau, F. Petroff, P. Eitenne, G. Creuzer, A. Friederich and J. Chazelas, Phys. Rev Lett. **61**, 2472 (1988).
- [26] G. Binasch, P. Grünberg, F. Saurenbach and W. Zin, Phys. Rev. B **39**, 4828 (1989).
- [27] I. Zutíć, J. Fabian and S. Das Sarma, Rev. Mod. Phys. **76**, 323 (2004)
- [28] O. Ujsaghy *et al.*, Phys. Rev. B **57**, 11598 (1998).
- [29] Kyoung-Whan Kim *et al.*, Phys. Rev. Lett. **111**, 216601 (2013).
- [30] I. Dzyaloshinskii, J. Phys. Chem. Sold. **4**, 241 (1958).
- [31] T. Moriya, Phys. Rev. **120**, 91 (1960).
- [32] F. Mei *et al.*, Scientific Reports **4**, 4030 (2013).
- [33] PM. Zarea *et al.*, Phys. Rev. Lett. **108**, 046601 (2012).
- [34] M. di Ventra, *Electrical Transport en Nanoscale Systems* (Cambridge University Press, Cambridge, 2008); S. Datta, *Electronic Transport in Mesoscopic Systems* (Cambridge University Press, Cambridge, 1995).

- [35] J. A. Hertz, Phys. Rev. B **14**, 1165 (1976).
- [36] W. L. McMillan, Phys. Rev. **175**, 537 (1968); Ya. V. Fominov, N. M. Chtchelkatchev and A. A. Golubov, Phys. Rev. B **66**, 014507 (2002).
- [37] J. Bardeen, Rev. Mod. Phys., **34**, 667 (1962).
- [38] see D. Dew-Hughes, Low Temp. Phys. **27**, 713 (2001).
- [39] A. Yu. Rusanov, M. B. S. Hesselberth, and J. Aarts, Phys. Rev. B **70**, 024510 (2004).
- [40] M. Yu. Kupriyanov and V. F. Lukichev, Fiz. Nizk. Temp. **6**, 445 (1980) [Sov. J. Low Temp. Phys. **6**, 210 (1980)].
- [41] P. G. de Gennes, *Superconductivity of Metals and Alloys*, p.182, (Perseus Books, Massachussets, USA, 1999).
- [42] K. Maki, Progr. Theor. Phys. **29**, 333 (1963).
- [43] D. Dalidovich and P. Phillips, Phys. Rev. Lett. **84**, 737 (2000).
- [44] see M. di Ventra, *Electrical Transport en Nanoscale Systems* (Cambridge University Press, Cambridge, 2008).
- [45] S. Takei and Y.B. Kim, Phys. Rev. B **78**,165401 (2008).
- [46] P. M. Hogan and A. G. Grenn, Phys. Rev. B **78**, 196104 (2008).
- [47] D. E. Feldman, Phys. Rev. Lett. **95**, 177201 (2005).
- [48] F. Deus, *Transporte em Ponto Quântico no Regime de Bloqueio de Coulomb*, Master Dissertation presented in CBPF - Centro Brasileiro de Pesquisas Físicas (2011).
- [49] Fernanda Deus, Alexis R. Hernandez and Mucio A. Continentino, J. Phys.: Condens. Matter **24**, 356001 (2012).
- [50] S. V. Tyablikov, *Methods in the Quantum Theory of Magnetism* (Plenum, New York, 1967).
- [51] A. R. Hernandez, F. A. Pinheiro, C. H. Lewenkopf and E. R. Mucciolo, Phys. Rev. B, **80**, 115311 (2009).
- [52] R. Bracewell, *The Fourier Transform and its Applications*, 3rd Ed. (New York: Mc Graw-Hill 2000).

- [53] M. Tinkham, *Introduction to Superconductivity* (New York: Mc Graw-Hill, 1975).
- [54] D. J. Thouless, *Annals of Physics* **10**, 553 (1960).
- [55] M. A. Continentino, *Quantum scaling in many-body systems* (World Scientific, Singapore, 2001).
- [56] D. C. Langreth, *Linear and Nonlinear Electron Transport in Solids* (Plenum, New York, 1976).
- [57] A. J. Millis, *Phys. Rev. B* **48**, 7183 (1993).
- [58] A. Mitra, S. Takei, Y. B. Kim and A. J. Millis, *Phys. Rev. Lett.* **97**, 236808 (2006); A. Mitra and A. J. Millis, *Phys. Rev. B* **77**, 220404 (2008).
- [59] F. Deus and M. A. Continentino, *Phil. Magazine* **93**, 22 (2013).
- [60] S. M. Ramos *et al.*, *Phys. Rev. Lett.* **105**, 126401 (2010).
- [61] E. D. Bauer *et al.*, *Physica B* **359**, 35-37 (2005).
E. D. Bauer *et al.*, *Phys. Rev. B* **73**, 245109 (2006).
- [62] I. T. Padilha and M. A. Continentino, *J. Magn. Magn. Mater.* **321**, 3466 (2009).
- [63] M. A. Continentino, I. T. Padilha and H. Caldas, *J. Stat. Mech.*, P07015 (2014).
- [64] R. Julien and B. Coqblin, *Phys. Rev. B* **8**, 5263 (1973).
- [65] A. Ramires, P. Coleman, A. H. Nevidomskyy and A. M. Tsvelik, *Phys. Rev. Lett* **109**, 176404 (2012).
- [66] M. A. Continentino, F. Deus, I. T. Padilha and H. Caldas, *Ann. Phys.* **348**, 1-14 (2014).
- [67] E. Majorana, *Nuovo Cimento* **14**, 171 (1937) - In Italian.
- [68] J. Alicea, *Rep. Prog. Phys.* **75**, 076501 (2012).
- [69] T. D. Ladd, F. Jelezko, R. Laflamme, Y. Nakamura, C. Monroe, J. L. O. Brien, *Nature* **464**, 45 (2010).
- [70] J. Alicea, *Phys. Rev. B* **81**, 125318 (2010).

- [71] C. Zhang *et al.*, Phys. Rev. Lett. **101**, 160401 (2008).
J. D. Saw, S. Tewari and S. Das Sarma, Phys. Rev. B **84**, 085109 (2011).
- [72] M. Gong, S. Tewari and C. Zhang, Phys. Rev. Lett. **107**, 195303 (2011).
- [73] G. H. Wannier, Phys. Rev. **52**, 191 (1937).
- [74] W. Kohn, Phys. Rev. **115**, 809 (1959).
J. de Cloizeaux, Phys. Rev. **129**, 554 (1953)
- [75] D. J. Griffiths, *Introduction to Quantum Mechanics* (Prentice Hall, 1994).
- [76] D. J. Rowe, Rev. Mod. Phys. **40**, 153 (1968).
- [77] M. A. Continentino, H. Caldas, D. Nozadze and N. Trivedi, Phys. Lett. A **378**, 3340 (2014).
- [78] C. A. R. Sá de Melo, M. Randeria and T. R. Engelbrecht, Phys. Rev. Lett. **71**, 3202 (1993).
- [79] N. Read and D. Green, Phys. Rev. B **61**, 10267 (2000).
- [80] A. J. Millis, Phys. Rev. Lett. **86**, 268 (2001).
- [81] J. M. D. Coey, *Magnetism and Magnetic Materials* (Cambridge University Press, 2010).
- [82] A. Thiavile *et al.*, Eur. Phys. Lett. **100**, 57002 (2012).
- [83] M. Heide *et al.*, Phys. Rev. B **78**, 140403 (2008).
- [84] A. Fert *et al.*, Nature nanotechnology **8**, 152 (2013).
- [85] N. Nagaosa *et al.*, Rev. Mod. Phys. **82**, 1539 (2010).
- [86] E. I. Rashba, Sov. Phys. Solide State **2**, 1109 (1960).
- [87] J. J. Sakurai, *Advanced Quantum Mechanics* (Addison-Wesley, 1967).
- [88] Y. A. Bychkov and E. I. Rashba, J. Phys. C **17**, 6039 (1984).
- [89] Dresselhaus, Phys. Rev. **100**, 580 (1955).
- [90] P. Bruno, Phys. Rev. B **39**, 865(R) (1989).

- [91] M. Cinal, D. M. Edwards and J. Mathon, Phys. Rev. B **50**, 3754 (1994).
- [92] A. F. Franco and H. Kachkachi, J. Phys.: Cond. Mat. **25**, 316003 (2013).
- [93] Q. Sun, J. Wang and H. Guo, Phys. Rev. B **71**, 165310 (2005).
- [94] A. Crépieux and C. Lacroix, J. Mag. Mag. Mat. **182**, 341 (1998).
- [95] C. D. Hu, J. Phys.: Cond. Mat. **24**, 086001 (2012).
- [96] D. A. Smith, J. Mag. Mag. Mat. **1**, 214 (1976).
- [97] A. Fert and P. Levy, Phys. Rev. Lett. **44**, 1538 (1980).
- [98] H. Imamura *et al.*, Phys. Rev. B **69**, 121303(R) (2004).
- [99] S. Herzog and M. R. Wegewijs, Nanotechnology **21**, 274010 (2010).
- [100] A. Kalitsov *et al.*, Phys. Rev. B **79**, 174416 (2009).